1-1-2009

Development of techniques using finite element and meshless methods for the simulation of piercing

Mbavhalelo Mabogo
Cape Peninsula University of Technology, mabogo@sun.ac.za

TITLE OF THESIS

Development of techniques using finite element and meshless methods for the simulation of piercing

by

Mbavhalelo Mabogo

Thesis submitted in fulfilment of the requirements for the degree

Magister Technologiae:
Mechanical Engineering

in the Faculty of Engineering
at the

CAPE PENINSULA UNIVERSITY OF TECHNOLOGY

Supervisor:
Prof Graeme John Oliver

Cape Town
February 2009

DECLARATION

I, Mbavhalelo Mabogo, declare that the contents of this thesis represent my own unaided work, and that the thesis has not previously been submitted for academic examination towards any qualification. Furthermore, it represents my own opinions and not necessarily those of the Cape Peninsula University of Technology.

Signed …… Date……

ABSTRACT

Finite element analysis modelling of sheet metal stamping is an important step in the design of tooling and process parameters. One of the critical measurements to determine the effectiveness of a numerical model is its capability of accurately predicting failure modes. To be able to make accurate predictions of deformation, tool force, blank design, etc computer simulation is almost necessary. In the automotive industry the tooling design can now be made by computer and analysed with FEA, and the amount of prototypes required for qualifying a design before manufacturing commences is greatly reduced.

Tool design is a specialized phase of tool engineering. While there are many die-cutting operation, some of which are very complex, they can all be reduce to plain blanking , piercing, lancing, cutting off and parting, notching, shaving and trimming.
The cutting action that occurs in the piercing is quite similar to that of the chip formation ahead of a cutting tool. The punch contact the material supported by the die and a pressure builds up occurs, When the elastic limit of the work material is the exceeded the material begins to flow plastically (plastic deformation). It is often impractical to pierce holes while forming, or before forming because they would become distorted in the forming operation.

The aim of the research is to develop techniques that would reduce the amount time spent during the tool qualifying stage. By accurately setting a finite element simulation that closely matches the experimental or real-life situation we can great understand the material behaviour and properties before tool designing phase commences. In this analysis, during the piercing process of the drainage hole for a shock absorber seat, there is visible material tearing (on the neck) which as a result the component is rejected. This results in material wastage, and prolonged cycle time since the operation has to be now done separately at a different workstation.

The initial phase of the simulation is to duplicate the current tearing in the production phase of the piercing process with the harder material (TM380), and the second phase is to eliminate the tearing by using a softer material (HR190) with different punch design and material data input. Several punch design have be designed and were simulated. By closely matching the simulation and the actual physical behaviour we can then make further recommendation for the piercing process and further improvements to the finite element simulation of such processes. Real values where used in the simulations, to make the results as accurate as possible. The FEA focuses on the behaviour of the blank material as a result of the punching load to produce the drainage holes. Different factor like work hardening, strain hardening play an influencing role since the piercing forms part of a progressive operation. The die and punch behaviour did not form part of this analysis.

The continuum model and Smooth Particle Hydrodynamics (SPH) setup were used in the simulations setup. In the continuum model, solid elements were used in the blank material definition. Since the piercing required involves material removal over a thickness, a tetrahedron mesh was used. Special failure criterions were used in the defining element deletion upon reaching specified strain level.

Using SPH improved the results dramatically by allowing the blank material to be defined in terms of particles rather than mesh. The particles are defined with a mass and cohesion distance is set between interacting particles. When the distance between particles is more than the critical distance, specified, then each particle no longer contributes to the strain calculated at the other and the corresponding cohesive component of the stress disappears. Hence failure of material occurs.

The simulations were conducted in an iterative process, starting with the harder material (TM380) and the softer material (HR190). Such an approach was geared towards modelling of material failure, either in form of material separations, or any material causing effects, e.g. stress raisers, abnormal burrs, excessive material stretching, etc. and then modelling of the improved material.

ACKNOWLEDGEMENTS

The author would like to thank Prof. Graeme Oliver for the supervision and guidance for the duration of this research. Your commitment to making this research paper a success is greatly appreciated.

The author would also like to thank Precision Press Pty (Ltd), for being an industrial research partner. This is also to thank Barend Burger for the assistance in defining the problem situation and for providing relevant information, guidance and advice.

The author would like to thank Peter Vogel and Zafer Celik at the DYNAMORE GmbH, Germany for the constant technical support and advice for the duration of the research.

Great thanks to the Institute for Advanced Tooling for making the available the infrastructure that made the research more smooth and possible.

I would like to thank my Pastors at the Restoration Life Ministry (RLM) in Cape Town. Your constant guidance and care made me believe indeed that I can do all things. The special bond we share has carried me during confusing times, your prayers where the oil in my wheels during dry times.

Most importantly I would like to thank my father for believing in me, for the inspirations from the sitting room, to the regular coaching and directive. Thanks for encouraging me to think ‘big’ and for all the support during my lowly days. You are magnificent.

Greatest thanks to Thando Ntshangase who inspired me to study towards the Masters research in the beginning. Many thanks also to my closest friends, Cullen, Chipanga, Patrick, Ayodele, and The Counsel, your encouragement was relevant and top quality.

The financial assistance of Cape Peninsula University of Technology towards this research is acknowledged. Opinions expressed in this thesis and the conclusions arrived at, are those of the author, and are not necessarily to be attributed to the Cape Peninsula University of Technology.

TABLE OF CONTENTS

TABLE OF FIGURES

TABLE OF TABLES

1 INTRODUCTION

Tooling forms a very important part to the contribution towards the gross domestic product of any country, and a country with a good tooling capacity stands a good chance for economic survival. According to the FRIDGE (Fund for Research into Industrial Development Growth and Equity) studies [1], conducted by the Department of Trade and Industry (DTI), the packaging and the automotive industries represent 90% of the local Tool Design and Manufacturing (TDM), which was valued at R3.3 Billion in South Africa in 2004.

The term tooling refers to any injection moulding, press tooling, jigs and fixtures, casting dies, etc [2]. Tooling often fails, and some reasons for failure can be as a result of wear and tear, fatigue, with fracture as the most dominant one. Some failures (however) are just a mere result of negligence during assembly or operation. This is often detrimental to production companies since it's often unplanned and unexpected. This consequently affects production, increases downtime, unplanned maintenance, and cost companies high monetary value.

Manufacturing defects and operating errors and play a major role in tool service life. Tool life reduction originates from the heat treatment process due to its large significance in altering the properties of the tool material. Heat treatment in press tools problems are mostly attributable to a lack in structural toughness, resulting in premature failure in the form of tool breakage/fracturing.

2 PURPOSE OF RESEARCH

The aim of this study is to analyze the failure that happens during the piercing of a shock absorber seat drainage hole (see Figure 2.1 for a shock absorber seat). This will be done by means of simulating the process with a Finite Element Analysis (FEA) package. Currently the piercing process, which forms part of a progressive tool, has a failure rate of 70% as a result of the tearing near valve seat neck. This is due to the high stresses subjected over the small distance between the drainage hole and the valve seat neck.

This research aims (also) to provide suggestions to tooling design optimizations and strategies to eliminate such tearing defects. Such capabilities also should form a good platform for suggestions of improved tool designing concepts and approaches to tool designer/tool makers and decision makers.

This research also aims to developing the capability of simulating such process in FEA for the local tooling industry in order to better predict the behaviour of the material. As a result better design strategies can be used, before any manufacturing can begin. Such approaches will minimise the amount of time spent during tool try-out and reduces the amount of prototypes required tool qualification.

Figure 2.1: Shock absorber seat

3 SCOPE OF RESEARCH

This study will focus on the modelling of the tearing during the piercing process, rather than performance of the progressive tool as a whole. Thus, no modelling or analysis of the pre-piercing processes (e.g. forming, trimming, etc) will be done, even though such stages of the process are critical to the piercing quality being simulated.

The simulation also assumes that no deformation will take place on neither the punch nor the die. This engineering approach assumes that the die-face deformations (also) during the piercing process are negligible and the industrial practice has proved the validity of this assumption. This notion of an ideally rigid die construction may nevertheless be questionable when it comes to the punching/forming of high strength steel due to higher forming loads.

The fracture modelling of the process will be limited to the tearing as defined by the failure criterion. No specific fracture model will be used. The failure criterion is such that when an element reaches a certain strain limit, it is deleted from the system. This could result in cumulative errors, as the elimination of elements from the system has an effect on the energy balance during the simulation.

4 PIERCING

4.1 INTRODUCTION

The technology of sheet-metal presswork emerged with the development of the steel industry, and to a large degree we owe our present standard of living to the production of stamped metal parts. The numerically controlled machine tool is an important contribution. Press machines and press tools are considered as a backbone of a modern machine shop of large industry set up producing a wide variety of articles such as vehicle bodies, electrical accessories, etc. Large number of metal components can be produced in a short time with the help of press tools without removal in the form of chips [2].

Press tool designers have to make proper selection of the type of press to be used and also the kind of press tools to be provided. The critical press information that must be taken into consideration is the press tonnage, press stroke, shut height and the die space [32]. The types of presses available for metal cutting and forming operations are varied depending upon the type of operation. These are classified by these (but not limited to):

4.2 PRESS CLASSIFICATION

TYPE OF FRAME

The frame of the press is fabricated by casting or by welding heavy plates. Cast frames are quite stable and rigid, but expensive. The general classification by frame includes the gap frame and straight side. This gap frame is cut below the ram to form the shape of the letter C.

This allows feeding of raw material (strip) from the side. Some gap-frame presses have an open back to permit strip feeding from front to back or ejection of finished

parts out of the back. Cast frame construction also has the advantage of placing mass of material where it's needed most. Welded frames are generally less expensive and are more resistant to shock loading because of greater toughness of the steel.

SOURCE OF POWER

The great majority of presses receive their power mechanically or hydraulically. A few manually operated presses are hand-operated through levers or screws, but are hardly suited for high production. Mechanical presses use a fly-wheel driven system to obtain ram movement. The heavy flywheel absorbs energy from the motor continuously and delivered its stored energy to the workpiece intermittently. The motor returns the flywheel to operating speed between strokes.

Hydraulic presses have a large cylinder and piston, coupled to a hydraulic pump. The piston and ram is one unit. The tonnage capacity depends upon the cross section of the piston (or pistons) and the pressure developed by the pump. The cylinder is double acting in order to move the ram in either direction. The advantage of a hydraulic press is that it can exert its full tonnage at any position of the ram stroke. In addition the stroke can be varied to any length within the limits of the hydraulic travel.

METHOD OF ACTUATION OF SLIDES

The flywheel of the press drives the main shaft, which in turns changes the rotary motion of the flywheel into linear motion of the slide of the ram. This is generally accomplished by incorporating crankpins or eccentrics into the main drive shaft. The most common driving device is the crankshaft, although many newer presses use the eccentric for ram movement. The main advantage of the eccentric is that it offers more surface area for bearing support for the pitman, and the disadvantages is its limitation on the length of the stroke. In addition to eccentrics and crankpins, slides can also be actuated by cams, toggles, rack and pinions, screws, and knuckles.

NUMBER OF SLIDES INCORPORATED

The number of slides incorporated in a single press is called the action i.e. the number of rams or slides on the press. Thus a single action has got one slide. A double action has two slides, an inner and an outer slide. This type of press is generally used for drawing operations during which the outer slide carries the black holder and the inners slide carries the punch. A triple action press is the same as a double-action with the addition of a third ram, located in the press bed, which moves upward in the bed soon after the other two rams descend [32].

The piercing process uses a 702 hydraulic press machines (Figure 4.1). Below are the press specifications (table 4.1 for Press machine specification).

Variable	Specification
Table size	1.110 – 1.070 mm
T Slot width	21 mm Top (Ram) – 16 mm Bottom (Machine bed)
Distances between T slots centres	230 mm Top (Ram) - 212 mm Bottom (Machine bed)
Stroke	200 mm
Minimum shut height	230 mm
Press speed	50 strokes/min

Table 4.1: Press machine specifications

Figure 4.1: 702 Press machine

5 PIERCING PROCESS

Tool design is a specialized phase of tool engineering. While there are many die-cutting operation, some of which are very complex, they can all be reduce to plain blanking , piercing, lancing, cutting off and parting, notching, shaving and trimming, etc. The design of the die block depends mainly on the workpiece size and thickness. The design of the punches largely is influenced by the area to be pierced and the pressure required penetrating the workpiece. The area to be pierced determines the method to penetrate the method of holding the punch.

The cutting action that occurs in the piercing is quite similar to that of the chip formation ahead of a cutting tool. The punch contact the material supported by the die and a pressure builds up occurs, When the elastic limit of the work material is the exceeded the material begins to flow plastically (plastic deformation).

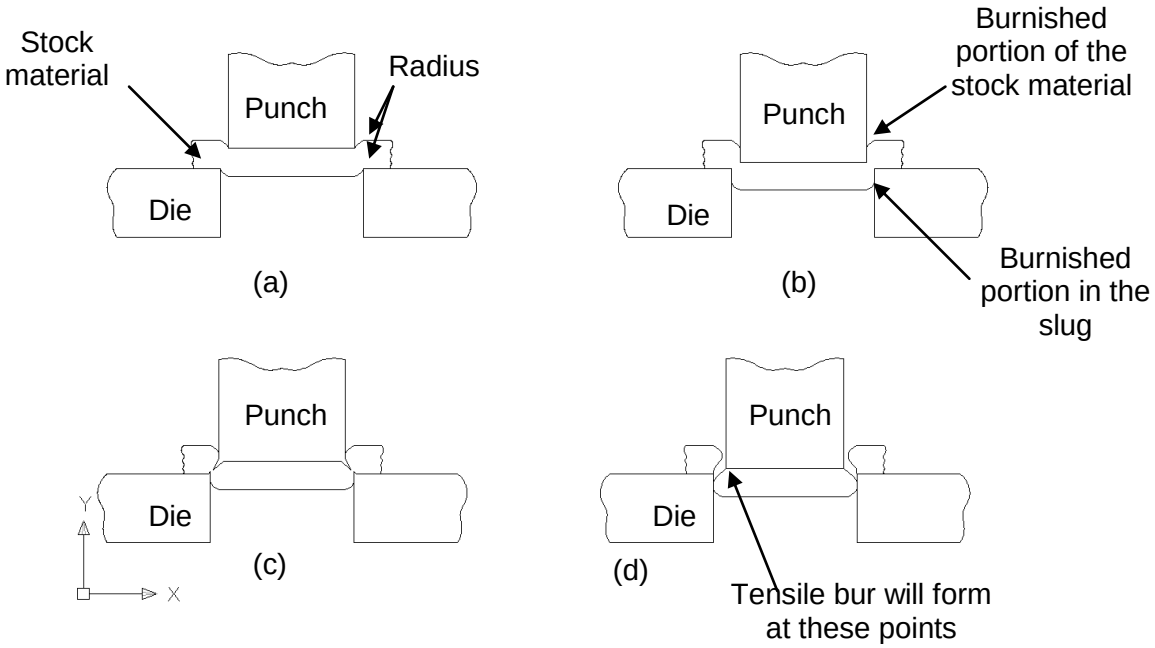

Figure 5.1: Cutting-action progression when blanking or piercing metal
(Adapted from Donaldson, 1976:651)

It is often impractical to pierce holes while forming, or before forming because they would become distorted in the forming operation [33]. The punch penetrates the work material, and the slug/blank is displaced in the die opening a corresponding amount. In such cases they are piercing in a piercing die after forming. During the piercing process the punch penetrated the work material and the blank, often referred to as the slug, and is displaced into the die opening.

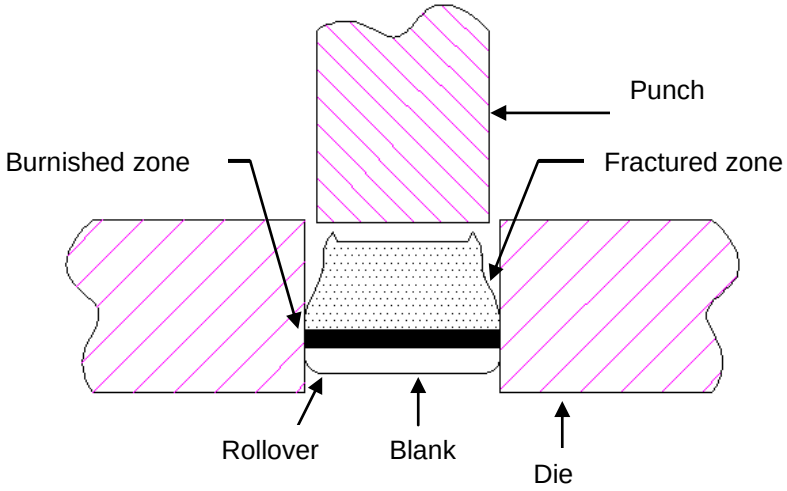

Figure 5.2: Characteristic appearance of the cutting edges
(Adapted from Donaldson, 1976:652)

Upon observation of the cutting surface, a radius formed on the top edge of the hole and the bottom edge of the blank (See Figure 5.1: Cutting-action progression when blanking or piercing metal). This radius is often referred to as the rollover and its magnitude is dependant on the ductility of the material. Compression of the blank against the walls of the die opening burnishes a portion of the edge [32]. Further continuation of the punching pressure then starts the fracture at the cutting edge of the punch and die. For good quality piercing, a clearance between the die and punch should always be assigned (see Figure 5.2 above for a characteristic appearance of the cutting edges). Angular clearance is also assigned to prevent the back pressure caused by the blank build-up especially when the punches or die block are fragile. Recommended angular clearance is caries from 0.25^0 to 2^0 per side.

6 LITERATURE STUDIES

Research and development on tooling optimization has been done in the past, [9, 13, 30, and 31]. The vast majority of work was done on cold forging dies and die casting dies. Limited research and development has been done on press tooling, injection moulds, jigs and fixtures. The tearing during the piercing process can also be highly influence by the physical properties of the punch and the die. Residual stresses in the influence highly on the die life. . These are stresses that are inside or locked into a component or assembly of parts. Residual stresses can accumulate at different phase of the tools manufacture, viz machining, grinding, heat treatment, etc. [4, 10]. Common examples of these are bending, rolling or forging, or thermal stresses induced when welding, esp. in jigs, fixtures, and castings. These stresses can be sufficient to cause a metal part to suddenly split into two or more pieces after it has been resting on a table or floor without external load being applied.

Cracks contribute to a majority of failures in steels components, particularly those that are subjected to cyclic loading, fluctuating stresses, etc. Cracks are more likely to occur in areas where stress concentration is present (e.g. holes, notches, corners, etc), slip beginnings, corrosion, material degradation, etc. Cracks normally occur in brittle steels, (brittleness as a result of heat treatment) where the application of repeated loads or a combination (cyclic and thermal) of loads is applied. Griffith Criterion is a common method that is used for failure of any structure with initial cracks. Griffith proposed the principle of energy balance between the strain energy lost in propagation of a crack and the surface energy of newly created fracture surfaces [11].

According to I. Jung [10], heat treatment contributes to most premature failures of tools with major causes being quench stress cracking, retained austenite and grain boundary carbides. Quench stress cracking is a stress relieving phenomenon produced by high thermal and transformation stresses, usually during quenching from hardening temperature. It is facilitated by unfavourable tool geometry, such as uneven mass distribution with pronounced differences in cross section, the notch effect of sharp edge radii, etc. Grain boundary carbides occur when heat treated structure consists of inadequately tempered martensite which additionally exhibits carbide banding along the grain boundaries.

Retained austenite phenomenon also plays a major role. This is when elevated austenite remains in the steel during cooling from hardening. The presence of retained austenite normally results in tool breakage after very short service periods and is currently one of the main failures caused in tools made of cold work and high speed steels with carbon concentration exceeding 0.8% by weight [10]. The effects of this retained austenite range from reduction of hardness of steel, which would affect the fatigue life, increase the brittleness of steels, volume expansion resulting in linear expansion, etc. Cold treatment, plastic deformation and tempering are normally used for the elimination of this state.

Several researches have already been conducted in the sheet metal forming optimisation process with few on the piercing process. This is because the piercing process involves the removal of the material in a continuum space and hence a dedicated software and attention to simulation setup required. The removal of the solid elements also makes the simulation unstable. A similar simulation research [15] was done on the air bending of a high strength steel using LS DYNA. The research presented a model for simulation of material behaviour of Ultra High Strength Steel. The bending simulation was conducted for different plate thickness over different die gaps (longitudinally and transversely).

Because of the high anisotropic behaviour of the studied steel, a special material in LS DYNA (Mat 37) was used for definition of thick elements. The model setup included punches, dies and blanks. The blank used an elasto-plastic material model for behaviour definition with shell and solid elements for mesh definition.

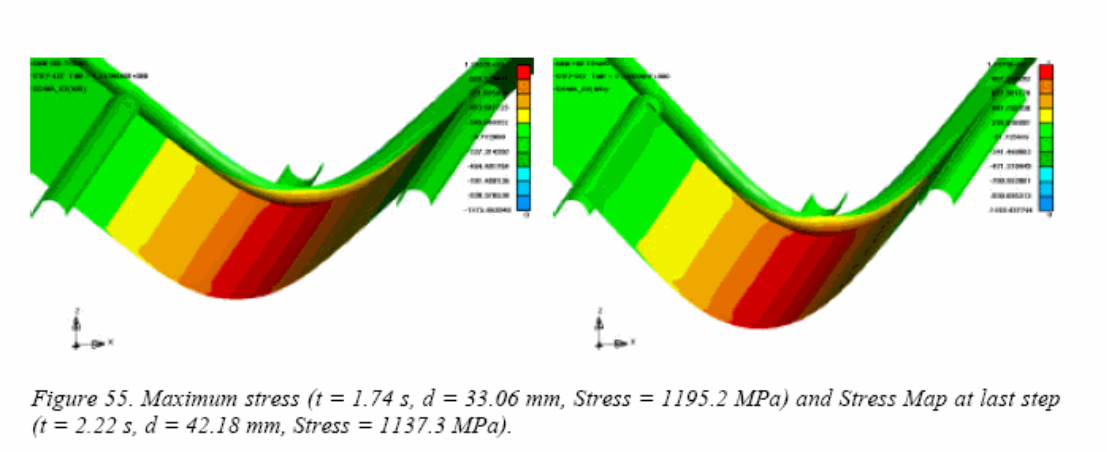

Figure 55. Maximum stress (t = 1.74 s, d = 33.06 mm, Stress = 1195.2 MPa) and Stress Map at last step (t = 2.22 s, d = 42.18 mm, Stress = 1137.3 MPa).

Figure 6.1: Simulation results for 6mm thickness with 106 die gap transversally
(Adapted from Satorres, 2005:64)

For definition of the solid elements, a special material model (Mat 24) was also used in the definition of solid elements within the simulation. This is a three dimensional elasto-plastic material with an arbitrary stress versus strain curve and arbitrary strain rate dependency can be defined. Also, failure based on a plastic strain or a minimum step size can be defined. This study concluded that the using solid elements yield much more results than using thick shell elements. (See figure 6.1 for results on a simulation for 6mm thickness with 106 die gap transversally). Thick elements are highly depended on mesh configuration and are susceptible to errors if not define properly. This also is highly depended on the software capability. This model was used as benchmark for the piercing simulation.

A similar study conducted by Anders Jenberg [16] also was presented at a 4th European LS DYNA user's conference for formulating a method for modifying the tool geometry to compensate for springback effects during the forming process. This paper proposes that the only way to get the required geometry for sheet metal process is to have a punch that is different to the desired final shape geometry. This could be done by of means an iterative method called the Heuristic methods. Using this method, the results from one forming simulation and one on spring back simulation gives input on how to proceed in the next simulation (See Figure 6.2 for a deviation and punch setup iterative step). This is probably what is happening in the metal workshops during too try-out. Such approaches eliminate the number of prototypes required and the amount of time spent in getting the final geometry.

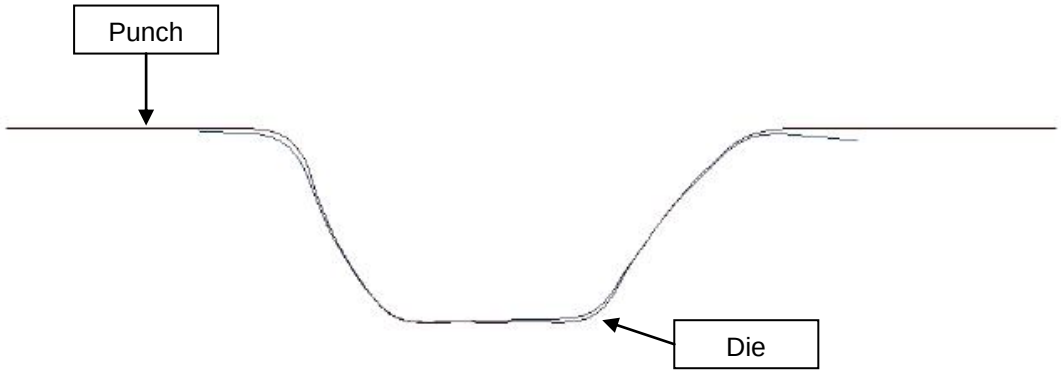

Figure 6.2: Deviation between punch and die before final iterations
(Adapted from Jenberg, 2003:8)

There are few similarities between the simulation of springback for tooling geometry modification (as shown above) and the piercing process, as there is little consideration for springback. The study does however give an indication of the capabilities and diversity of LS DYNA in handling complex calculation. Such forms a good basis for this piercing process.

Failure prediction in such simulation is quite critical and proper configuration is vital as it can hugely affect the results. These simulation dependants can vary, from mesh size, punch velocity, strain rates effects, etc. This failure can usually be determine by using a Forming Limit Diagram (FLD). An FLD is a useful tool in sheet metal manufacturing analysis (see Figure 6.3 for an example of an FLD). This curve shows the critical combinations of major strain and minor strain in the sheet surface at the onset of necking failure. Both experimental and numerical results in the literature have shown that the level of the FLD is strongly strain path dependent and the prediction of FLD depends on the shape of the initial yield function and its evolution [43].

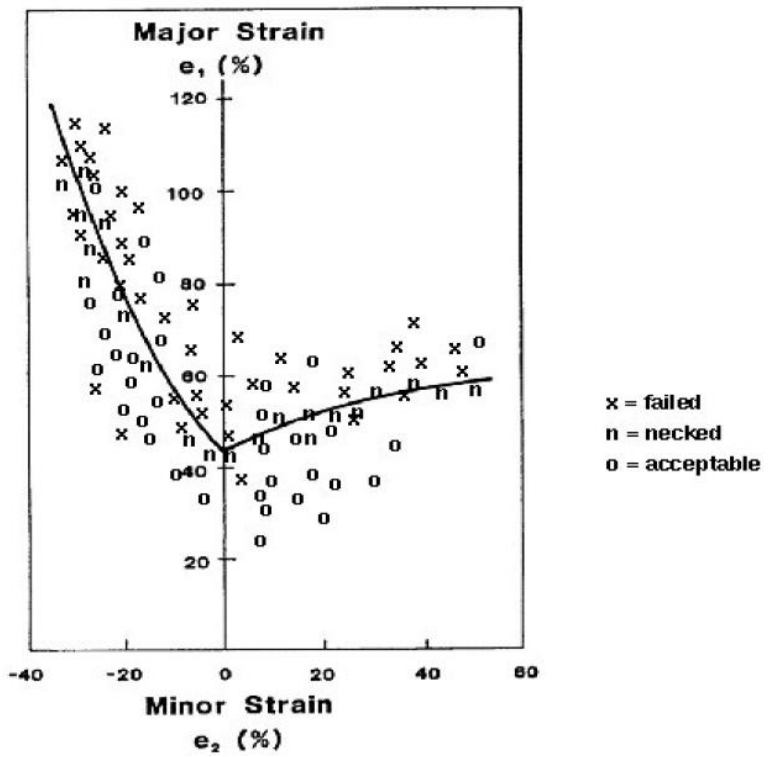

Figure 6.3: Forming Limit Diagram for sheet metal forming simulation
(Adapted from DYNAFORM training manual 2007:87)

In the FLD, any strains levels above the curve will cause failure in the manufacturing and the strain below the curve would probably fine for manufacturing. If a forming limit diagram has been determined for a particular alloy and gauge, then it can be used in conjunction with finite element models to evaluate the likelihood of splitting in a given forming operation.

Gernot. O, et al [18], conducted a study using FLD and concluded that the FLD has limitation, since it is only valid for linear straight paths. The FLC cannot be used in a complex nonlinear history of a deep drawing or a successive stamp and crash process which includes a significant change in strain rates. It is recommended that the LS DYNA be coupled with an algorithm (in this case CRACH). This software was developed to enhance the failure prediction of forming limit of sheets for non linear straight paths. In this case, a the coupling was done through material interface. Strain and incremental tensor are transferred to a submodule for filtering the input data used in the algorithm CRACH.

The coupling of LS DYNA with CRACH showed the potential to predict potential fracture in deep drawing and crash loading in early design stage and allowed to optimise geometry and material quality to significantly reduce later problems in real components.

For non-solid solid elements simulation, the time can be drastically increased. To reduce this, mass scaling and adaptive meshing is employed. Since volume mesh can considerably be a time consumption task, mass scaling and adaptive meshing was assigned also. Mass-scaling refers to a technique whereby non-physical mass is added to a structure in order to achieve a larger explicit timestep. Mass scaling therefore reduces the CPU cost (time) and improve the performance. Mass scaling is also recommended to be used when performing explicit analysis.

Adaptive meshing (other well know as look “ahead meshing”) helps you improve a mesh by moving nodes, splitting elements, or remeshing the model, this is done by the software to reduce elemental distortion or refine a mesh in areas where error estimates are highest. The software derives the new mesh by analyzing the data variation along the boundaries and within the interior regions of the faces. During adaptive meshing, the software may encounter singularities in your model. A singularity represents infinite stresses that theoretically occur at singular points, sharp corners, or geometric discontinuities.

To account for singularities, adaptive meshing slows down the refinement of the meshing in these areas. The software averages the mesh weight of the points surrounding a singularity, instead of deriving the weight at the site of the singularity. The software attempts to refine the mesh adequately near the singularities and satisfy the specified energy error norm. At the site of a singularity, infinite mesh refinement is required for convergence. Here the software attempts to avoid the extremely fine levels of mesh refinement occurring at a singularity. Although you can run adaptive meshing as many times as you need to smooth a mesh and/or generate more elements, you must also consider factors such as computer run times, resources, and input time. With some models, you could run adaptive meshing many times to find an infinite solution at an artificial, singular point. Though each run may yield a finer mesh, it's rarely practical to go beyond two or three runs. A document, Input Parameters for Metal Forming Simulation using LS-DYNA [19], drafted by the Livermore Software outlines the procedure on how to setup the simulation for efficient and accurate results without maxing the computer run times.

S.W. Lee, M.S. Joun [17] conducted a study on the finite element analysis of the piercing process in the automatic simulation of multi-stage forging processes. In this study, it was assumed that the fracture in piercing takes place at the instant when the maximum accumulated damage around the shearing region reaches the critical damage value of the material and that separation is made along the line connecting the two die edges. A tensile test experiment was conduct at a speed of 0.5 mm/s (tensile test machine cross head velocity) in order to find the correct damage value to be input in the simulation. The critical damage value was obtained from correlation of a tensile test and its computer simulation.

The comparison of predictions with experiments in pierced shape and forming load variation verified the validity of the approach in a quantitative manner. This damage value approach has emphasis on the effect of the strain hardening exponent on the critical damage value. The approach was verified by a test piercing process with a medium-carbon steel and is applied successfully to the automatic simulation of a sequence of six-stage compound forging processes. From the application and simulation results, it was assumed that fracture during piercing takes place when the accumulated damage value reaches the critical damage value at any element around the shearing region and that the line connecting the two die edges is the separation line of the fracture. The approach was successfully applied to the automatic simulation of a sequence of the compound forging process.

M.j. Ward et al [44] also conducted a study on the Simulation of a multi-stage railway wheel and tyre forming process using DEFORM™-2D metal forming program. The objective of the simulation was to determine whether alternative pre-form configurations of material and tooling could result in a final component with superior geometrical and physical properties .This simulation covered the all the stages, including heat loss between forming operations in the thermo-mechanical simulation. Piercing was modelled by the fracture capability of the code, employing the Cockcroft and Latham damage criteria.

$$C = \int_0^{\varepsilon_f} \left(\frac{\sigma^*}{\bar{\sigma}} \right) d\varepsilon \qquad (1)$$

Where: C is the normalised Cockcroft and Latham fracture criterion

: ε_f is the fracture strain

: σ^* is the peak stress level

The piercing simulation was also axisymmetric and was based on a damage criterion based element-deletion method. This method involves comparing some measure of cumulative damage in each element with a fracture criterion. Any element for which the accumulated damage is greater than the fracture criterion is deleted. The trail of deleted elements simulates the effect of crack propagation. A C = 0.89 was used in the simulation. During the piercing process of such a process, angles of less than 8° resulted in the workpiece sticking to the tooling after forging. Therefore, only angles greater than this were considered. (See Figure 6.4 showing the simulation with different simulation bore angles).

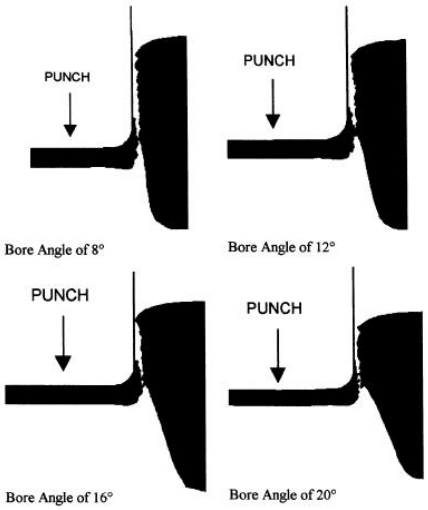

Figure 6.4: Piercing simulation with different bore angles.
(Adapted from Ward, 1998:211)

Such finite element simulation can aid the tool designer in achieving appropriate tool configurations without the need to perform time consuming and expensive physical trials.

Smooth Particle Hydrodynamics (SPH) is another computational method that has been used in similar simulations. This is a mesh-free Lagrangian method (where the co-ordinates move with the fluid), and the resolution of the method can easily be adjusted with respect to variables such as the density [14]. The method was developed to avoid mesh tangling encountered in extreme deformation within the finite element method. The main difference between the classic method and SPH is the absence of a grid. Therefore the particles are a computational framework of which the calculations are based [LS DYNA Theory Manual]. The method is mostly used for modelling complex simulations .e.g. blast loading, hypervelocity impacts, ballistic penetration, etc. Consider the material model in Figure 6.5 (below) where different particles as Define in SPH.

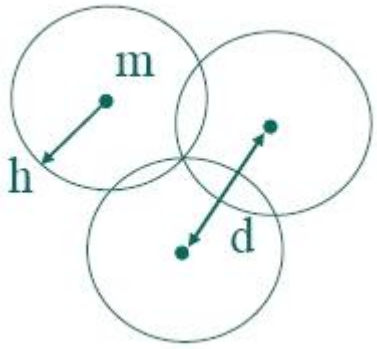

Figure 6.5: Material model for SPH

Where m: mass of particle

h: smoothing length

d: distance between particles

Particle methods are based on the quadrature formulas on moving particle $(x_t(t), w_t(t))_{t\in P}$. P is the set of particles, $x_t(t)$ is the location of particle i

and is the $w_t(t)$ weight of the particle. The particles are moved along the characteristic curves of the field v and also modify the weights with the divergence of the flow to conserve the volume [46]. Where:

$$\frac{d}{dt}x_t = v(x_t, t) \tag{1}$$

$$\frac{d}{dt}w_t = div(v(x_t, t))w_t \tag{2}$$

Each particle interacts with all other particles that are within a given distance (usually assumed to be) from it, that distance is addressed as smoothing length. The interaction is weighted by the function which is called the smoothing (or kernel) function. To define the smoothing kernel, first an auxiliary function θ is introduced. The most useful function in the SPH community is the cubic B-spline which has the good properties of regularity. It is defined by:

$$\theta(d) = C \times \begin{cases} 1 - \frac{3}{2}d^2 + \frac{3}{4}d^3 & \text{si} \quad 0 \le /\text{d}/ \le 1 \\ \frac{1}{4}(2-d)^3 & si \quad 1 \le /d/ \le 2 \\ 0 \quad \text{elsewhere} \end{cases} \tag{3}$$

Where C is the normalisation that depends on space dimension [49].

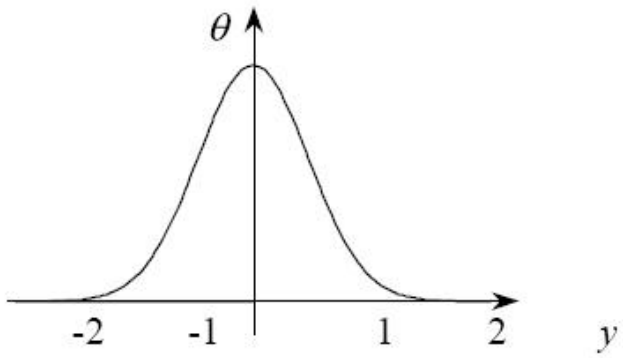

We have then enough elements to define the smoothing kernel W:

$$W(d,h) = \frac{1}{h^{\alpha}(x,y)}\theta\left(\frac{d}{h(x,y)}\right) \qquad (4)$$

FAILURE CRITERION USING SPH

It is not mandatory to define particular failure criterion (maximum plastic strain or maximum stress) in SPH calculations. Here the kinematics of material separation are accommodated in a manner that neither involves the loss of material, requires foreknowledge of the locus of separation, nor requires special numerical treatment. Material damage is incorporated at SPH nodes through a loss of cohesion as neighbouring SPH particles separate from each other. When the distance between particles is more than the critical distance, h, then each particle no longer contributes to the strain calculated at the other and the corresponding cohesive component of the stress disappears. Hence failure of material occurs.

BOUNDARY CONDITIONS

As SPH mainly deals with the particles, to control the motion of each particle "SPC NODES" (single point constraint on nodes) is applied. Nodal displacements in direction can be constrained using "SPC NODES".

CONTACT MODELLING

For modelling contact between work-piece and tool *CONTACT AUTOMATIC NODES TO SURFACE is used, wherein work-piece is modelled by SPH nodes (slave part) and tool (master part) is modelled by Lagrangian elements [50].

CRITICAL PARAMETERS

*CONTROL_SPH: Which defines the general control parameters needed for the calculation.

*SECTION_SPH: This defines parameters for every part of SPH particles.

*ELEMENT_SPH: This defines every particles, assigns its part ID and mass.

Murat Buyuk et al [35] conducted a study to find out which is the most suited analysis method for ballistic impact. A comparison between the Lagrangian, Eulerian, ALE (Arbitrary Lagrangian - Algerian) and SPH was conducted. This is necessary because in a numerical model of a continuum, the material is discretisized into finite sections. The way in which discretisation takes place leads to different numerical methods to be used.

In Lagrangian solver, the numerical mesh moves and distort with the physical material. This material is widely used because of its advantage, such as being able to track accurately and efficiently material interfaces and incorporates complex material models. In Eulerian solver, the numerical mesh is fixed in space and the physical material flows through the mesh. This formulation is generally used to represent fluids and gases. In the ALE solver, solver allows for “automatic rezoning”, which can be quite useful for certain problems. Depending on the specified motion, the ALE can be completely Lagrangian, completely Eulerian or something in-between.

The Naval Explosive Ordnance Disposal technology division [20] conducted an impact experiment using SPH. This was study the simulation of the process of perforating plates with projectiles at high velocity. The target plates included 3 plate thicknesses 3, 6, 12 mm or three materials (A36 Steel, 6061 – T65 Aluminium, and C6200 Brass). The projectiles were of different types also (0.5 Caliber, PAN Steel, PAN Aluminium slug). The nominal normal projectile data included: pre and post impact projectile speed and orientation, post- test deformed projectile, plate deformed profiles, plate plug masses for perforated plates, flash X ray images and post – test photographic documentation.

The plate impact simulations were performed independent of the and without knowledge of the experimental results. Two constitutive models were used in the plate impact simulation, the Johnson Cook method for the target plate and associated Equation of state and a simple Von Mises stress for the projectile. Overall the model simulation was successful, however a trend was noticed that under predict the measured residual projectile velocity as the projectile became more deformed. (See Figure 6.5 below for the simulation results).

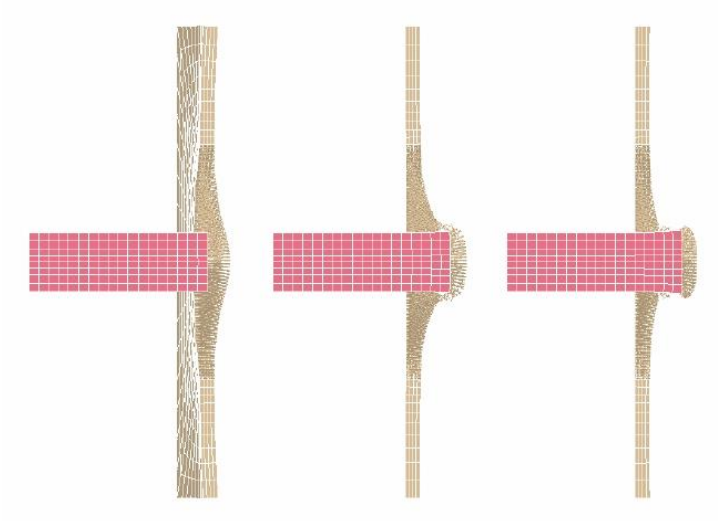

Figure 6.5: Deformation of a 6mm plate with a 0.5 Caliber projectile
(Adapted from Schwer, 2006:8)

The high handiness of SPH allows the resolution of many problems that are hardly reproducible with classical methods. Dominic Lacerda, et al [22], conducted a research of an aluminium sphere impacting an aluminium plate at 6.64 km/s and a steel sphere impacting an aluminium plate at 5.53 km/s using SPH. Few experimental features are available for such velocities. These simulations can be

used to understand the events. The two simulations of hypervelocity impacts were compared with experimental results.

Experimental and numerical results are in good agreement. The difference between results is around 10%. SPH method is able to reproduce the global shape of the debris cloud and to predict the resultant velocity. The results could be improved with more particles using a 2D axi-symmetric model. (See Figure 6.6 below for results comparison between the experiment and SPH). Such abilities to simulate complex large deformation can also results in high computation time also. According to Gregg Skinner and Dennis Lam [21], major performance issues can be encountered using SPH if proper care has not being in vectorizing all related subroutines, even though using supercomputers.

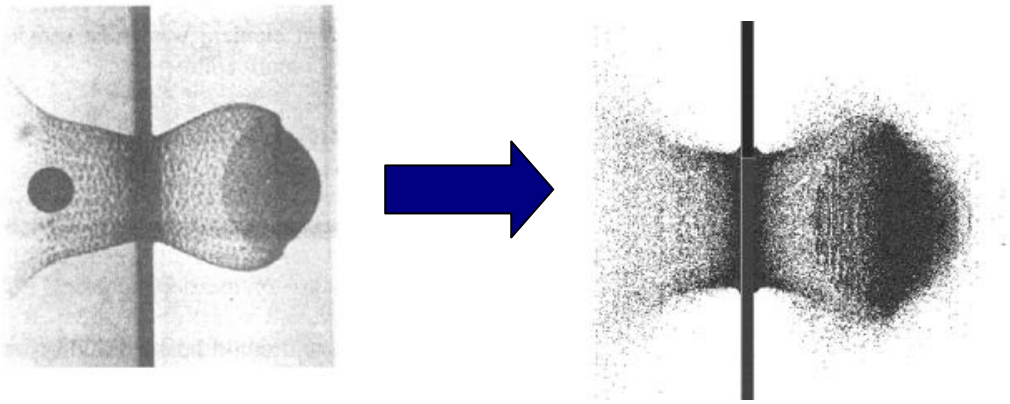

(a) *(b)*

Figure 6.6: Debris Cloud from experiment and Debris cloud with SPH (**Adapted from Larceda)**

A study conducted by Ambati R. [50] was used as the base and benchmark for these simulations in this research. In this research, two techniques, i.e. adaptive remeshing and smoothed particle hydrodynamics are were implemented to simulate high speed machining processes like cutting and drilling with LS-DYNA. Along with cutting and drilling processes using LS-DYNA, structural analysis of hole and drill tool, coupled with transient thermal analysis using ANSYS were also performed

During the high speed cutting, characteristics of metal under high speed metal cutting are defined mainly based on high deformations in the work piece. Large deformations are imposed on the work-piece material at high speed in a very small area. In the initially stage, stress in chip reaches maximum normal stress, the chip weakened locally and thus removed from the work-piece as segments. Two maximum criteria were used, maximum stress and maximum stress at failure.

As cutting and drilling are highly deformable processes large plastic strains occurs due to high deformations in the elements. Severe distortion in the elements can be controlled by adaptive meshing since the simulation is 2D (adaptive meshing cannot be implemented in 3D solid elements). The study concluded that using a single point cutting tool the cutting force varies with different rake angles used. The study also concluded that with the variation of friction coefficients, cutting force varies proportionally. From Figure 6.7 below, during cutting action, Von-Mises stresses are very high at primary shear zone compared to secondary and tertiary shear zones. In tertiary shear zone, residual stresses developed due to plastic deformation are reformulated with remeshing thus resulting in diminishment of residual stresses.

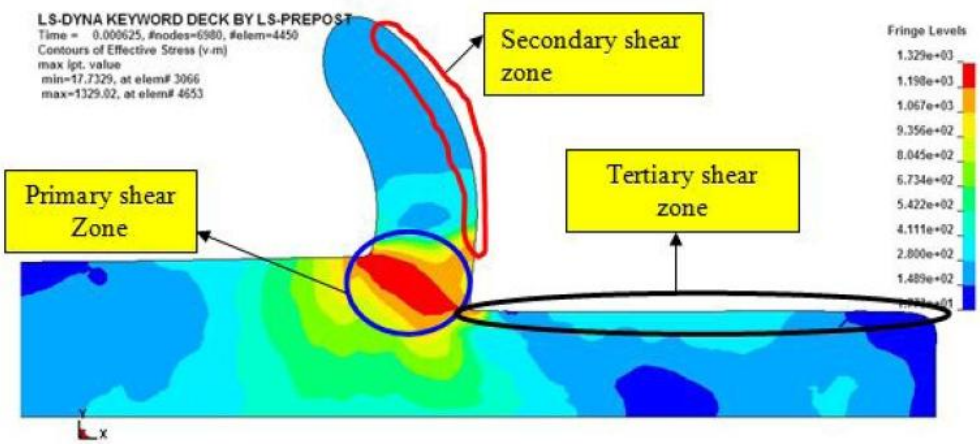

Figure 6.7: Von Mises stresses distribution in 2D during cutting
(**Adapted from Ambati)**

The simulations were also done in 3D using SPH. Here material properties are calculated at discrete set of disordered points called SPH particles, this avoids problems associated with mesh tangling and high strains which usually occurs in Lagrangian analysis. In SPH, Material damage is incorporated at SPH nodes through a loss of cohesion as neighbouring SPH particles separate from each other.

In this simulation, a good cutting force approximation was achieved. The cutting forces were compared to the cutting force using adaptive meshing and experiment. The cutting forces required dropped and were at similar level and behaviour as the experimental results. SPH also allowed the analysis of important factors nature of chip flow, which is high dependant on tool velocity, tool geometry and feed. The results also concluded that chip segmentation depends on the cutting velocities. With increase in cutting velocity, segmentation of chip occurs more frequently. See Figure 6.7 for a step by step illustration of the Von Mises distribution during cutting in 2D using SPH.

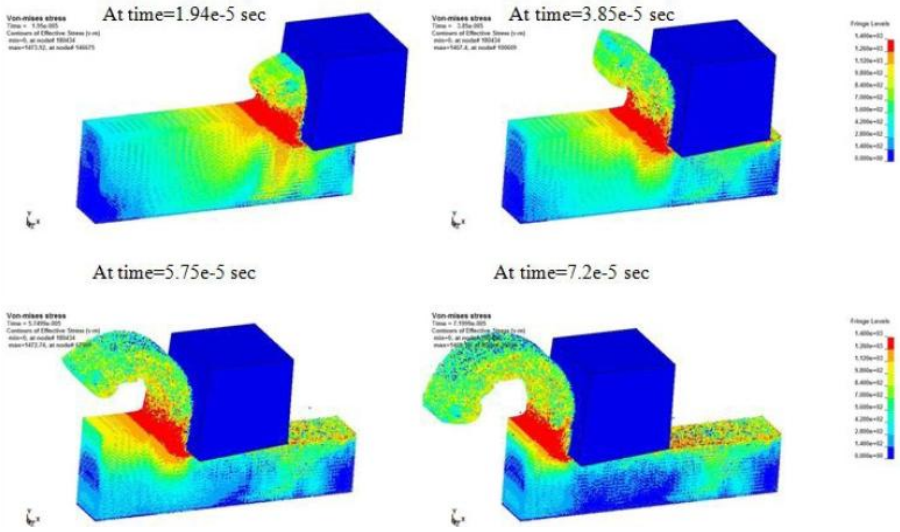

Figure 6.8: Von Mises stresses distribution in 3D using SPH
(Adapted from Ambati)

SPH was also used in the simulation of drilling using 3D. The work-piece was modelled using "Johnson Cook" material model as that of in 2D and 3D cutting simulations. The material model will show the dependency of flow stress on strain rates and temperatures which are near to the realistic conditions. The tool is set to be the master object and the work-piece is the slave object, meaning that the work-piece will deform according to the tool movement.

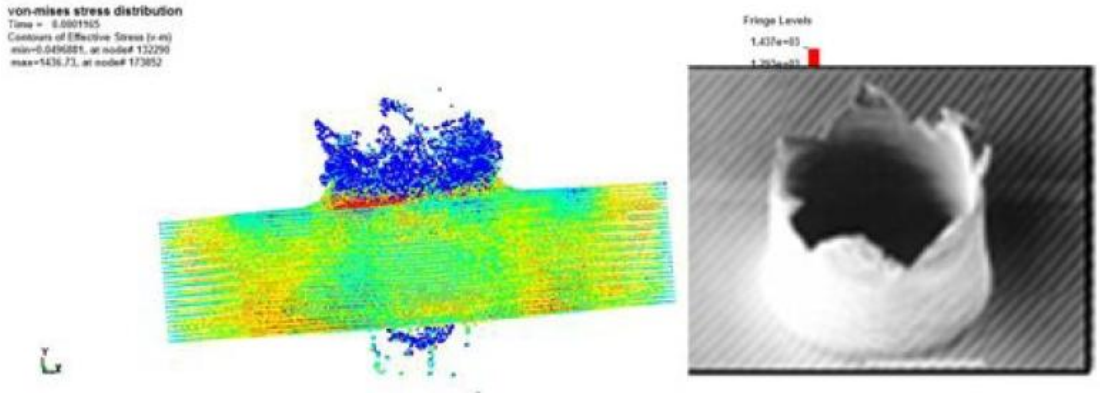

Figure 6.9: Von Mises stresses distribution during cutting
(Adapted from Ambati)

Blue particles in Figure 6.9 above are due to the material flowing up as a form of chip. Burr minimization, however still needs to be improved.

7 SUPRAFORM AND ITS CHARACTERISTICS

The FEA focuses on the behaviour of the blank material as a result of the punching load to produce the drainage holes. Different factor like work hardening and strain hardening play an influencing role since the piercing forms part of a progressive operation. The punch and die are made from hardened die steel (P20 pre hardened steel). The analysis assumes that the behavioural response of the die and punch is negligible and hence does not form part of this analysis.

7.1 SUPRAFORM®TM

7.1.1 MAIN PROPERTIES

The blank material is a hot rolled high strength low alloy structural steels SUPRAFORM®TM-380. This is archived by reduced pearlite, i.e. low carbon content, which also imparts excellent weldability and toughness to the steel. The high strength is derived from precipitation hardening by micro alloying elements (mainly niobium) and carefully controlling the processing parameters during hot rolling [23].

During steel making, the steel is calcium treated to reduce the sulphur content to very low values and also to effect inclusion shape control. The heat is processed to a high standard of steel cleanliness, which results in excellent notch toughness properties.
Severe forming can readily be carried out on TM 380 due to its superior formability, thus further increasing the steel's versatility. With the need for higher yet stronger structures, effective mass savings can be achieved without the penalty of reduced overall strength by selecting a steel which has a combination of higher tensile and yield strengths and reduced thickness.

Some typical application for this steel are body chassis components for the automotive and truck industry, bumper brackets, engine mounting brackets and wheel centres, crane jibs and booms and wide variety of mining equipment and cold formed sections.

7.1.2 MECHANICAL AND CHEMICAL PROPERTIES

See *Table 7.1* and *Table 7.2* for chemical composition and mechanical properties as stated in the data sheet.

Grade	C	Mn	Si	P	S	Al	Nb
TM 340	0,05	0,50	0,03	0,015	0,005	0,04	0,015
TM 380	0,06	0,65	0,03	0,015	0,005	0,04	0,025
TM 420	0,08	0,85	0,03	0,015	0,005	0,04	0,030
TM 460	0,10	1,25	0,04	0,015	0,005	0,04	0,030
TM 500	0,10	1,50	0,04	0,015	0,005	0,04	0,030

Table 7.1: SUPRAFORM®TM chemical properties (ladle analysis)

The high strength of the SUPRAFORM®TM grades is achieved by grain refinement and precipitation hardening of ferritic microstructure. In order to ensure that the mechanical properties are met, the ferritic grain size is carefully controlled and is finer that ASTM E112 plate No 1, grain size 8.

Grade	Yield strength (MPa)	Minimum tensile strength1 (MPa)	Minimum elongation[2] (%) for thickness t	Minimum elongation[2] (%) for thickness t
			for t≤3.0 mm	*for t≥3.0 mm*
TM 340	340 – 420	400	0.10	1.20
TM 380	380 – 460	450	0.10	1.20
TM 420	420 – 500	490	0.12	1.40
TM 460	460 – 560	530	0.12	1.60
TM 500	500 - 600	560	0.15	1.60

Table 7.2: SUPRAFORM®TM mechanical properties

7.2 SUPRAFORM® HR

7.2.1 MAIN PROPERTIES

SUPRAFORM® HR is also hot rolled structural steels with improved formability and good weldability. The SUPRAFORM® HR consists of four grades where the HR designations relate to the minimum respective yield strengths of each grade. I t has been developed mainly for application where pressing, stamping or forming has to be carried out on structural steel to produce a final product. Although the grades are

essentially structural steel grades perform very well in drawing and forming application. SUPRAFORM® HR cam be welded using any of the standard arc and resistance welding processes, usually without any special precaution.

Some typical application for this steel are body chassis components for the automotive and truck industry, bumper brackets, engine mounting brackets and wheel centres, any cold formed sections requiring sharp bends, container internal structure.

7.2.2. MECHANICAL AND CHEMICAL PROPERTIES

See *Table 7.3* and *Table 7.4* for chemical composition and mechanical properties as stated in the data sheet.

Grade	**C**	**Mn**	**Si**	**Al**	**P**	**S**
HR 190	0,04	0,20	0,03	0,04	0,015	0,015
HR 220	0,05	0,25	0,03	0,04	0,015	0,015
HR 250	0,12	0,55	0,03	0,04	0,015	0,015
HR 290	0,16	0,85	0,03	0,04	0,015	0,015

Table 7.3: SUPRAFORM® HR chemical properties (ladle analysis)

The high strength of the SUPRAFORM® HR grades is achieved by grain refinement and precipitation hardening of ferritic microstructure. In order to ensure that the mechanical properties are met, the ferritic grain size is carefully controlled and is finer that ASTM E112 plate No 1, grain size 8.

Grade	Yield strength (MPa)	Minimum tensile strength1 (MPa)	Minimum elongation[2] (%) for thickness t	Minimum elongation[2] (%) for thickness t
			2 ≤ t ≤ 4	*2 ≤ t ≤ 4*
HR 190	190 – 270	290	35	37
HR 220	220 – 300	320	32	34
HR 250	250 – 330	370	30	33
HR 290[4]	290 – 370	410	27	30

Table 7.4: SUPRAFORM® HR mechanical properties

In order to possess good drawing, forming and pressing properties, hot rolled strip have a homogeneous microstructure which can be achieved only if the strip temperature is accurately controlled during hot rolling.

8 MECHANICAL PROPERTIES

8.1 MODULUS OF ELASTICITY

The modulus of elasticity is a measure of the stiffness of the material, but it only applies in the linear region of the curve. Modulus of elasticity (or Young's Modulus) is a measurement of the rate of change of strain as a function of stress. It represents the slope of the straight-line portion of a stress-strain curve. With respect to tensile testing, it may be referred to as Tensile Modulus. This method of testing is used to determine a sample's behaviour under an axial stretching load. Common tensile test results include elastic limit, tensile strength, yield point, yield strength, elongation, and Young's Modulus. Young's Modulus is reported commonly as N/mm2.

8.2 YIELD STRENGTH

The yield strength or yield point of a material is defined in engineering and materials science as the stress at which a material begins to deform plastically. Prior to the yield point the material will deform elastically and will return to its original shape when the applied stress is removed. Once the yield point is passed some fraction of the deformation will be permanent and non-reversible. In the three-dimensional space of the principal stresses (σ_1, σ2, σ3), an infinite number of yield points form together a yield surface.

9 METHODOLOGY USED FOR SIMULATING THE PHYSICAL PIERCING PROCESS

A combination of FEA and experimental analysis will be used in this research. LS DYNA will be used for the FEA because of its ability to simulate the punching process while manipulating the material law (material failure criterion) for improved results. The simulation process will be defined in DYNAFORM as this is a dedicated software for defining such processes and LS PREPOST will be used in the definition of the blank since DYNAFORM cannot define solid elements. Mechanical tests (e.g. tensile test) will be conducted on the specimen to find the mechanical properties and

behaviour to be used in both the FEA and experimental analysis (See Figure 9.1 below for research outline of all the research procedures to be performed).

The initial phase of the simulation is to duplicate the blank tearing that takes place when using the TM380 material. A material failure criterion will be applied to the blank. An erosion criterion (e.g. maximum stress at failure) will be set such that, if an element reaches a certain strain level it gets deleted from the solution. This can be defined by means of an erosion criteria or a failure flag in the material input deck. Data required for the simulation are the material yield strength material Ultimate Tensile Stress (UTS), stress strain behaviour curve. Since LS DYNA is an explicit dynamic finite code, gradually loads can be applied to deform a blank.

Press machine data is also critical for the simulation (e.g. punching speed). This is because the blank material definition is rate dependant and different velocities would yield different results. The simulation time should be stable without putting a strain on computational time. Different punch geometries will be used in the simulation (e.g. Single and double shearing punches and profiled punches). This will be done to observe different stress distribution during the process. Shearing punches are most probable to yield improved results however are not favourable in the metal workshops as they require attentive maintenance for them to be effective.

The similar simulation will be run with the HR190 material. This is a much softer material (as compared to TM380) with improve ductility and improved response. Since the press machine that is used in the press workshop is old and punching speed cannot be changed, the same punching velocity will be used.

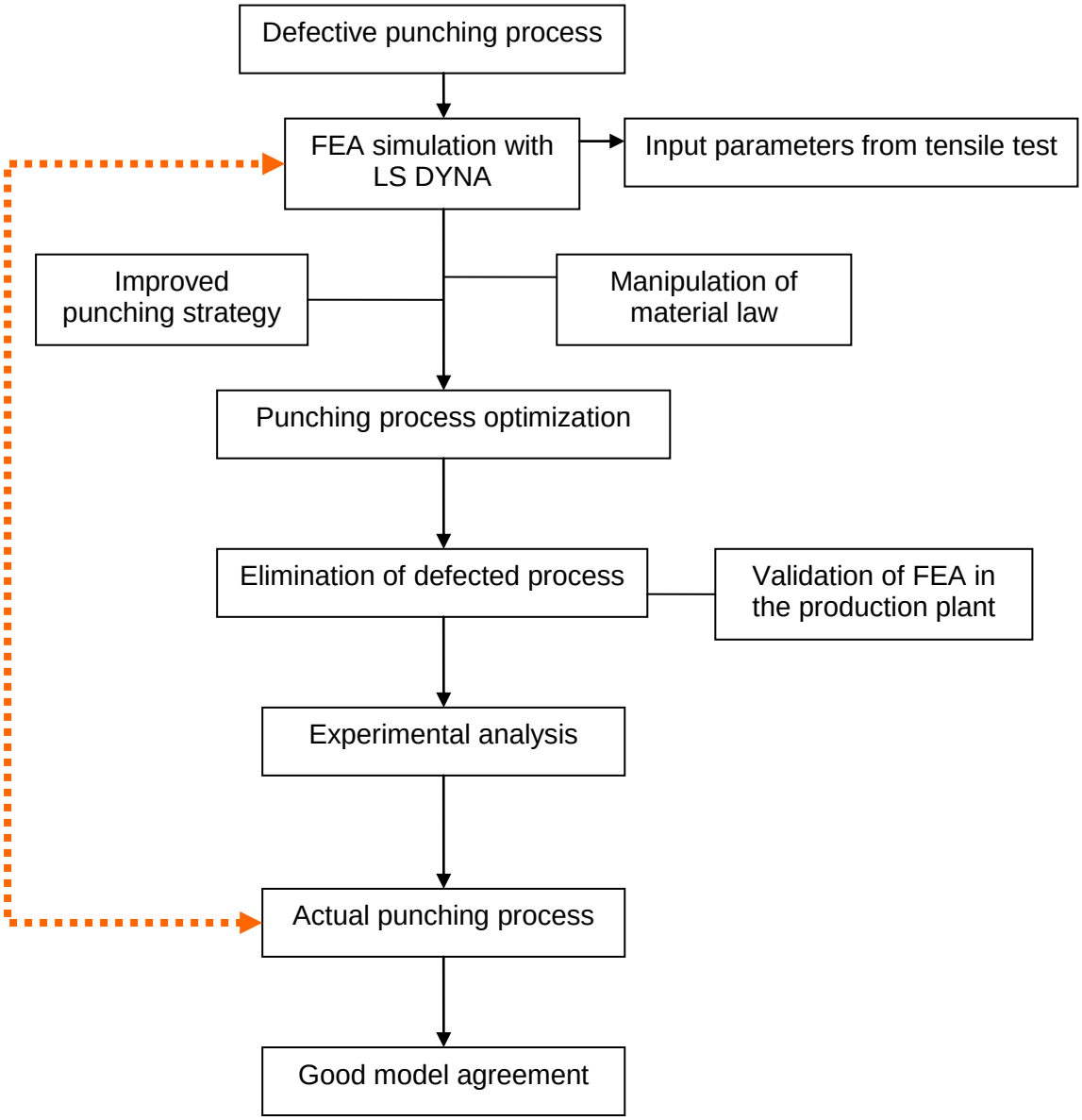

Figure 9.1: Research Methodology process

The improved strategy will be a combination of different punch geometries, blank material thickness and improved failure criteria definition. The results would be experimentally tested by using the softer material in the production process (pending on automotive regulation approval for using a different material).

Because of allowable downtime on the press tool, only the softer (HR190) material will be tested experimentally as the probable solution. This is because of the prolonged time required in changing the punches. The primary solution therefore is to simulate the softer material with the same punch (flat punch) and the secondary is stress distribution with different punch geometries. The punches will be subjected to operational loads and stresses and reactions will be studied, interpreted and compared with experimental results. A good model agreement is vital for the validation of the FEA with actual experimental work.

Figure 9.1 shows how we start off with a defective punching process and improve it through and iterative process of simulation, adjustment to the physical parameters and verification. Through this we can arrive at a simulation that matches the physical phenomena and which we can then use to arrive at an improved piercing process.

10 THE TENSION TEST AND STRAIN RATES

The most common mechanical test for characterizing metals is the tension test. A specimen (see Fig 10.2 for a sub sized specimen as per ASTME handbook) is mounted in a machine which pulls it at a prescribed rate and simultaneously records the load on the specimen. The material is said to yield at the point where it stops behaving like an elastic material, at this point typically occurs a small fraction of a percent of strain. After this point, if the load is removed, the specimen retains a permanent deformation called the plastic deformation (See Figure 10.1 for a typical stress-strain curve).

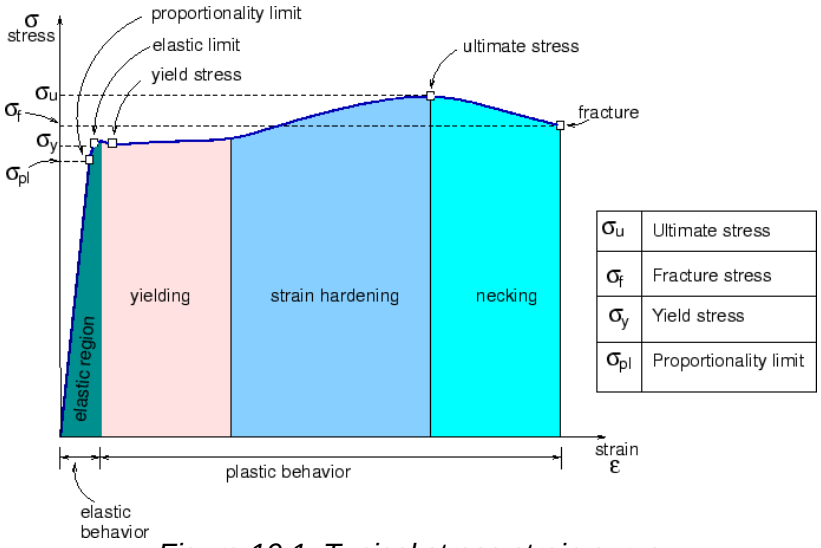

Figure 10.1: Typical stress strain curve

Three criteria for the initiation of yielding are most commonly used, the elastic limit, the proportional limit, and the yield strength. The Elastic limit is the greatest stress that the material can withstand without any measurable permanent strain remaining after the complete release of the load whereas the proportional limit is the highest stress at which stress is directly proportional to the strain. This is obtained by observing the deviation from the straight line portion of the stress – strain curve. The yield strength is the stress required to produce a small specified amount of plastic deformation. This is often referred to as the yield point. A material is said to have deformed plastically if it doesn't return to its original shape after the load is removed.

Machined test specimens are expected to meet size specifications, and should be measured to ensure dimensional accuracy. Test specimen measurements determine the initial cross sectional area and poses important since they will be measured against the final cross section area after the test (See Table 10.1 for specimen dimensions used in the tensile test). According to the ASTME, measurement of elongation requires marking the gage length of the test specimen. The gage length should be placed on the test piece such that when fracture occurs, the fracture will be located within the centre one-third of the gage-length marks.

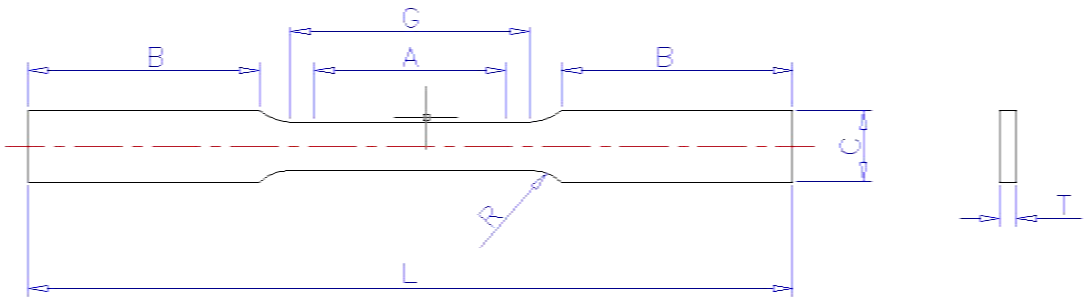

Figure 10.2: A typical sub-sized specimen as per ASTM standard handbook

Where:

Specimen Variable	Value
G – Gauge Length	24.5 mm
W – Width	6.125 mm
T – Thickness	2.2 mm
R – Radius	6.125 mm
L – Overall length	98 mm
A – Length of reduced section	30.625 mm
B - Length of grip section	40 mm
C – Width of grip section	9.187 mm

Table 10.1: Uniaxial testing specimen specification

In the conventional engineering tension test, an engineering stress – stress curve is constructed from the load elongation measurements made on the specimen [ASTM E8]. The engineering stress used in the stress-strain curve is the average longitudinal stress in the tensile test and can be described in the form:

$$s = \frac{P}{A_0} \tag{5}$$

This is obtained by dividing the load (*P*) by the original area of the cross section of the specimen. The strain *e* used for the engineering stress-strain is the average strain, which is obtained by dividing the elongation of the gage length of the specimen ΔL by its original length $L_{0.}$

$$e = \frac{\Delta L}{L_0} = \frac{L - L_0}{L} \tag{6}$$

The stress that the specimen undergoes is expressed by dividing the load *P* with the sectional area $A_{0.}$

$$\sigma = \frac{P}{A} \tag{7}$$

The engineering stress-strain curve however does not give a true indication of the deformation characteristics of a metal because it is based entirely on the original dimensions of the specimen, and these dimensions change continuously during the test. The cross-sectional area also of the specimen is decreasing rapidly at the stage of necking, and the load required continuing deformation falls off. This makes the conversion from engineering to true stress prior to necking vital in getting realistic results [43]. The derivation of the above equation assumes both constancy of volume and a homogenous distribution of strain along the gauge length of the tension specimen (see below for true and engineering stress conversion).

$$\sigma = S(1 + e) \tag{8}$$

$$\varepsilon = \ln(1 + e) \tag{9}$$

Where: σ : True Stress

S: Engineering Stress

ε : True Strain

E: Engineering Strain

The general shape and magnitude of the stress-strain curve of any metal will however depends on its composition, heat treatment, prior history of plastic

deformation, strain rate, temperature, and state of stress imposed during the testing. The parameters, which are used to describe the stress-strain curve of a metal, are the tensile strength, yield strength or yield point, percent elongation, and reduction of area. The first two are strength parameters; the last two indicate ductility

Strain rate is defined as the rate at which deformation occurs, therefore varying speeds will help achieve different strain rates and hence different mechanical behaviour. Higher speeds increase the deformation rate thus achieving high strain rate. Average tensile quasi-static testing for metallic materials is performed at strain rates of approximately $1X10^{-3}$ s^{-1}[7]. Strength properties for most material tend to increase at high rates of deformation. Different strain rates from a critical part of the experiment as the component that is used is assumed to be a rate dependant material. The ASM E8 prescribes an upper limit of deformation rate as determined qualitatively during the test by one of the following methods (listed in decreasing order of precision):

- Rate of straining
- Rate of stressing
- Rate of cross head separation
- Elapsed time
- Free running crosshead spring

10.1 RATE DEPENDANT AND RATE INDEPENDENT MATERIALS

In the mathematical description of material behaviour, the response of the material is characterized by a constitutive equation which gives the stress as a function of the deformation history of the body. A different constitutive relation allows us to distinguish between a viscous fluid and a rubber or concrete. In one-dimensional solid mechanics, the constitutive relations are often referred as the stress- strain law for the material.

A material for which the stress-strain response is independent of the rate of deformation is said to be rate-independent; otherwise rate-dependant. The material for the simulation has been defined as rate-dependant. (See Figure 10.3 below for typical stress strain curves for rate-independent and otherwise rate-dependant material)[41].

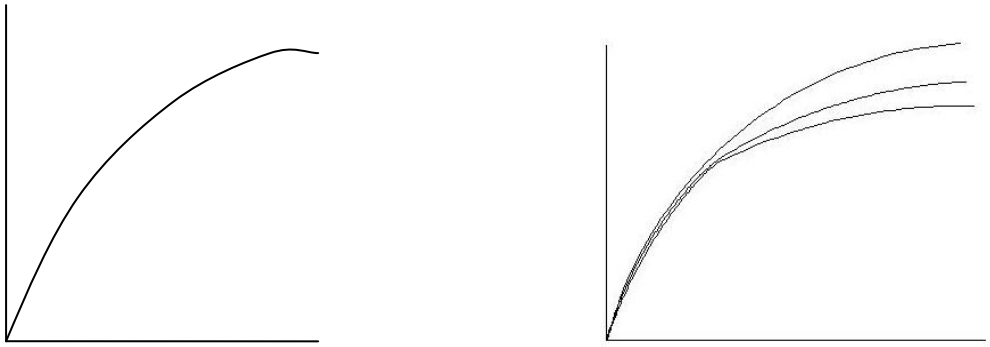

(a) *(b)*

Figure 10.3: Rate dependency in engineering stress-strain curve
(*a) rate-independent material (b) rate-dependant material*.
(Adapted from Belytschko, 2000)

In rate-dependant plasticity, the plastic response of the material depends on the rate of loading. For plastic deformation to occur, the yield condition must be met or exceeded, in contrast to rate-independent plasticity where the condition can not be exceeded, the plastic strain is given by the combined isotropic hardening and kinematic hardening [41].

A universal testing machine for tension & compression testing connected to the computer was used for the test. The testing machine used can achieve a maximum force of 50 KN and a speed of 500mm/min. The tensile test was conducted at a cross head velocity of 5 mm/s for both the TM380 and HR190. The gage length is 25.4 mm and a strain rate of 0.16 s^{-1}.

10.2 TENSILE TESTING PROCEDURE

a) Measure dimensions of each specimen and record them accordingly. They are useful in calculating properties such as stress.
b) Switch on machine, ensure that correct load cell & grips (wedge type grips for thin plate) are used, setup specimen correctly with the gauge length in the middle.
c) Setup speed correctly to give the required strain rate.
d) Proceed with tests when setup is satisfactory.

e) Once the test for a single sample is complete store its results & measure the specimen to obtain new length & cross sectional dimensions (where failure occurs)
f) Repeat steps “a - e” with higher speeds (increasing strain rate).

10.3 EXPERIMENTAL RESULTS

Below are the results from the tensile test (Figure 10.4 and 10.5). These results were used in the LS DYNA simulation for description of the material behaviour, in form of a load curve, during the piercing simulation. See Table 10.2 for Stress/Strain tensile test results of the materials (TM380 & HR190).

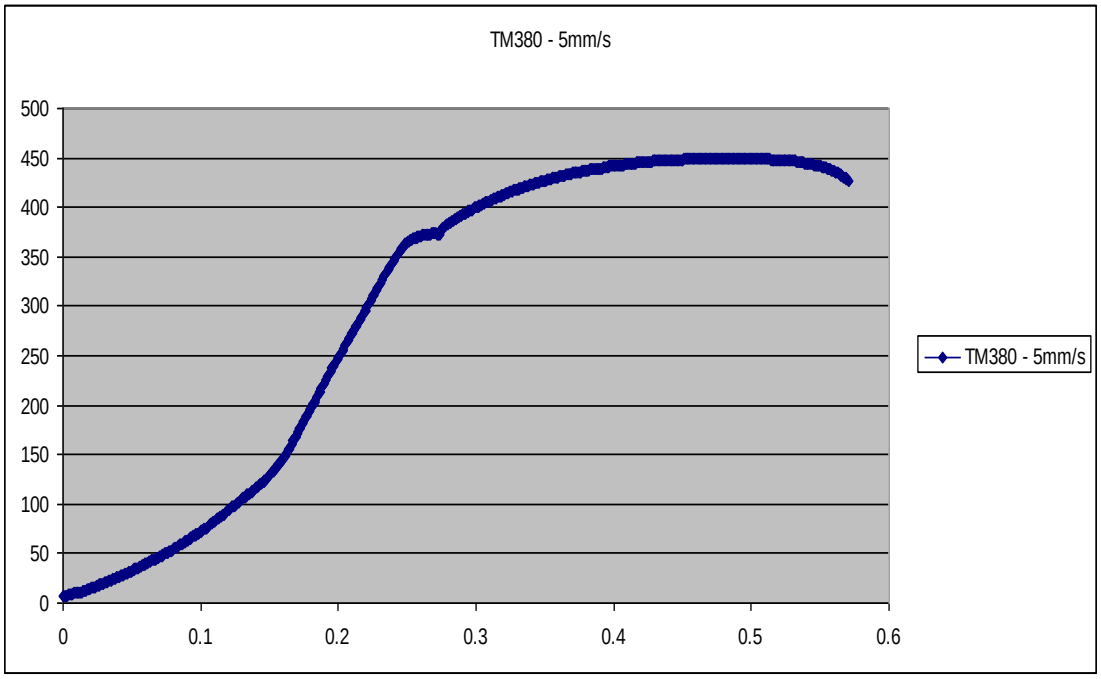

Figure 10.4: Stress/Strain behaviour for TM380

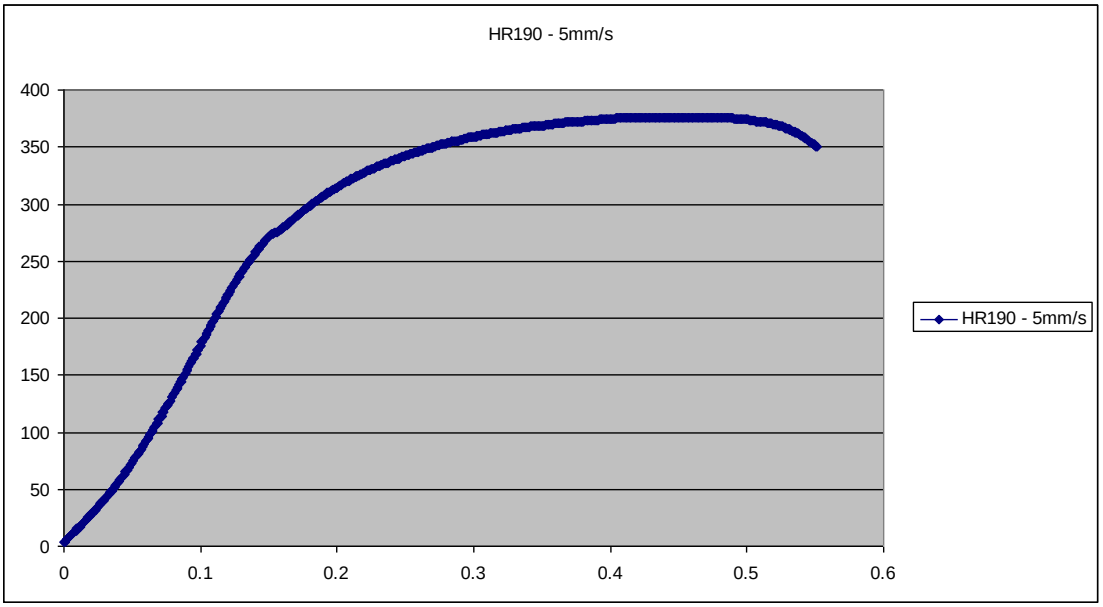

Figure 10.5: Stress/Strain behaviour for HR190

Material	Cross head velocity	Yield Stress	Ultimate Tensile Stress
TM380	5mm/s	375 Mpa	492 Mpa
HR190	5mm/s	270 Mpa	376 Mpa

Table 10.2: Stress/Strain data from the tensile testing

11 FINITE ELEMENT FORMULATION

11.1 FINITE ELEMENT ANALYSIS

Finite Element Analysis (FEA) is a computer simulation technique used in engineering analysis. It uses a numerical technique called the finite element method (FEM). FEA consists of a computer model of a material or design that is stressed and analyzed for specific results. It is used in new product design, and existing product refinement. For an existing product or structure it is utilized to qualify the product or structure for a new service condition. In case of structural failure, FEA may be used to help determine the design modifications to avoid failure. (See Figure. 11.1 for an example of a finite element analysis model).

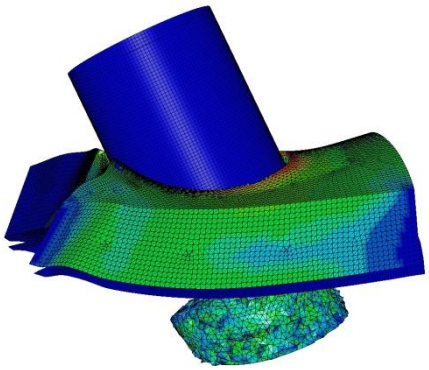

Figure 11.1: Finite element analysis model

FEA uses a complex system of points called nodes which make a grid called a mesh. This mesh is programmed to contain the material and structural properties which define how the structure will react to certain loading conditions. The mesh acts like a spider web in that from each node, there extends a mesh element to each of the adjacent nodes [6].

Recent experiment(s) [9] where conducted on the failure analysis of cold forging dies using FEA. A finite Element package called DEFORM-2D^{TM} v6.0 running on a UNIX based Silicon Graphics O2^{TM} was used to simulate and predict ductile fracture in a forging die. The size of the trim die analyzed was an M6, related to the size of the bolt produced. A total of 11 FEA models were simulated, each one giving different results with different input parameters (trim die final stopping distance ranging from 0.25 to 0.75mm in steps of 0.05mm). These results would have been difficult to obtain unless an FEA was utilized.

Peder Skov-Hansen, et. al [13], also conducted a tool life analysis of fatigue in cold forging dies. In order to predict the tool life of a critically loaded punch in the flange operation, an elastic FEM analysis was performed, calculating the strain and stress distribution using ANSYS. The predicted tool life corresponding to the low cycle fatigue test was 782 cycles, and using dynamic fracture mechanics the calculated additional tool life was 82 cycles.

12 FAILURE CRITERION

A yield criterion, often expressed as yield surface, is a hypothesis concerning the limit of elasticity under any combination of stresses. Since stress and strain are tensor qualities that can be described on the basis of three principal directions

$$\left(\sigma_1, \sigma_2, \sigma_3\right)$$

Maximum Principal Stress Theory – Yield occurs when the largest principal stress exceeds the uniaxial tensile yield.

$$\sigma_1 \leq \sigma_y$$

Maximum Principal Strain Theory – Yield occurs when the maximum principal strain reaches the strain corresponding to the yield point during a simple tensile test.

$$\sigma_1 - \nu\left(\sigma_2 + \sigma_3\right) \leq \sigma_y$$

Maximum shear Stress Theory – Also known as the Tresca Criterion, this assumes that yield occurs when the shear stress τ exceeds the shear yield strength τ_y

$$\tau = \frac{\sigma_1 - \sigma_3}{2} \leq \tau_{ys}$$

Total Strain Energy Theory – This theorem assumes that the stored energy associated with elastic deformation at the point of yield is independent of the specific stress tensor and thus yield occurs when the strain energy per unit volume is greater that the strain energy at the elastic limit in simple tension. For a 3 dimensional stress state this is given by:

$$\sigma_1^2 + \sigma_2^2 + \sigma_3^2 - 2\nu\left(\sigma_1\sigma_2 + \sigma_2\sigma_3 + \sigma_1\sigma_3\right) \leq \sigma_y^2$$

13 STATIC AND DYNAMIC ANALYSIS

Time integration techniques are used for simulation of the code by means of time steps in the forming process. The software will formulate the equations to be solved, based on geometry, boundary conditions, and material properties where:

- The information at the first time step is used to calculate the nodal deflections at the second time step.
- Information at the first two time steps may be used to calculate the nodal deflections at the third time step.
- This process, called time integration is continued until the end of the analysis is reached.

This process, called time integration is continued until the end of the analysis is reached. These time integration techniques are static implicit time integration and dynamic explicit time integration.

13.1 STATIC IMPLICIT ANALYSIS

Implicit formulation allows static and a dynamic approach for finite element simulation. In the static case where acceleration and velocity forces are neglected, the principle of virtual work leads to:

$$[K]\{u\} = \{F\} \qquad (10)$$

Where:

[K] is the stiffness matrix

{u} is the displacement vector

{F} = is the applied load

13.2 DYNAMIC EXPLICIT ANALYSIS

For sheet forming problems with large numbers of nodes and elements in contact, implicit codes will usually encounter severe convergence problems. For these reasons, it is strongly recommended to use explicit finite element methods [43]. LS-DYNA is (predominantly) an explicit dynamic finite element code. This implies that, for any given calculation. In static analysis deformation is not time dependant and does not allow gradually applied loads/deformation.In the implicit dynamic case where acceleration and velocity forces are carried,

$$[M]a + [C]v + [K]x = F \qquad (11)$$

Where:

F is the applied loads
[K] is the stiffness matrix
[C] is the damping matrix
[M] is a mass matrix
x are the nodal deflections
v are the nodal velocities
a are the nodal accelerations

For a given magnitude of loading, dynamic response may be greater or less than static loading. Dynamic analysis is relevant for this analysis since the deformation is time dependant and allows for gradually applied loads/deformation. Dynamic analysis also allows localized deformation.

13.3 MATERIAL MODELS

LS DYNA uses different material models types for the definition of the material behaviour. A wide range of material models are available within LS DYNA, some material include strain rate sensitivity, failure, equation of state, thermal effects, etc.

Ductile materials can sustain large plastic deformation without fracture. However, will fracture when the strain becomes large enough - this is as a result of work-hardening of the material, which causes it to become brittle. This behaviour was described using the Distortion Energy theory which proposes that the total strain energy can be separated into two components: the volumetric (hydrostatic) strain energy and the deviatoric stress (distortion or shear) strain energy. It is proposed that yield occurs when the distortion components exceeds that at yield point for a simple tensile test [45]. This is generally referred to as the Von Mises Criterion, Where:

The stress is described by a system of differential equation:

$$\dot{\varepsilon} = \dot{\varepsilon}^{e} + \dot{\varepsilon}^{p} \tag{12}$$

Where:

$\dot{\varepsilon}$ is strain rate

$\dot{\varepsilon}^{e}$ is elastic strain rate

$\dot{\varepsilon}^{p}$ is plastic strain rate

$$\dot{\sigma} = C\,\dot{\varepsilon}^{e} \tag{13}$$

C is the elastic tangent modulus

Using the additive decomposition and solving the elastic strain rate, the stress rate is expressed as:

$$\dot{\sigma} = C\left(\dot{\varepsilon} - \dot{\varepsilon}^{p}\right) \tag{14}$$

Inside the yield function the response is elastic regardless of direction of the stress rate, and the plastic strain rate is exactly zero $\left(\varepsilon^{p}=0\right)$. The choices for defining the equivalent stress and plastic strain aren't unique. The equivalent stress is the Von Mises stress,

$$\bar{\sigma}=\sqrt{\frac{3}{2}\sigma'_{ij}\sigma'_{ij}} \tag{15}$$

Where σ'_{ij} is the deviatoric stress:

$$\sigma'_{ij}=\sigma_{ij}-\frac{\sigma_{kk}}{3}\delta_{ij} \tag{16}$$

Where σ_{kk} is the trace of σ'_{ij}

Which can also be expressed in the form:

$$\sigma'=\sigma-\frac{tr(\sigma)}{3}I \tag{17}$$

For the purpose of this analysis the constitutive model MAT_24 (Piecewise Linear Elasticity) was used. Such material is suited since it allows strain rate effects. This material is an elasto-plastic material which has got an arbitrary stress versus strain curve and arbitrary strain rate dependency. Deviatoric stresses have to satisfy the Yield Condition:

$$\phi=\frac{1}{2}\sigma'_{ij}\sigma'_{ij}-\frac{\sigma_y^2}{3}\leq 0 \tag{18}$$

Where ϕ is the Yield function and σ_y is the material yield stress where:

$$\sigma_y=\beta\left[\sigma_o+f_h(\varepsilon_{eff}^{p})\right] \tag{19}$$

Where: σ_o is the threshold stress (initial stress)

$f_h(\varepsilon_{eff}^p)$ is the hardening function and,

(ε_{eff}^p) is the effective plastic strain, which can be expressed in the form:

$$\varepsilon_{eff}^p = \int_0^t \left(\frac{2}{3} \dot{\varepsilon}_{ij}^p \dot{\varepsilon}_{ij}^p \right)^{1/2} dt \tag{20}$$

Where:

$$f_h(\varepsilon_{eff}^p) = \mathrm{E}_p(\varepsilon_{eff}^p) \tag{21}$$

E_p is the current plastic hardening modulus and is expressed in the form:

$$\mathrm{E}_p = \frac{\mathrm{E}_t E}{E - E_t} \tag{22}$$

E_t is the input tangent modulus and β is the account for strain rate effects. Strain rate effects (β) may be accounted for using the Cowper Symonds model which scales the yield stress with the factor:

$$\beta = 1 + \left(\frac{\dot{\varepsilon}}{C} \right)^{1/p} \tag{23}$$

Where: C and p are the Cowper Symonds material parameters

In the implementation of this material model, deviatoric stresses are updated elastically, the yield function is checked, and if it satisfied the deviatoric stresses are accepted. If it is not, an increment in plastic strain is computed:

$$\Delta\varepsilon_{eff}^p = \frac{\left(\frac{3}{2} \sigma'^*_{ij} \sigma'^*_{ij} \right)^{1/2} - \sigma_y}{3G + E_P} \tag{24}$$

14 CONTACT

Contact treatments forms an integral part of many large deformation problems. Accurate modelling of contact interfaces between bodies is crucial for the prediction capability of the finite element simulation. In LS DYNA contact is defined by identifying (via parts, part sets, segment sets, or node sets) locations that are to be checked for potential penetration of a *slave* node through a *master* segment (See Figure 14.1 for a contact illustration). This contact for this tearing analysis uses a CONTACT_AUTOMATIC_SINGLE_SURFACE keyword. This is a single surface contact, that is, the contact is defined wholly by the slave side [46]. By convention slave and master terminology is used where one body is designated as master, the other is designated as slave. Slave nodes are checked for penetration through master segments.

The failure nodes have been assigned as specific strain level such that when it reached a certain limit, the node must be deleted. The characteristics of this type of contact are that only slave side is defined and no segment orientation is required. The effects of friction will have a major impact on the wearing of the punch and die. For the purpose of the analysis a standard coefficient of friction between two metals is assigned.

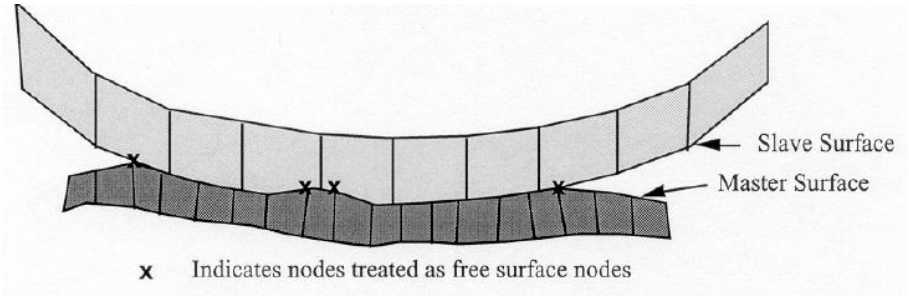

Figure 14.1: Contact between master and slave surface
(Adapted from LS DYNA support)

A search for penetrations, using any of a number of different algorithms, is made every time step. LS DYNA makes one pass to eliminate any detected penetrations by removing the penetrating slave nodes to the master surface. Not all initial penetration will be necessarily removed as this can lead to non physical contact behaviour.

Contact treatment is internally represented by linear springs between the slave node and the nearest master segments. The stiffness of these springs determines the force that will be applied to the slave nodes and master nodes. In the case of a penalty-based contact, when a penetration is found a force proportional to the penetration depth is applied to resist, and ultimately eliminate, the penetration.

The penalty method defines the restoring forces as:

$$k = \frac{f_s \times Area^2 \times K}{Volume} \tag{25}$$

Where:

Area is area of contact

K is Bulk modulus of contact elements

Fs is SLSFAC X SFS (26)

Where SLSFAC refers to Penalty scale factor(0.1 default) and SFS refers to the scale factor on default on slave/master penalty stiffness.

This method is the default method and uses the size of contact segments and its material properties to determine contact spring stiffness. As this method depends on the material constants and the size of the segments, it works effectively when the material stiffness parameters between the contacting surfaces are of the sane order of magnitude.

14.1 STRESS MODEL UPDATE

In the implementation of this material model, deviatoric stresses are updated elastically, the yield function is checked, and if it satisfied the deviatoric stresses are accepted. If it is not, an increment in plastic strain is computed:

$$\Delta\varepsilon_{eff}^{p} = \frac{\left(\frac{3}{2}s_{ij}^{*}s_{ij}^{*}\right)^{1/2} - \sigma_{y}}{3G + E_{P}} \tag{27}$$

Is the shear modulus and E_P is the current plastic hardening modulus. G is the modulus of rigidity.

The trial deviatoric stress state s_{ij}^{*} is scaled (to satisfy the yield condition) back as described by Hallquist [24]:

$$s_{ij}^{n+1} = \frac{\sigma_{Y}}{\left(\frac{3}{2}s_{ij}^{*}s_{ij}^{*}\right)^{1/2}} s_{ij}^{*} \tag{28}$$

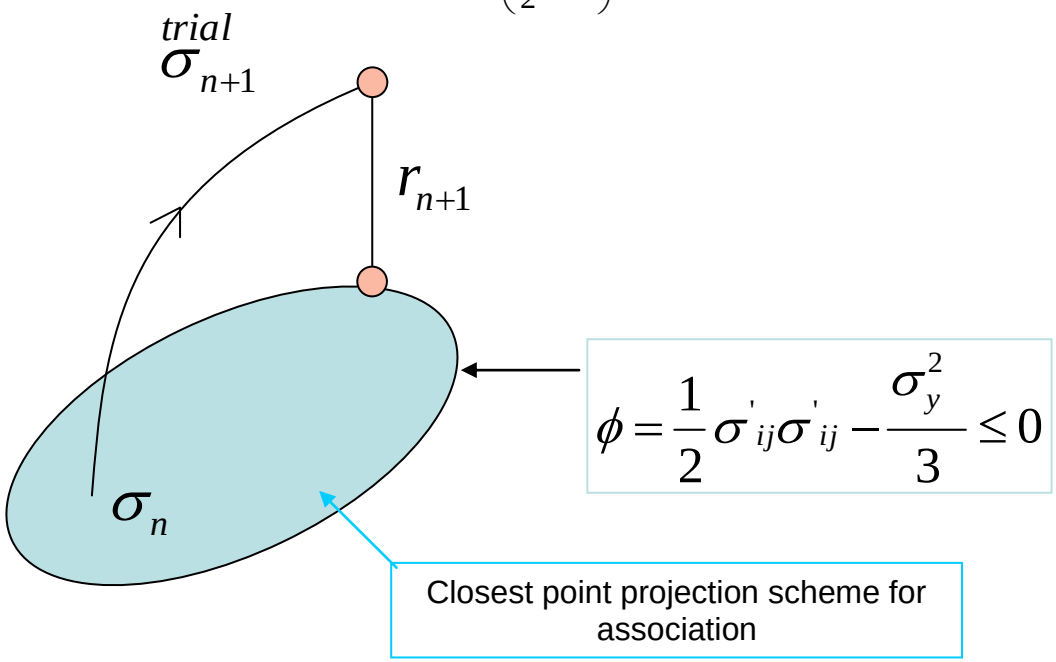

Figure 14.2: Prediction and correction illustration

15 GENERAL SOLID MATERIAL EROSION CRITERIA

Many constitutive elements in LS DYNA do not allow for failure and erosion. The ADD_EROSION options provide a way of including failure in models although the option can also be applied to constitutive models with other failure/erosion criteria [46]. Each of the criterion defined are applied independently, and once any one of them is satisfied, the element is deleted from the calculation. A typical EROSION input deck allows for failure to be defined is several form, namely:

- $P \geq P_{\min}$ Where P is the Pressure and $P_{\min}$ is the pressure at failure.

- $\sigma_1 \geq \sigma_{\max}$ Where σ_1 the maximum principal is stress and $\sigma_{\max}$ is the principal stress at failure.

- $\sqrt{\frac{2}{3}\sigma'_{ij}\sigma'_{ij}} \geq \sigma_{\max}$ where σ'_{ij} is the deviatoric stress components and $\sigma_{\max}$ is the equivalent stress at failure

- $\varepsilon_1 \geq \varepsilon_{\max}$ Where ε_1 the maximum principal is strain and $\varepsilon_{\max}$ is the principle strain at failure.

- $\gamma_1 \geq \gamma_{\max}$ Where γ_1 is the shear strain and $\gamma_{\max}$ is the shear strain at failure.

For this simulation, the maximum principal stress ($\sigma_{\max}$) at failure was used to define erosion failure.

16 DYNAFORM AND LS DYNA

16.1 DYNAFORM

DYNAFORM is the complete die system simulation solution. DYNAFORM allows the organization to entirely bypass soft tooling, reducing overall tryout time, lowering costs, increasing productivity and providing complete confidence in die system design. It also allows evaluation of alternative and unconventional designs and materials for an optimal solution. DYNAFORM is inclusive of such modules for tooling analysis application:

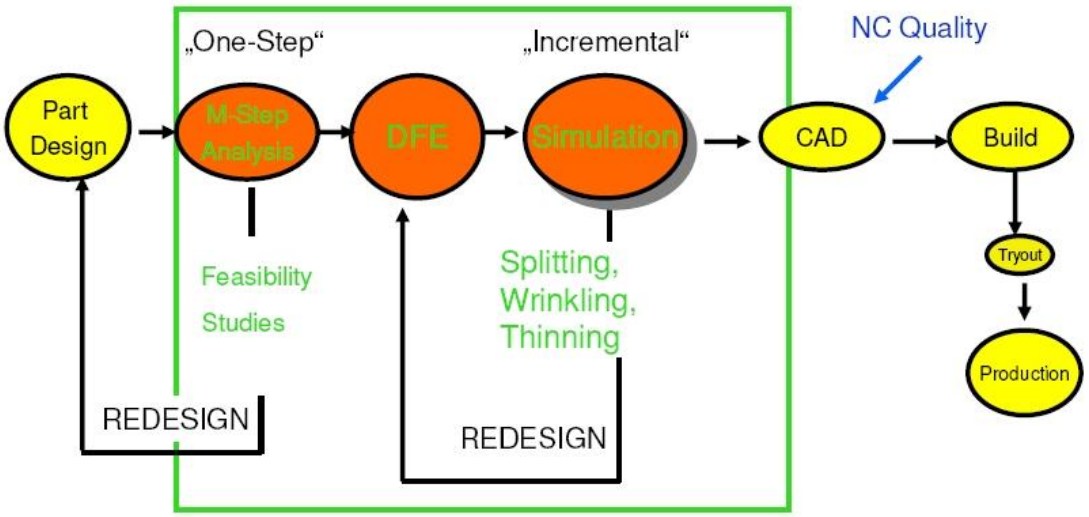

Figure16.1: Tool design development strategy with simulation
(Adapted from ZA Training Overview)

The use DYNAFORM and LS DYNA eliminates any probable risk during manufacturing and tool tryout. This is as a result of built models (BSE, DFE, FS, etc) which do all the pre-manufacturing analysis and stress prediction. (See Figure 19 for a development strategy as suggested by DYNAFORM).

The BSE module is a complete solution for accurate blank size estimation, nesting to maximize material utilization, piece price and scrap calculation. BSE is based on a one-step algorithm for rapid calculation. Potential forming failure due to excessive blank thinning is detected through an inverse method. BSE also creates a forming limit diagram (FLD) map for feasibility review.

Based on the product design of a panel, the DFE module offers capabilities of both CAD surface and CAE meshing tools. DFE Interactively generates binder surfaces, addendum profiles/surfaces, PO Lines and layout drawbeads with full associativity between FEA mesh and surfaces. A preliminary die face is created for further formability studies with an iterative process until die face validation is achieved.

The FS module is a complete incremental die simulation program for quickly generating formability results at a very early stage of the product design cycle. It is suited for design feasibility analysis and verification. Stress, strain and thickening results are plotted and a complete forming limit diagram (FLD) is generated. It is a proven tool for uncovering hidden problem areas [DYNAMORE USER WEBSITE].

DSA offers an LS-DYNA based FEA solution to analyze die system operations including scrap shedding/removal, die structural integrity and sheet metal transferring/handling. Further development will include trimming, flanging and hemming operations [47].

16.2 LS DYNA

LS DYNA is a powerful dual-solver is the engine that powers the efficient processing environment of DYNAFORM, making it a complete simulation solution package. LS-DYNA uniquely offers both explicit & implicit solutions that can be seamlessly switched to correctly simulate the physics of virtually all engineering concerns of a die system including formability, springback, springback compensation, trimming, and flanging [47].

One of LS-DYNA's most widely used applications is sheetmetal forming. LS-DYNA accurately predicts the stresses and a deformation experienced by the metal, and determines if the metal will fail. LS-DYNA™ is a trademark of Livermore Software Technology Corporation. LS-DYNA supports both 2-D and 3-D explicit elements, and features an extensive set of single-surface, surface-to-surface and node-to-surface contact as well as a contact analysis option that automatically creates the contact surfaces. LS-DYNA has over one hundred metallic and non-metallic material models: Elastic, Nonlinear Elastic, Elasto-plastic, Foam, Damage, Equations of State, etc. Over 25 different contact options are available. These options primarily treat contact of deformable to deformable bodies, single surface contact in deformable bodies, and deformable body to rigid body contact.

Multiple definitions of contact surfaces are possible. (LS-DYNA Developed by Livermore Software Technology Corp. Contact: 1).A special option exists for treating contact between a rigid surface (usually defined as an analytical surface) and a deformable structure. One example is in metal forming, where the punch and die surface geometries can be input as IGES- or VDA-surfaces which are assumed rigid. Another example is in occupant modelling, where the rigidbody occupant dummy (made up of geometric surfaces) contacts deformable structures 37 such as airbags and instrument panels. (LS-DYNA Developed by Livermore Software Technology Corp. Contact: 1).

17 SIMULATION SETUP

The piercing simulation was designed and pre-processed with Eta/DYNAFORM. With this tool it is possible to mesh any kind of surface. This includes the definition of the process, assigning of punch velocity and direction, definition of supporting die and contact (as illustrated in Figure 17.1). Eta/DYNAFORM also allows the ability to define the material model and assign the failure criterion for the elements.

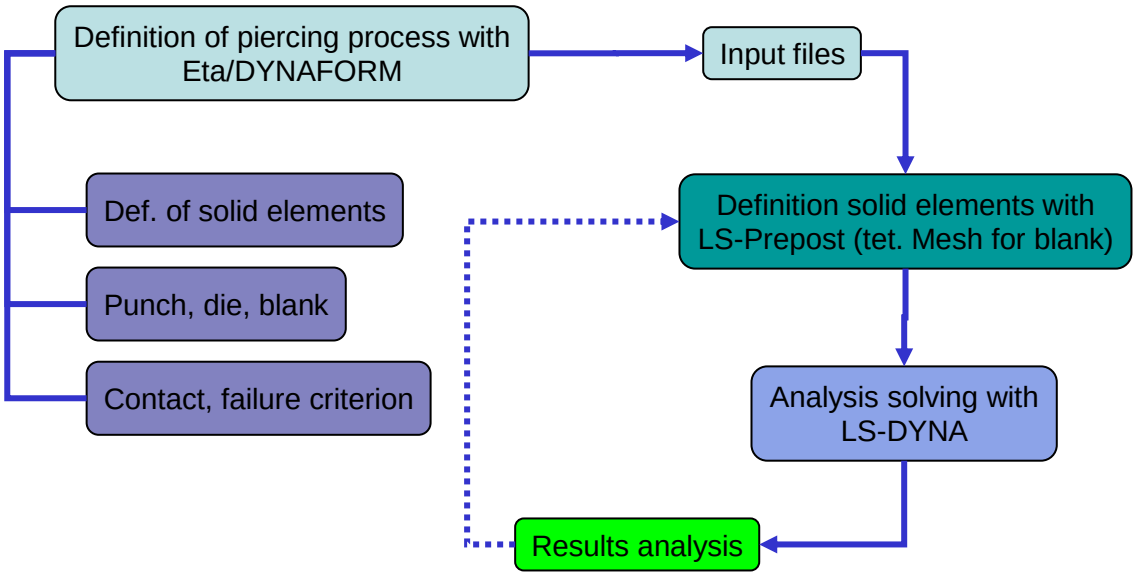

Figure 17.1: FEA design modeling process

It is however not possible to define solid elements in DYNAFORM and hence LS Prepost was used in define the tetrahedron mesh.

17.1 INTIAL SETUP

The initial FEA simulation consisted of a flat punch, blank material (blank Mat 1 & 2), and supporting die (See Figure 17.2 for punch simulation initial setup). A failure criterion was however applied on blank mat 1 only. This implied that material erosion will only take place on material and no stresses will be transferred to blank material 2. The setup also implied that a failure gap (0.5 per side) had to be assigned. This consequently affected the punch (green) diameter as a diameter 9 punch (9 + 0.5 +0.5 =10 mm punch diameter) had to be used. The punch was meshed as a shell element and assigned a velocity boundary condition. Shell elements were assigned because failure/deformation on the punch did not form part of the scope of the analysis. The mesh density of the punch was not critical and it is assigned as a rigid (indeformable) body in the simulation.

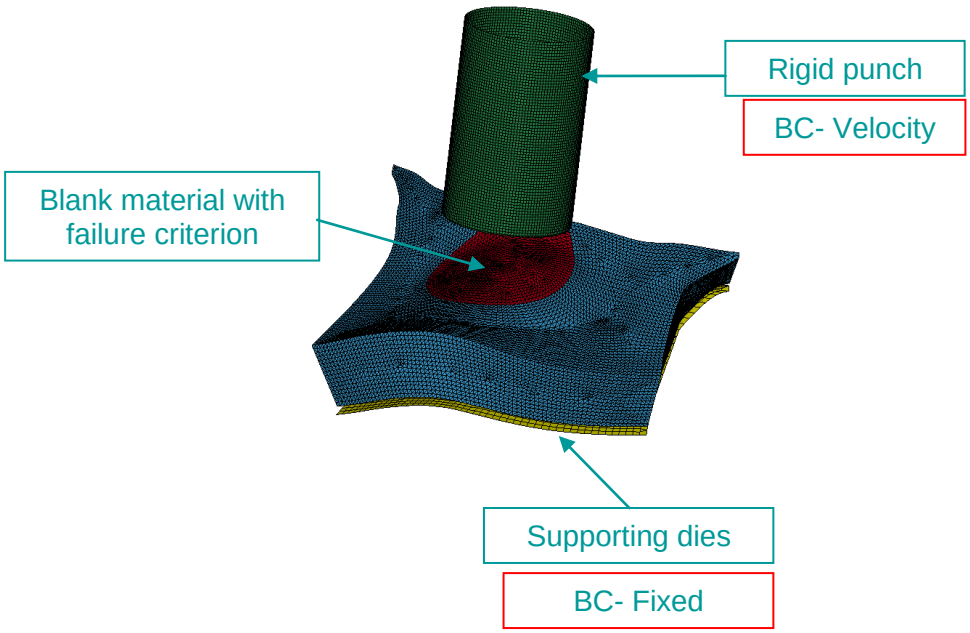

Figure 17.2: FEA piercing simulation initial setup

Element size was however an important factor. A balance had to be achieved such that the size was small enough to give accurate results but big enough to optimize analysis time. Figure 17.1 and 17.2 shows the part mesh data for initial setup and material properties (respectively) for the intitial setup.

INTIAL SETUP					
Part	Mesh	No of shells	No. of solids	Total No. of elements	Total No. of nodes
1. Punch & supporting dies 2. Blank Mat 1 & 2	DYNAFORM LS - PREPOST	13 786 -	- 383 215	- -	- -
Total		13 786	383 215	397 001	86 749

Table 17.1 : Part meshes data for initial setup

17.2 SOLID ELEMENTS

Since the piercing required involves material removal over a thickness, a tetrahedron mesh was used for the definition of blank material (See Figure 17.3 for a typical tetrahedron mesh. The tetrahedron (tetmesh) is one kind of pyramid that has a flat base and a triangular face above it. The base can also be of any polygon shape. For volume mesh generation, tetrahedral meshes are widely used for number viscous flows, structural/fracture analyses etc. due to their simplicity in terms of mesh generation). Table below contains simulation setup information about solid elements mesh. (Refer to table 9 for tetmesh data).

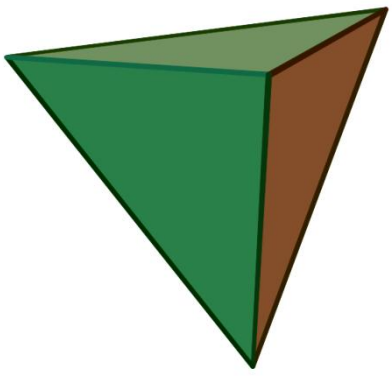

Figure 17.3: A typical tetrahedron mesh

A skin mesh of 0.1255 and 0.8117 was used for the min and max edge size respectively.

17.3 MATERIAL MODEL

Material Model 24 (MAT_PIECEWISE_LINEAR_PLASTICITY) was chosen for the blank material. This as a three dimensional elasto-plastic material with an arbitrary stress versus strain curve and arbitrary strain rate dependency can be define. Table below contains simulation setup input data and values required for the definition of the material properties.

Variable	Description	Value	Comments
MIS	Material identification	1	
RO	Density	7.850E-09	
E	Young's modulus	2.070E+05	
PR	Poisson's ratio	0.28	
SIGY	Yield stress	375 Mpa	(1)
ETAN	Tangent modulus	-	(2)
FAIL	Failure flag	-	
TDEL	Minimum time step size for automatic element deletion		
C	Strain rate Parameters C	-	(3)
P	Strain rate Parameters P	-	(3)
LCSS	Load curve ID defining effective stress versus effective plastic strain.	2	

Table 17.2: Part meshes data for initial setup

Comments

(1) Supplied data / from test.

(2) No need to be used.

(3) Different value depending on the transversally or longitudinally simulation. It is not an important value, because if LCSS is defined, program does not use this value and takes effective stress at failure.

Tool motion is imposed using the BOUNDARY_PRESCRIBED_MOTION_RIGID keyword. This keyword follows used a load curve (user defined) to define its movement whereby when the punch proceeds towards its final position, the blank experiences a complex sequence of stresses and strains as it is formed into its final shape. See Figure 6 below for a typical displacement curve used in the analysis.

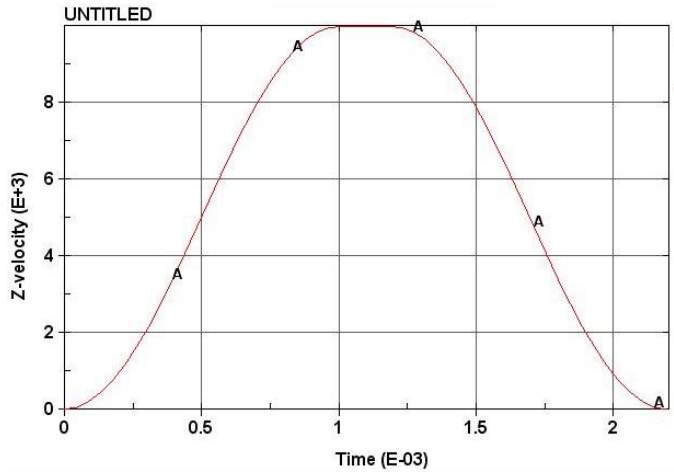

Figure 17.4: Displacement curve used for velocity definition

Tool motion (displacement or velocity) should vary smoothly with time, starting and ending with a velocity of zero. The maximum punch velocity of 10 000 mm/s was initially used for the simulation (DYNAFORM standard) (See Figure 17.4 for a velocity – time profile used).

Shell elements were also used to mesh the supporting die. A fixed boundary condition was assigned also, such that the die restricts any blank movement during the piercing process. The fixed boundary condition was also assigned to prevent any plastic strain on the blank during the piercing process.

The mesh density of the supporting die was also not important because it is assigned as a rigid (undeformable) body in the simulation. The shell element formulation is selected using the "elform" parameter on the *SECTION_SHELL keyword. The simulation was run for material TM380 and material HR190 with similar settings.

17.4 CRITICAL SIMULATION SETTINGS

PART

Parts identification (pid). This part has attributes identified by section identification (sid) and material identification (mid).

SECTION

Parts identified by (sid) are defined by this keyword. Element formulation, integration rule, nodal thicknesses and cross section properties are defined.

MAT

Parts identified by (mid) are defined as a Material Model by set of parameters.

ELEMENT

Three different element types can be defined: shell, thick shell and solid (brick) elements. Identified by element identification (eid), have the attributes of (pid) and are defined by the node list (nid).

CONTROL_TERMINATION

This control card is used in specifying when the software should stop the simulation calculation. This could in form of specifying the termination time, termination cycle, termination mass, percentage change in energy ratio. A termination time was specified for this simulation.

CONTACT

In LS DYNA contact is defined by identifying (via parts, part sets, segment sets, or node sets) locations that are to be checked for potential penetration of a *slave* node through a *master* segment. This contact for this tearing analysis uses a CONTACT_AUTOMATIC_SINGLE_SURFACE keyword.

MAT ADD EROSION

The ADD_EROSION options provide a way of including failure in models although the option can also be applied to constitutive models with other failure/erosion criteria.

INCLUDE

The *INCLUDE keyword provides a means of reading independent input files containing model data. The simulation contains "blk" file and "mod" files.

18 INITIAL SIMULATION RESULTS

18.1 INITIAL SIMULATION RESULTS – USING A CONTINUUM MODEL

The simulation was run on an Intel (R) Xenon(R) (8 CPUs) workstation. The contact assigned between punch and blank worked successful as the first element was eroded at 375 MPa. A hole diameter (of 10mm) equivalent to the blank (with failure criterion applied) was achieved (See Figure 18.1 for simulation results with cross section results).

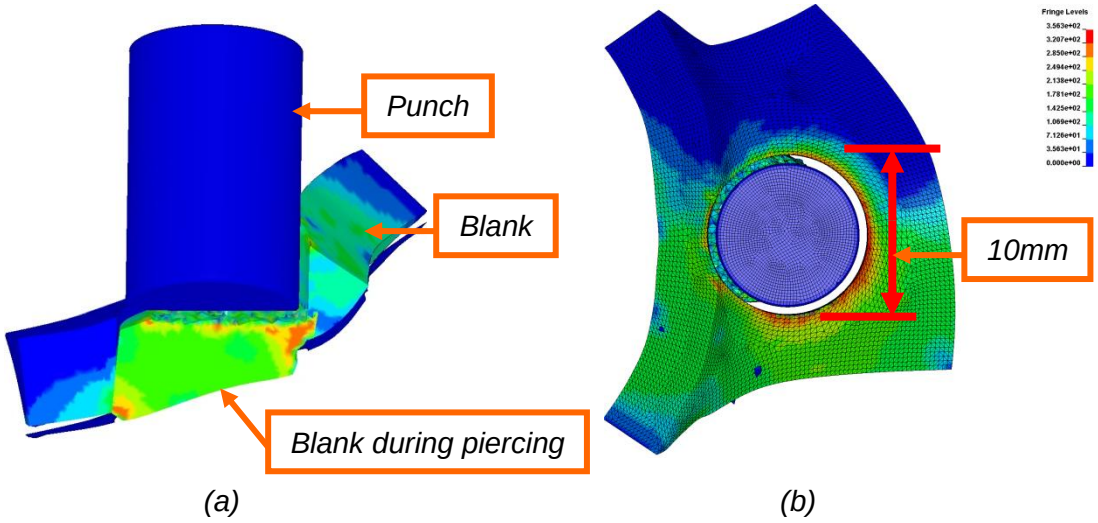

Figure 18.1: Initial setup punching simulation
(a) process sectional view (b) top view with final hole size.

From the simulation results, the stresses where only in the blank (area with failure criterion defined) and no stress where transferred to the surrounding region. The blank was merely sheared off the surrounding region and this was visible from the from piercing walls inspection. Refer to Figure 18.2 and 18.3 for effective plastic strain and effective stress in the initial setup respectively. The next chapter discusses all the changes that were done to improve the simulation results (e.g. process setup and failure criterion application, timesteps and punching velocity, etc).

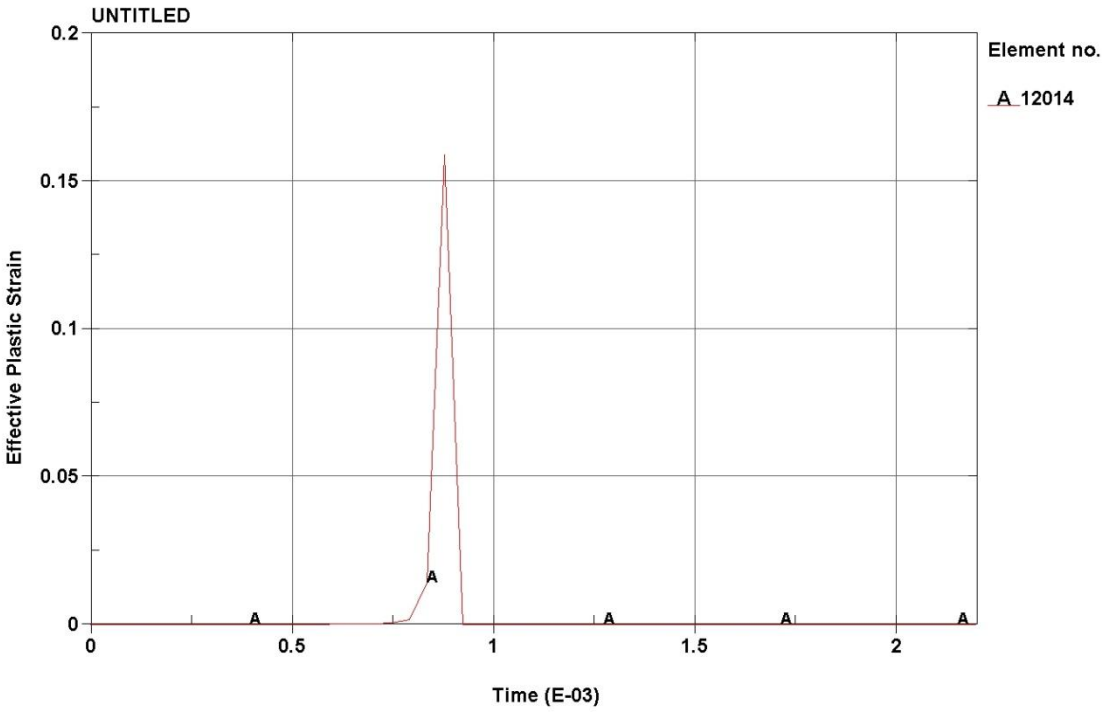

Figure 18.2: Effective plastic strain of a critical element in initial setup

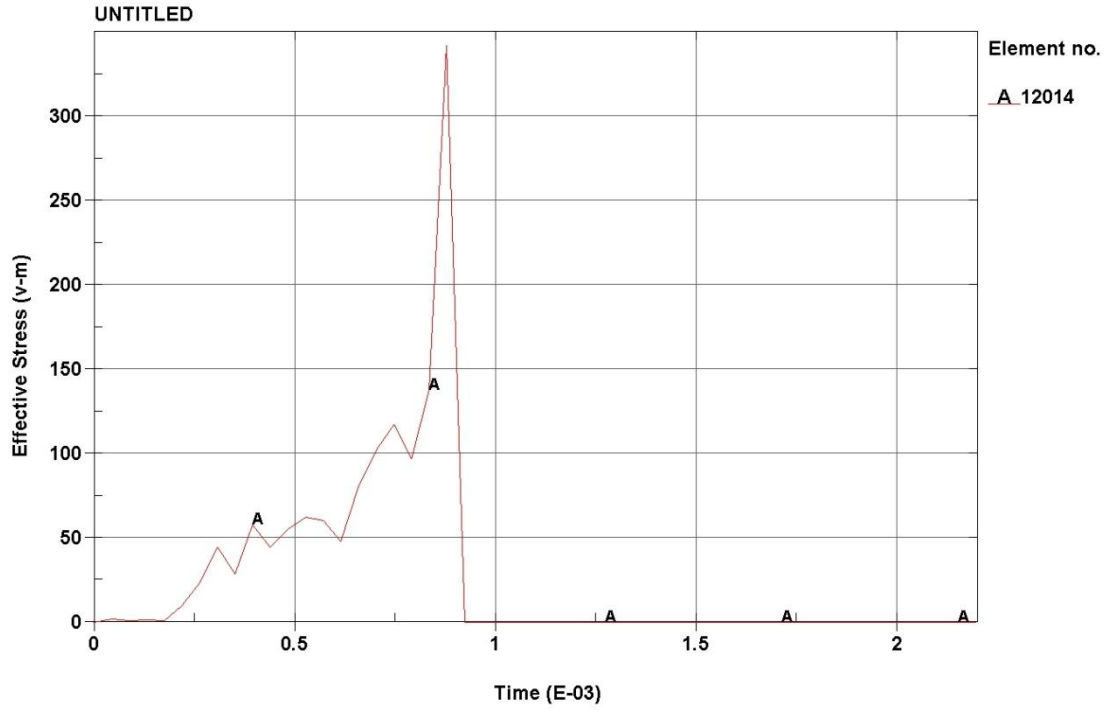

Figure 18.3: Effective stress of a critical element in initial setup

18.1 CONTINUUM MODEL LIMITATIONS

18.1.1 FAILURE CRITERION

The setup in LS DYNA allows for definition of failure criterion in many models. A method of define the plastic-strain-percentage-to-failure was used as a failure criterion. Failure flag of 0.2 which denotes a Yield stress at 0.2% plastic strain. (Figure 18.4 below a typical illustration of the stress/strain curve).

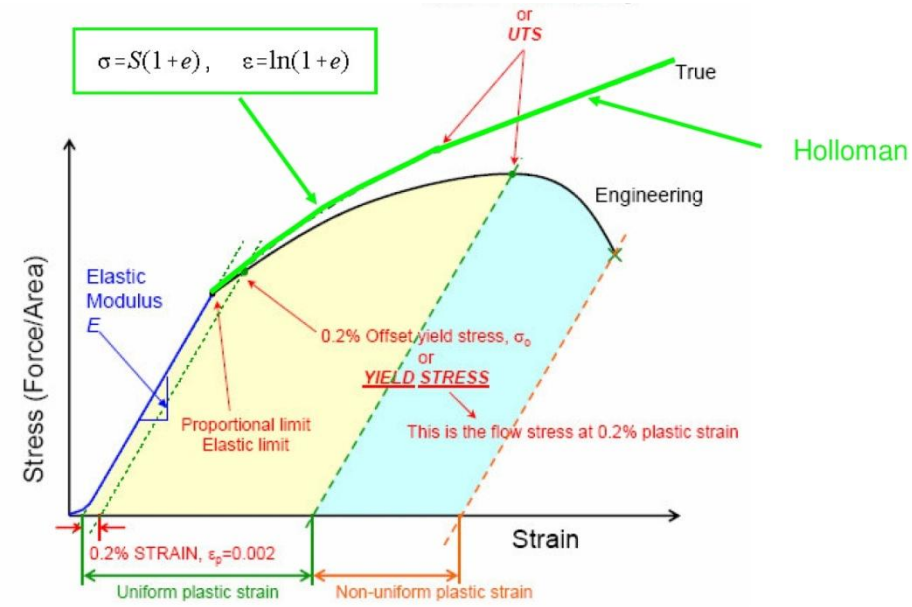

Figure 18.4 : Illustration of the stress/strain curve
(Adapted from DYNAFORM - ZA Training Overview)

This method was however not specific enough and couldn't account for the failure in the system. The MAT_ADD_EROSION option provided a way of including failure in models. When using this option several failure damage values (e.g. maximum pressure at failure, principal stress at failure, minimum principal stress at failure and so forth) can be assigned independently, once any one of them is satisfied, the element under the load is deleted from the calculation. Figure 18.5 below shows an extract from a typical input deck using in defining the failure criterion for the analysis. The inclusion of this input deck automatically overrides any failure criterion defined previously.

Card 1	1	2	3	4	5	6	7	8
Variable	MID	EXCL	MXPRES	MNPEPS				
Type	A8	F	F	F				
Default	none	none	none	none				

Card 2	1	2	3	4	5	6	7	8
Variable	PFAIL	SIGP1	SIGVM	EPSP1	EPSSH	SIGTH	IMPULSE	FAILTM
Type	F	F	F	F	F	F	F	F
Default	none	none	none	none	none	none	none	none

SGVM - Effective stress defined for failure in the analysis

Figure 18.5: Input deck used in defining the failure criterion

18.1.2 STRESS DISTRIBUTION

To facilitate the piercing in this analysis a failure criterion had to be assigned in the region equivalent to the drainage hole required. In the surrounding region (blue), a rigid property was assigned (See Figure 18.6 for the two different setups). Hence failure could only happen in the small region (red). Such an arrangement did not allow proper stress distribution and hence failure (cracking) in surrounding region could not occur. The presence of contact gap (between punch and red region) meant a reduction in the punch diameter (diameter 9mm instead of 10mm). This greatly influenced the accuracy of the results. For simulation Setup No. 2, the failure criterion was assigned to the whole blank material. Thus any material strain caused by the punch will transfer to the whole surrounding region (red).

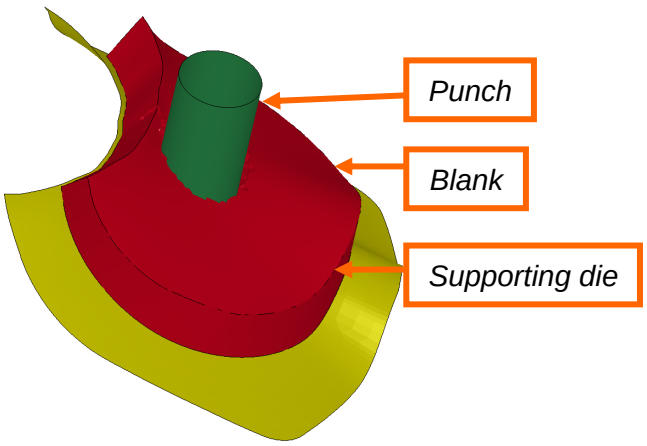

Figure 18.6: FEA simulation setup No. 2

SETUP No 2					
Part	Mesh	No of shells	No. of solids	Total No. of elements	Total No. of nodes
1. Punch & supporting dies 2. Blank Mat	DYNAFORM LS - PREPOST	5 425 -	- 278 814	- -	- -
Total		5 425	278 814	284 239	57 032

Table 18.1: Part meshes data for Setup No. 2

18.1.3 SIMULATION INPUT DATA

In addition to different material models in DYNAFORM, the software has template stress/strain curves that can be used to account for material behaviour. This is defined in form of a load curve. Power laws or Holloman's Law can be used to predict this curve, provided the important data about the material are known (Yield Stress, UTS, etc). This can be improved however by conducting a Stress / Strain experiment and using the Load / Extension curve for material behaviour.

The punch to timestep relationship was also. This is done in order to reduce any dynamic effects that can affect the results. The time step was reduced (from -1.200E-6 to -1.00E-7). This was because the initial model setup had a total mass of 22 Grams and the timestep was increasing by 22 Kilograms. This made the results very inaccurate and unreliable. The maximum punch velocity is 333 mm/s (as per machine specification) (See Figure 18.6 for an improved velocity – time profile used in the simulation).

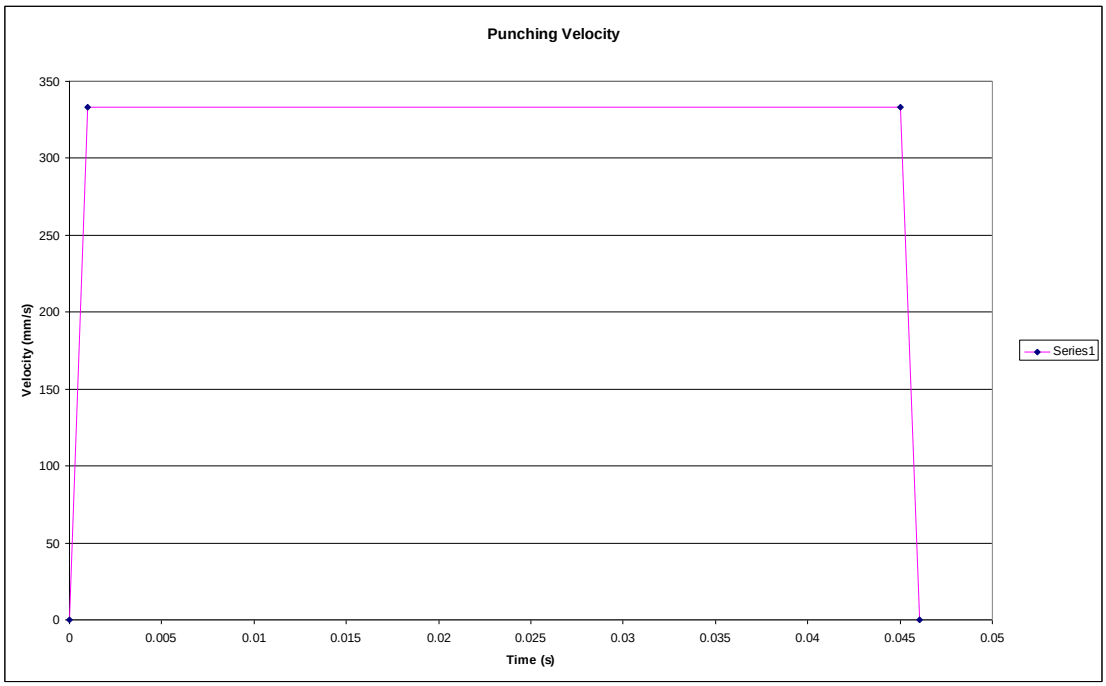

Figure 18.7: Punch velocity profile

Further suggestion for reducing dynamic effects are (as per LS DYNA training manual/overview) [43]:

- Prevent sudden starts and stops
- Use ramped or sinusoidal functions for forces and velocities
- Prevent small elements due mass scaling

19 SIMULATION RESULTS FOR TM380 USING CONTINUUM METHOD

19.1 SIMULATION RESULTS WITH A FLAT PUNCH – TM380

The simulation of the piercing process was done using three different punches with same simulation setup. This was done to check whether using different punch designs will yield different results and eliminate the tearing. This is a common practice is the shop floor e.g. using a shear punch to reduce the impact load on the material. This also assists in gauging the results sensitivity when using punches that approaches that material differently. Below are the punch designs used in the simulations on the continuum model.

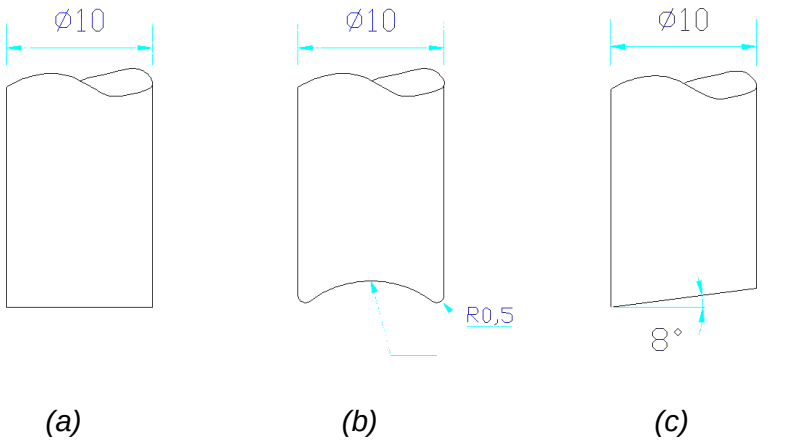

Figure 19.1: Punch designs used in the simulations of the continuum model setup (a) Flat punch (b) Concave punch (c) Shear punch

The simulation of the piercing was successful (See Appendix A for input deck for continuum model with TM380 material). At a stress 670 MPa (true stress) the element started to erode and piercing tool place (See Fig 19.2 for results of the piercing and Fig 19.3 for a simulation step).

19.1 SIMULATION RESULTS WITH A FLAT PUNCH – TM380

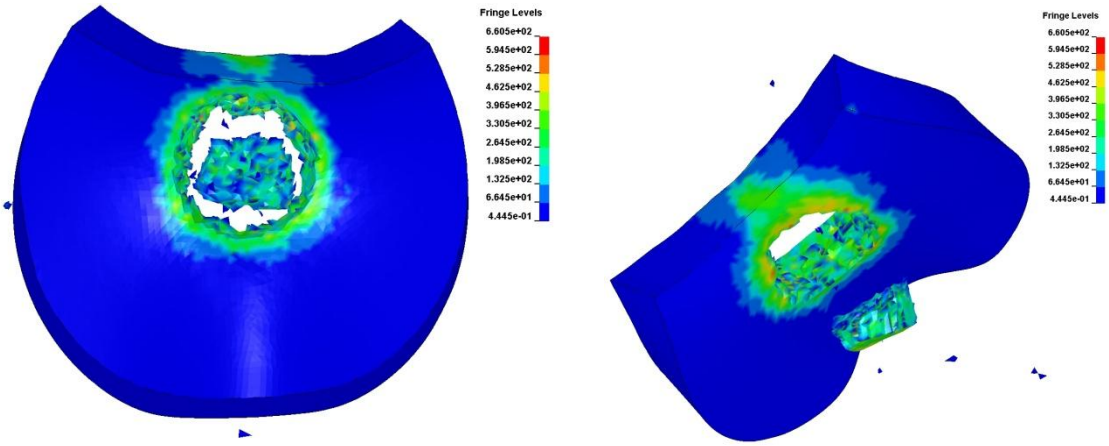

Figure 19.2: piercing simulation results for improved setup

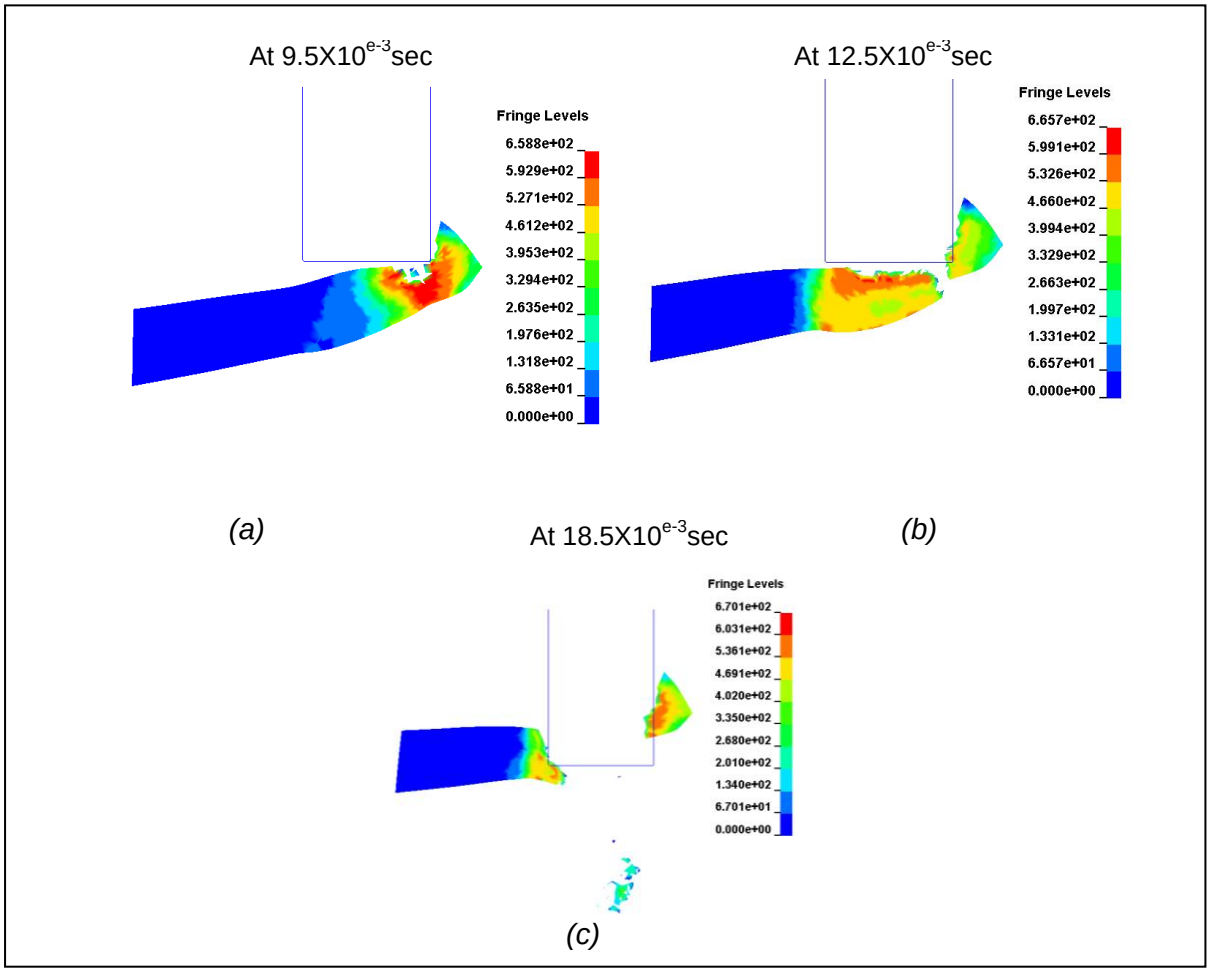

Figure 19.3: Simulation steps for material TM380 with a flat punch (a) punch makes contact with blank, (b) erosion of elements (c) black removed from material.

Maximum effective stress	Maximum plastic strain	Maximum eroded volume
660.518 MPa (Element 564941)	0.399 (435826)	abs = 2.302002e-002 ord = 5.648795e-002

Table 19.1: Simulation results for flat punch on TM380 material

19.2 SIMULATION RESULTS WITH A FLAT PUNCH – HR190

Similar piercing simulation was run on a HR190 and the results are shown in Fig 19.5 below. The material element erosion in this simulation starts earlier (550MPa) as compared to the TM380.

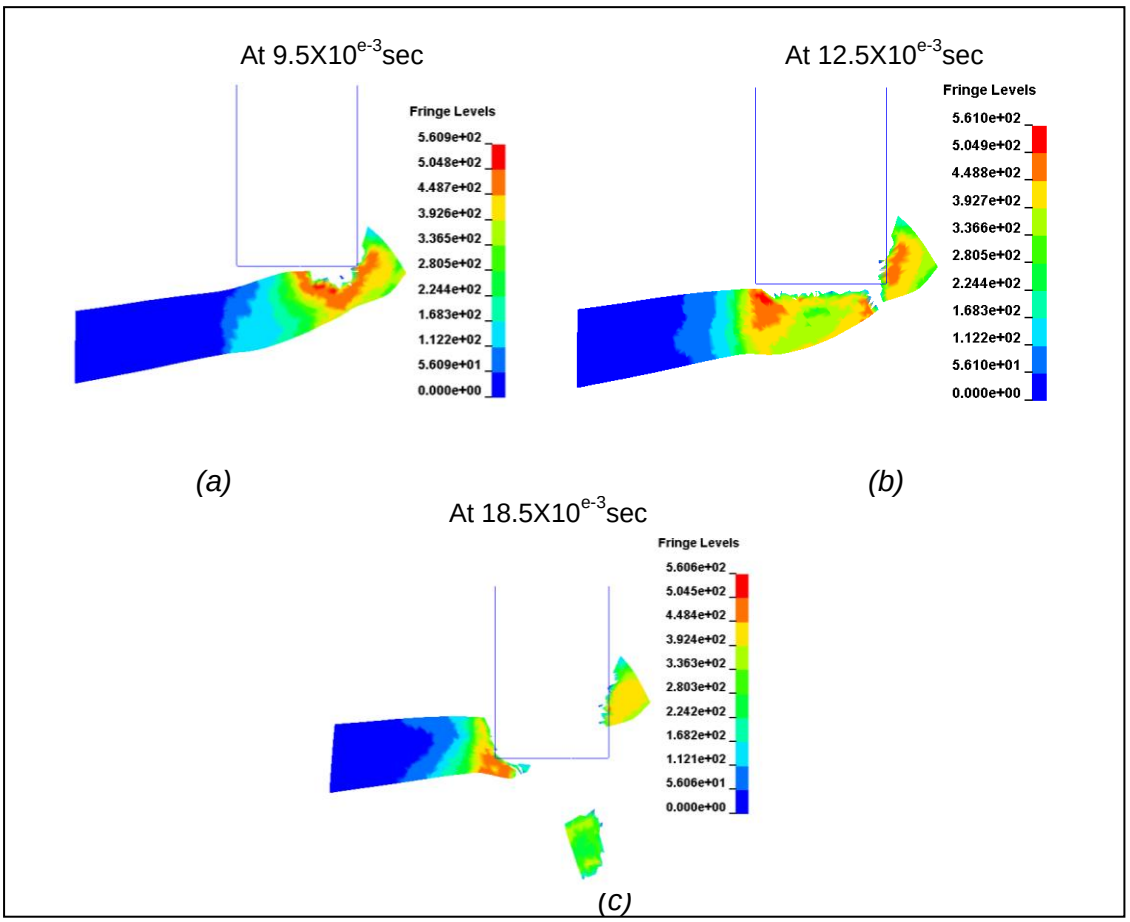

Figure 19.4: Simulation steps for material TM380 with a flat punch (a) punch makes contact with blank, (b) erosion of elements (c) black removed from material

Maximum effective stress	Maximum plastic strain	Maximum eroded volume
560.959 MPa (Element 300762)	0.405 (320860)	abs = 2.302002e-002 ord = 6.628364e-002

Table 19.2: Simulation results for flat punch on HR190 material

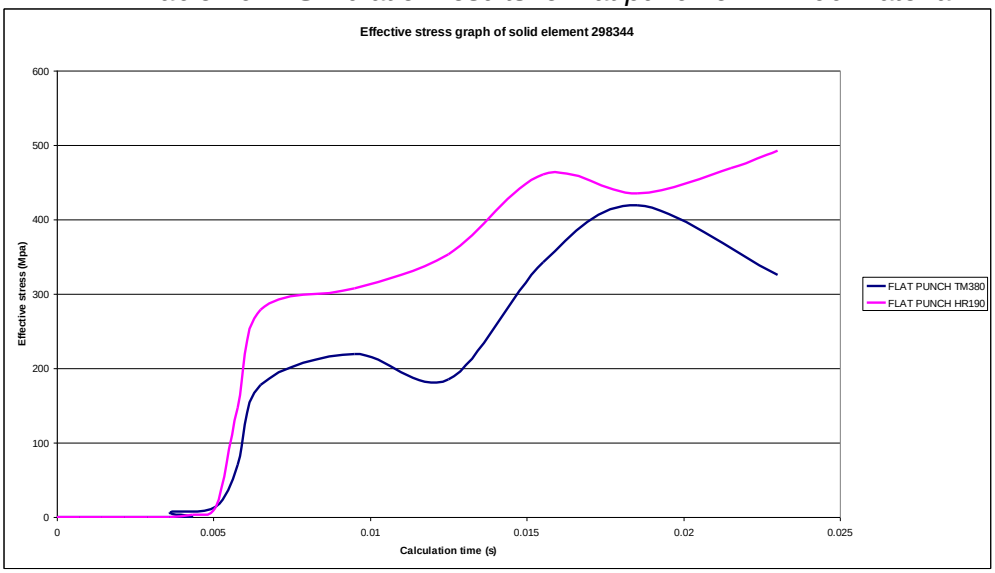

Figure 19.5: Effective stress comparison for solid element 298344 using flat punch for TM380 & HR190 material

A solid element (298244) was selected in a region where the material tearing is expected to occur. This region is where the blank material will experience the maximum plastic strain & thereby cause material failure upon reaching the strain limit. The stresses in this element would be as a result of shear bands created during the piercing process. These are regions of high strain as a result of severe plastic flow. The emergences of shear bands, often are precursors to failure, and can signify the possibility of further deformation.

From the simulation, the solid element in the HR190 material has higher stress loading at the end of the simulation. These could be a result of higher residual stresses in the system. Residual stresses are stresses that remain after the original cause of the stresses (external forces, heat gradient) has been removed. In both simulation no sufficient stresses is transferred to cause any material failure.

19.3 SIMULATION RESULTS WITH A CONCAVE PUNCH – TM380

Below is a sectional view (section normal to the X axis) of the contact during the piercing of a TM30 with a concave punch with a result table for the simulation.

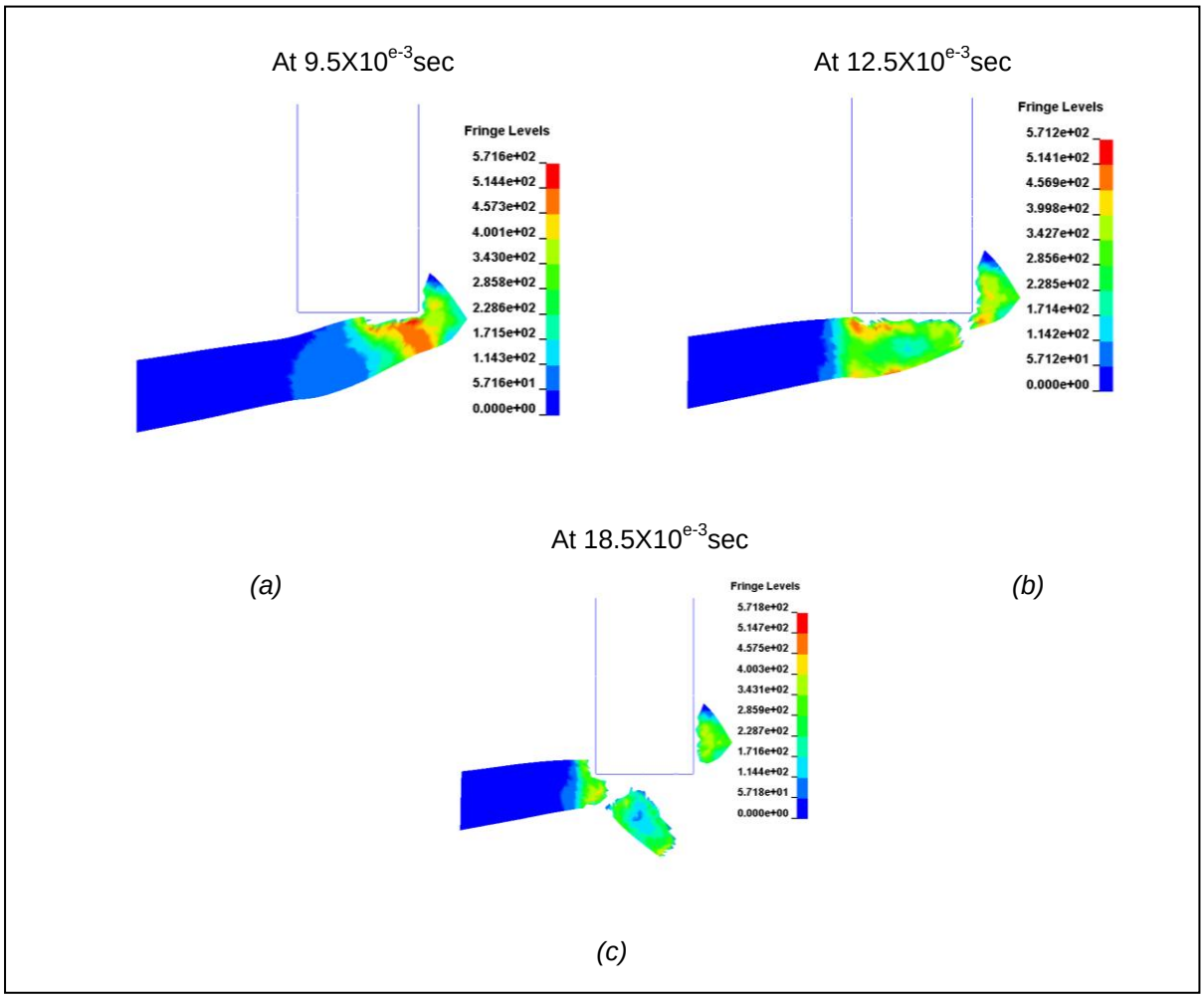

Figure 19.6 Simulation steps for material TM380 with a concave punch (a) punch makes contact with blank, (b) erosion of elements (c) punch makes full contact with blank (c) the blank removed from the blank material

Maximum effective stress	Maximum plastic strain	Maximum eroded volume
661.9 MPa (Element 456531)	0.399 (435826)	abs = 2.302002e-002 ord = 5.642320e-002

Table 19.3: Simulation results for concave punch on TM380 material

19.4 SIMULATION RESULTS WITH A CONCAVE PUNCH – HR190

Below is a sectional view (section normal to the X axis) of the contact during the piercing of a TM30 with a concave punch with a result table for the simulation.

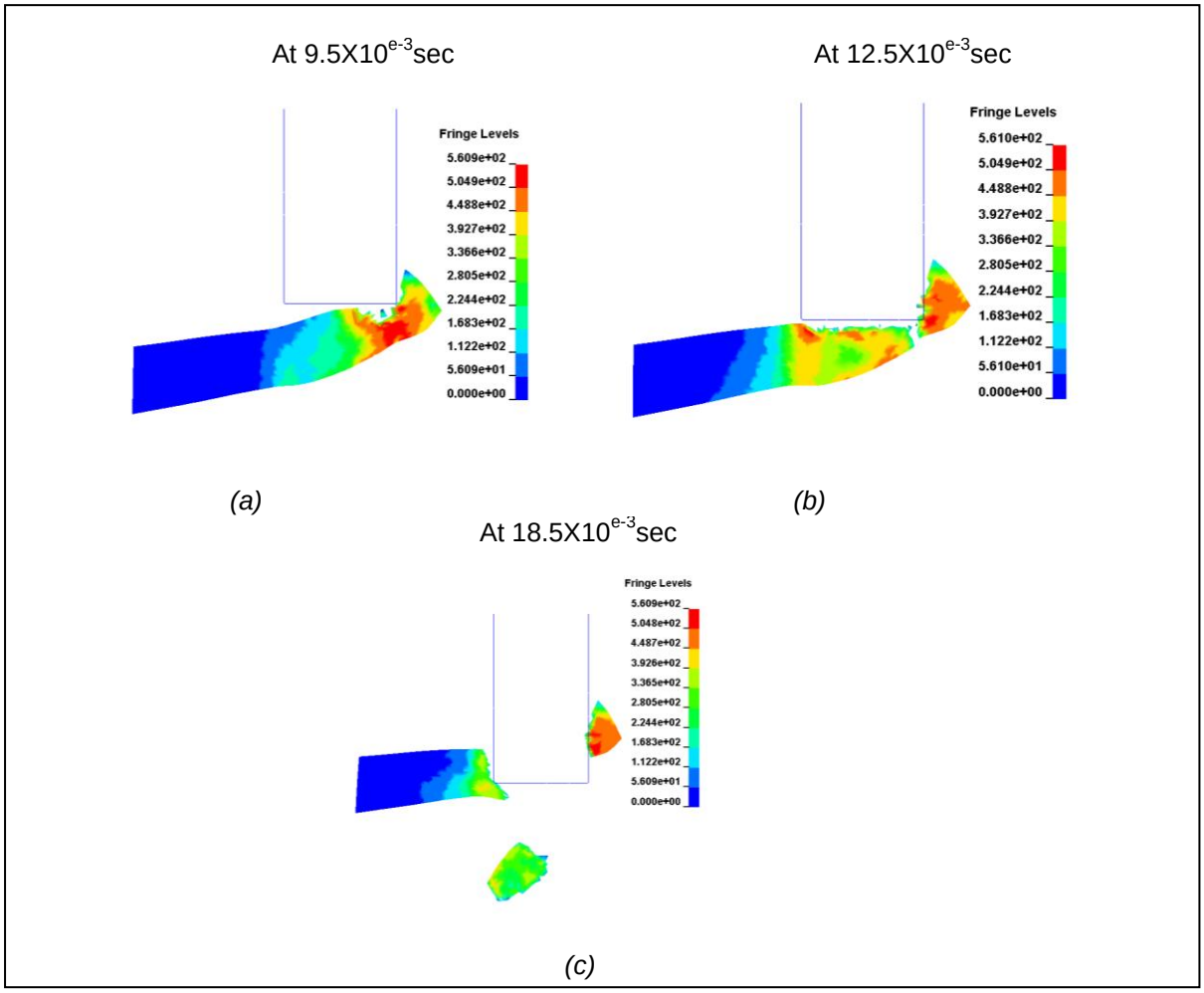

Figure 19.7 Simulation steps for HR190 material with a concave punch (a) punch makes contact with blank, (b) erosion of elements (c) punch makes full contact with blank (c) the blank removed from the blank material

Maximum effective stress	Maximum plastic strain	Maximum eroded volume
556.996 MPa (Element 360333)	0.405 (415992)	abs = 2.170368e-002 ord = 6.143400e-002

Table 19.4: Simulation results for concave punch on HR190 material

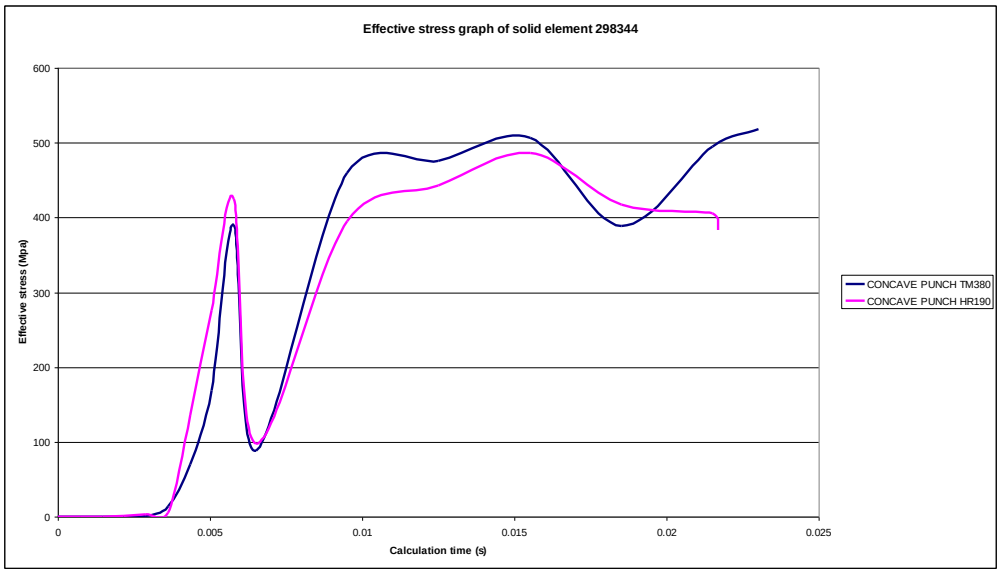

Figure 19.8: Effective stress comparison for solid element 298344 using concave punch for TM380 & HR190 material

Using a concave punch yielded better results. From the punching diagrams (Fig 19.6 & 19.7), the punch designs results in better hole size conformance. The drop in loaded stresses (Fig 19.8) is as a result of the shape punch, where there contact break after the punch starts piercing.

19.5 SIMULATION RESULTS WITH A SHEAR PUNCH – TM380

Below is a sectional view (section normal to the X axis) of the contact during the piercing of a TM30 with a concave punch with a result table for the simulation.

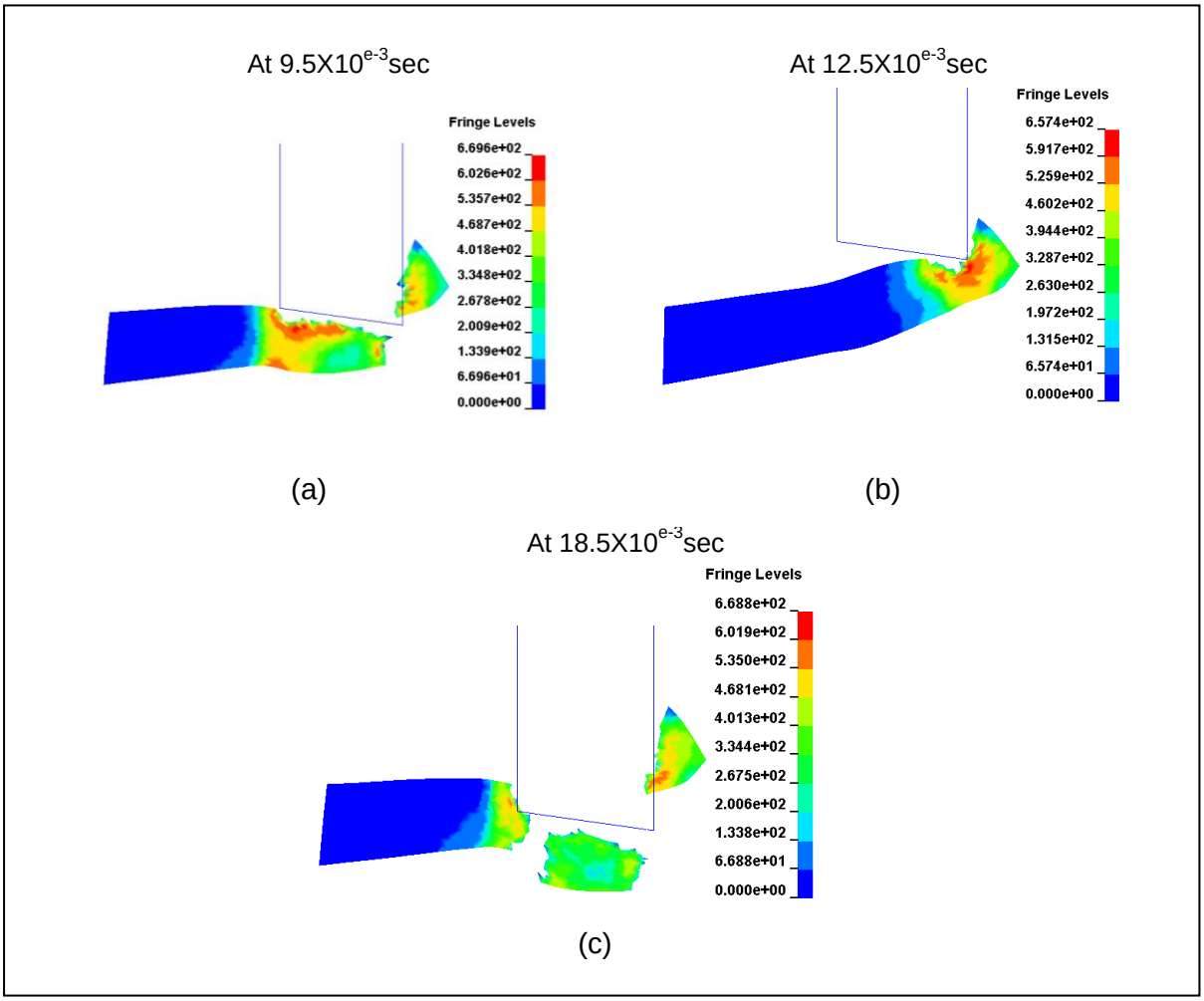

Figure 19.9 Simulation steps for material TM380 with a shear punch (a) punch makes contact with blank, (b) erosion of elements (c) punch makes full contact with blank (c) the blank removed from the blank material

Maximum effective stress	Maximum plastic strain	Maximum eroded volume
556.996 MPa (Element 360333)	0.405 (415992)	abs = 2.170368e-002 ord = 6.143400e-002

Table 19.5: Simulation results for shear punch on TM380 material

19.6 SIMULATION RESULTS WITH A SHEAR PUNCH - HR190

Below is a sectional view (section normal to the X axis) of the contact during the piercing of a HR190 with a concave punch with a result table for the simulation.

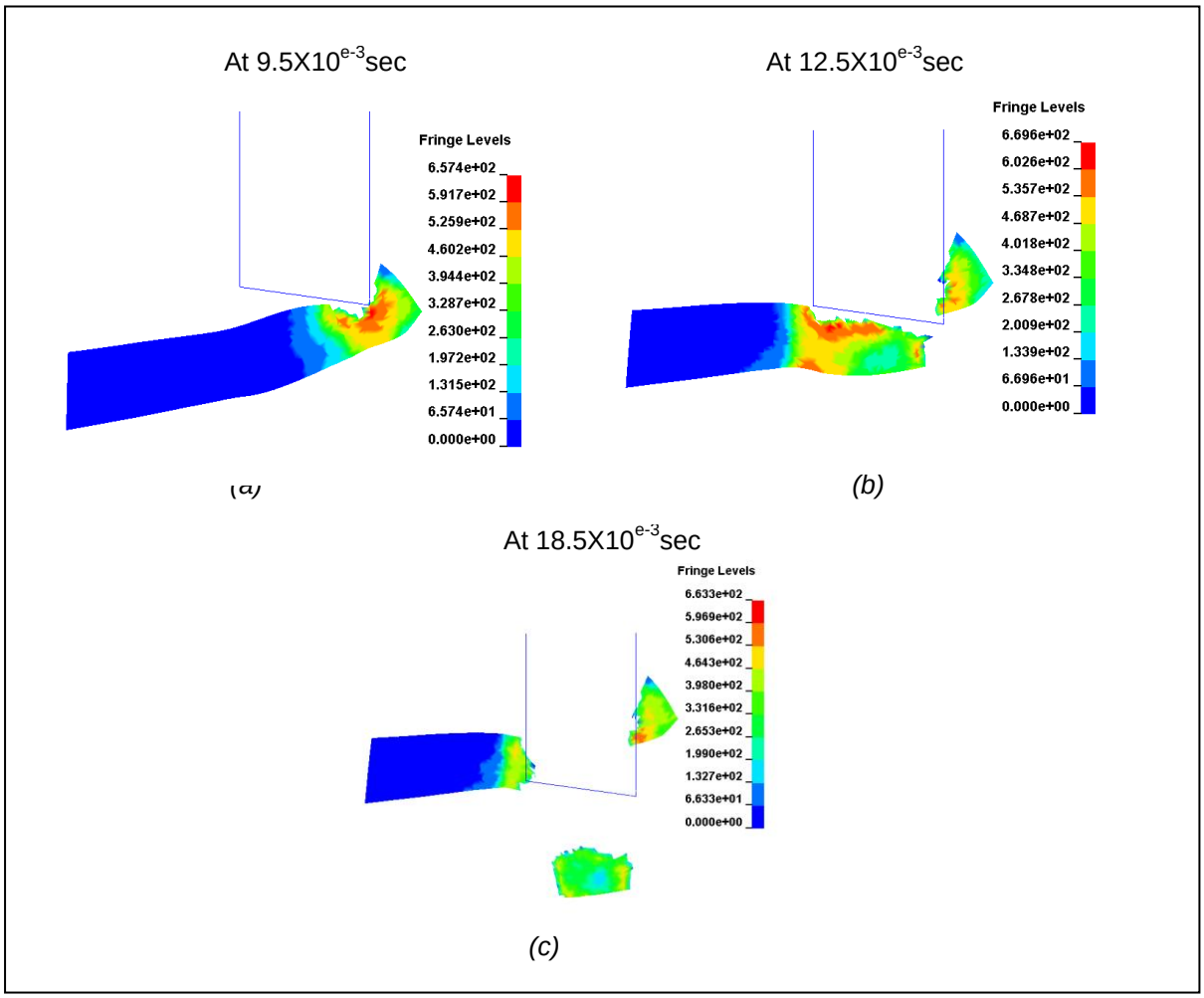

Figure 19.20 Simulation steps for material HR190 with a shear punch (a) punch makes contact with blank, (b) erosion of elements (c) punch makes full contact with blank (c) the blank removed from the blank material

Maximum effective stress	Maximum plastic strain	Maximum eroded volume
560.992 (Element 354789)	0.405 (512548)	abs = 2.302000e-002 ord = 5.731764e-002

Table 19.6: Simulation results for shear punch on HR190 material

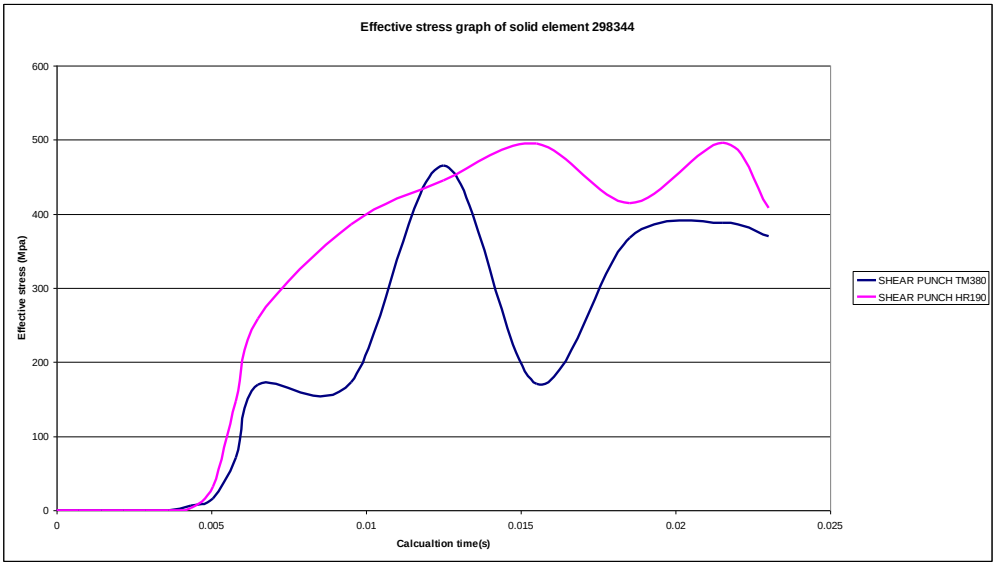

Figure 19.21: Effective stress comparison for solid element 298344 using shear punch for TM380 & HR190 material

19.7 CONCLUSION

Several piercing simulations were run with different punch design (i.e. flat, concave, shear) with the same model parameters on the two different material (TM380 & HR190). HR190 was used as an alternative material to see the simulation results when using a softer, more formable material. From the erosion graphs for each simulation, there is a similar amount of material eroded (+/-0.0564 for TM380 & +/-0.06143 for HR190) in all simulations.

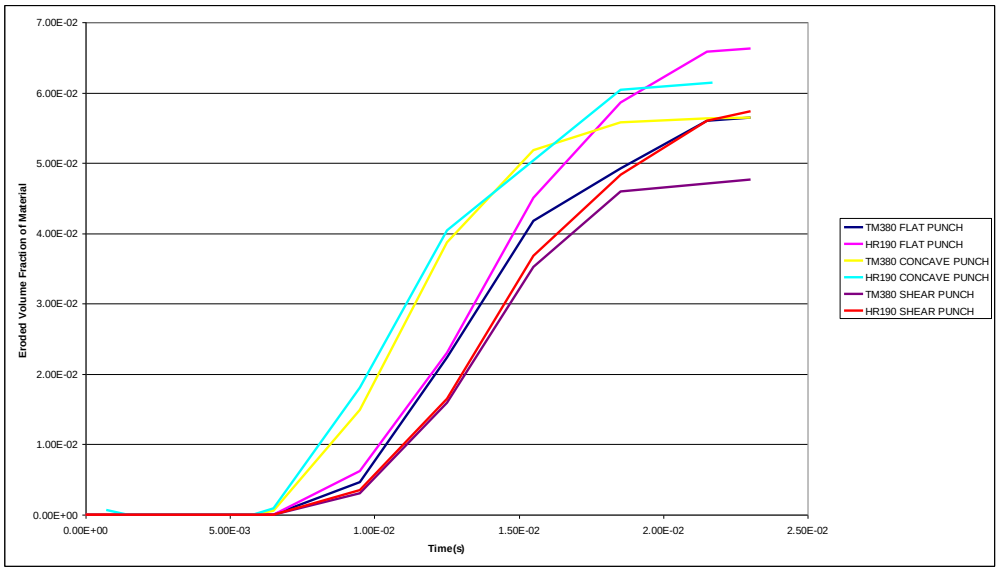

Figure 19.22 Volume of erosion fraction for TM380 & HR190 blank material with different punches designs

Erosion takes place when an element reaches a specified failure strain ot damage value, it is then deleted from the simulation and no longer form part of the calculation. This heavily affects the reliability of the results, since energy is lost, and is not recommended. From the results tables, also, the materials in all simulation experiences similar plastics strain (0.405 max.) with all different punches. This is also evident in the effective plastic graph behaviour. After the piercing process, strain in the system drastically drops.

Using such a continuum model makes it difficult to get proper shear bands to create material separation in the simulation. Shear bands are internal flaws inside the material ands is the key mechanism to explain failure in ductile materials. From the simulation, using all punches, insufficient stresses are transferred to the component neck to cause any material tearing. The absence of shear bands can be rectified by using a different material model which incorporates such material behaviour or using different simulation criteria.

20 IMPROVED SIMULATION RESULTS

20.1 SIMULATION RESULTS FOR TM380 USING SPH

SPH was used in blank definition for these simulations. In these setups the mesh grid is replaced by particles. The particles are defined with a mass and cohesion distance is set between interacting particles. When the distance between particles is more than the critical distance, h, then each particle no longer contributes to the strain calculated at the other and the corresponding cohesive component of the stress disappears. Hence failure of material occurs. Using such method avoids any possible mesh tangling that is normally caused by large deformations.

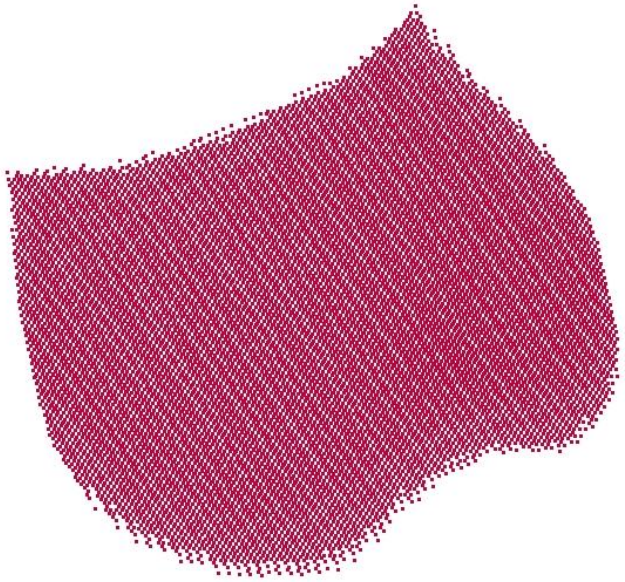

Figure 20.1: Blank definition using SPH

A mass of 9.8124997e-10 (ratio of the density to the volume of the blank) was assigned for each particle in the blank. Because of the lack of a numerical grid, the SPH processor requires some condition in setting the initial masses and coordinates. The particle mesh needs to be enough regular. It means that all the particles of a given neighbourhood need to be of the same masses. As a consequence all the particle of the same material, which have the same initial density, need to have the same initial volume.

The SPH processor has been developed as an extra layer of LS DYNA. Therefore all the actual features of LS DYNA can be used with the particles. Initial velocities, contacts, rigid walls, etc are defined using classical LS DYNA keywords [48]. The contact used in this simulation has been changed from CONTACT_AUTOMATIC_SINGLE_SURFACE to NODE_TO SURFACE. In this contact each slave node is checked for penetration through the master surface. Penalty forces are used to limit penetrations.

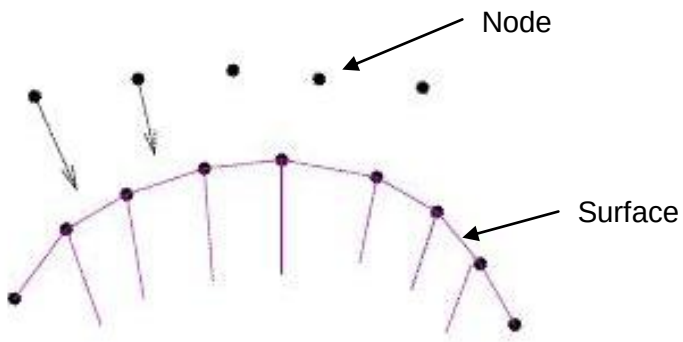

Figure 20.2: Node to surface contact used in SPH

The punching simulation was successful. As the punch made contact with the blank material and the loading caused the particles separations while forming the blank to the expected shape. Fig 20.3 shows a step simulation of the piercing with the TM380 blank material.

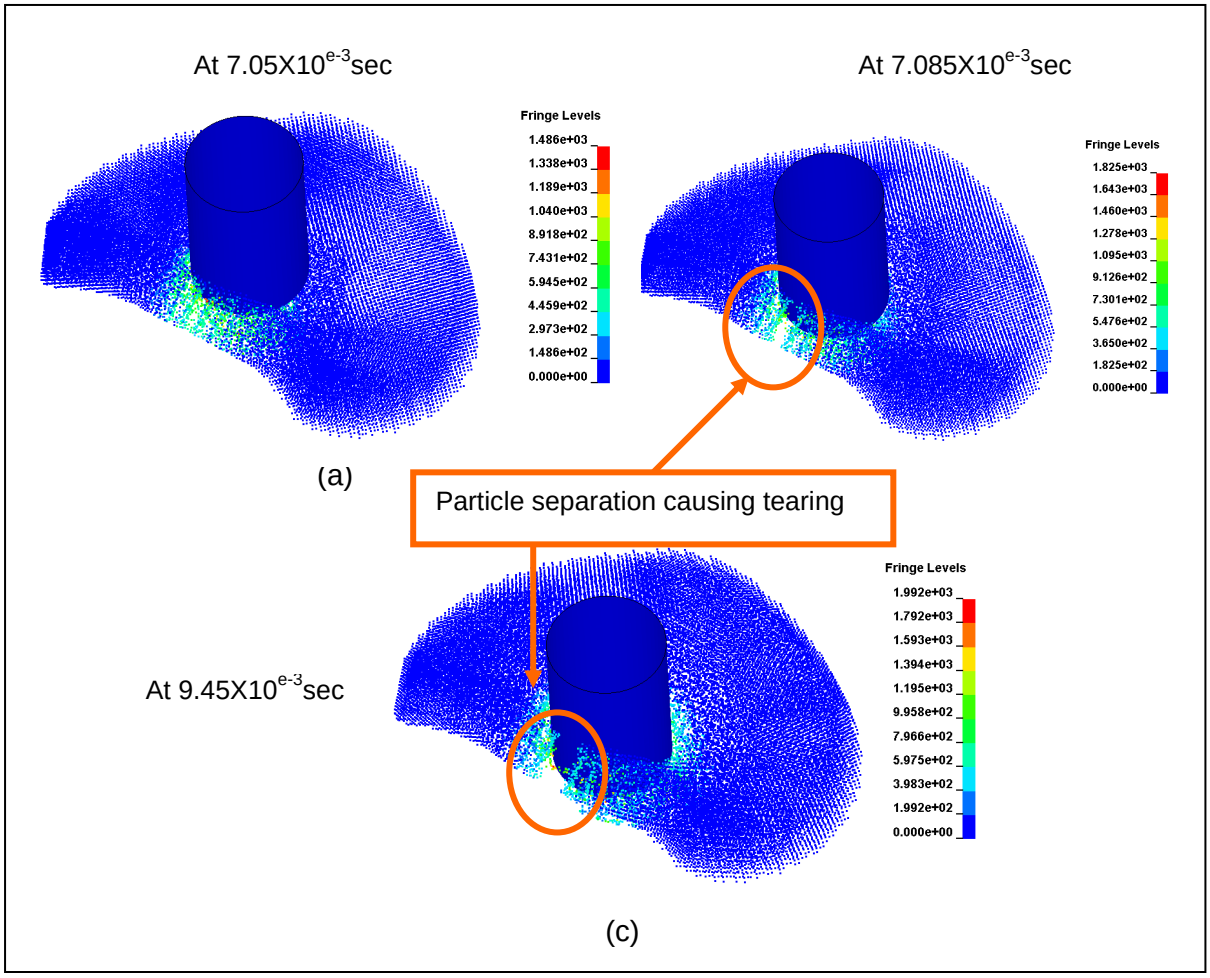

Figure 20.3: Simulation of TM380 with SPH
(a) punch makes contact with blank; (b) punch makes full contact (punch blanked out and material tearing initiation in red circle)(c) tearing initiation on the blank periphery (d) tearing propagate as blanks pushed out punch

From Figure 20.3, the tearing of the material starts from the periphery of the blank. This is as a result of loading on the particles exceeding the cohesion forces between them in that region. This tearing initiation is, however, contradictory to the expected tearing to start from the punch towards the periphery of the material and not vice versa. The higher plastic straining in that region causes the tear initiation (See Figure 20:4 below for component with excessive plastic straining in an unacceptable condition) that normally acts as stress raiser.

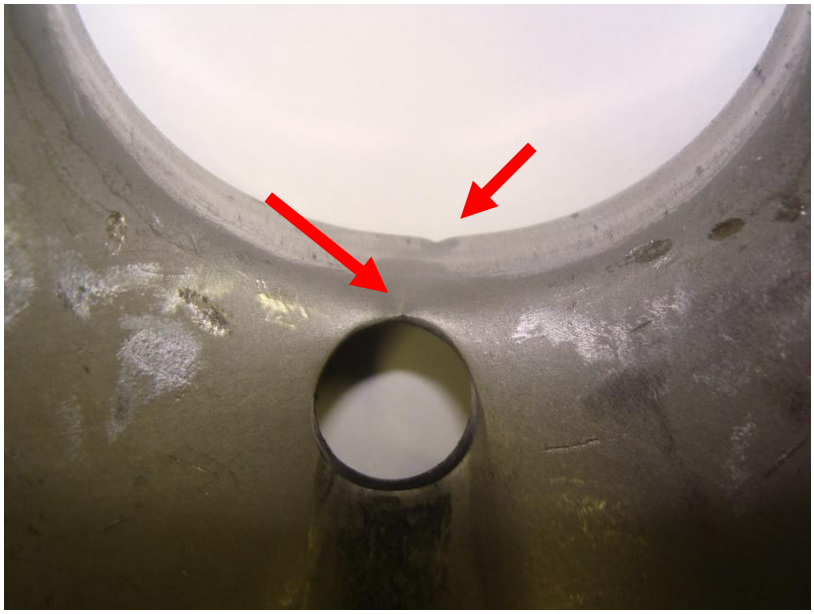

Figure 20.4: Component excessive plastic straining in an unacceptable condition

Since no material erosion in this simulation, little or no energy is lost in the system. The shape of the slug is also in the shape of the punch. This highly influences the reliability of the results.

20.2 SIMULATION RESULTS FOR HR190 BLANK MATERIAL

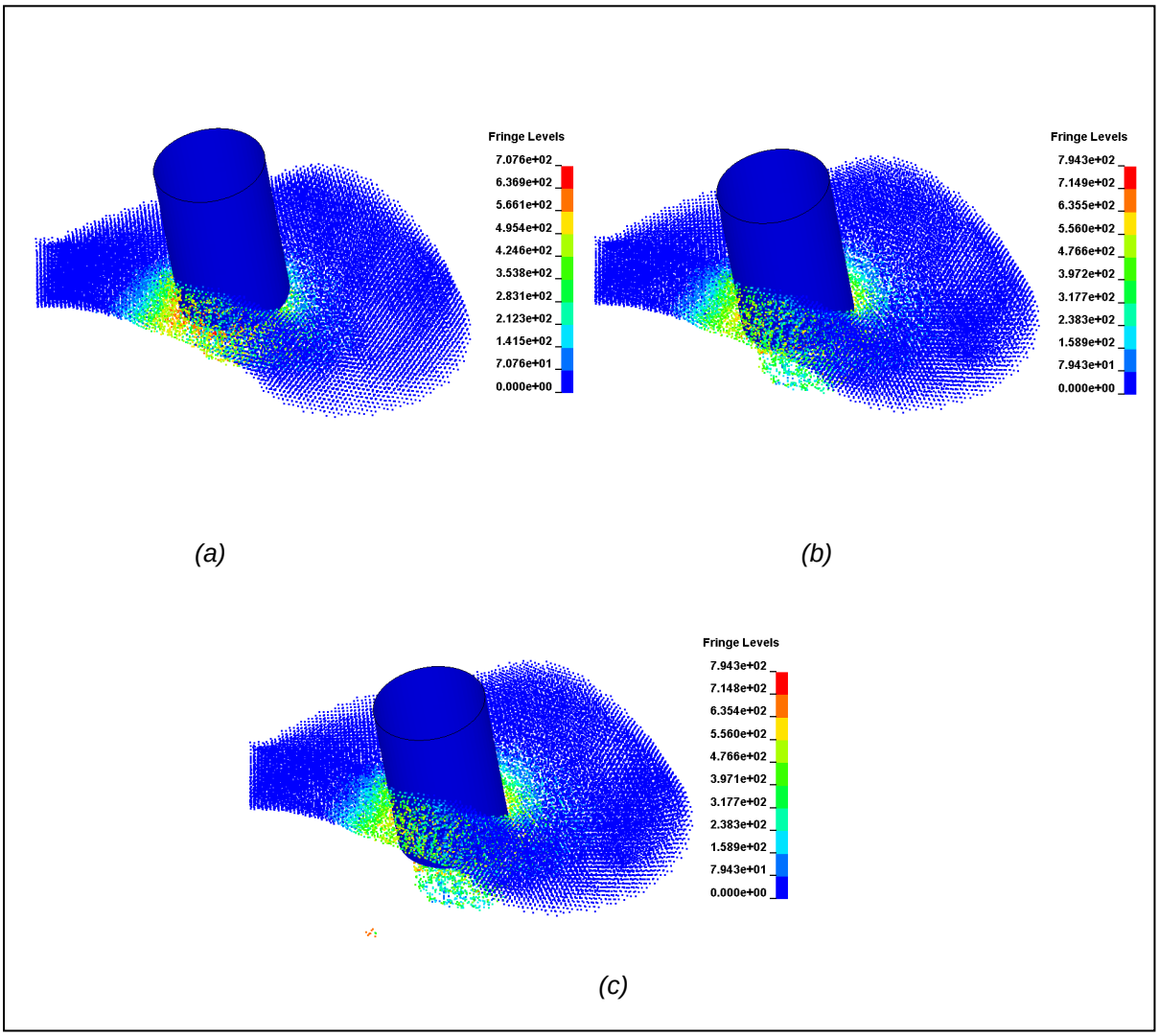

Figure 20.5: Simulation of HR190 with SPH
a) punch makes contact with blank; (b) punch makes full contact (punch blanked out) (c) tearing initiation on the blank periphery (red circle); (d) tearing propagate as blanks pushed out punch

The simulation of the piercing process with a softer HR190 blank material was successful. During the simulations, the setup remained unchanged, except using a material with lower UTS. As a result the material separation was eliminated. Using a softer material also meant that the few stresses distributed around the punch causing any load separation on the particles. Few burrs are evident when using such a material, however within controllable limits.

Figure 20.6: Component in an acceptable conditions

21 CONCLUSIONS AND RECOMMENDATIONS

21.1 SIMULATIONS SETUP

The simulations of the piercing process were done using both a continuum finite element solution method and using the Smoothed Particle Hydrodynamics method. For both the simulation methods the piercing process was successful. Actual process parameters, from a production facility, were used in the simulations, to make the results as realistic as possible. The punching speed was taken to be the press machine stroke speed. Tensile tests on the different blank materials were used for the input data for material behaviour definitions for the simulations. This was in the form of a flow curve.

The simulations were conducted for a range of process parameters, starting with the harder material (TM380) and the softer material (HR190) and using different punch geometries. Such an approach was geared towards modelling of material failure, either in form of material separation, or any defects, e.g. stress raisers, abnormal burrs, excessive material stretching, etc. and then modelling of the improved material. Such material conditions characteristics plays an important role since the operation in focus, forms part of a combination of pre and post operations (progressive tool) that could result in blank material failure.

Often tensile test specimens may have defects region that has a slightly lower load-carrying capacity than the material used for the operations however great care was taken into considerations to minimise any chance of such errors. Various material behaviour predictions laws with strain hardening definitions are also available in LS DYNA, e.g. Holloman's law, Power laws, etc for definition of material flow curves.

21.2 THE CONTINUUM MODEL

In the continuum model setup, solid elements, were used in the definition of the blank material, hence the results from the simulations becomes mesh dependant. Bigger elements size would yield different results as compared to smaller mesh size. Using a smaller elements size would have high computational time. An element size balance was reached such that the results would be as accurate as required without higher monetary costs as a result of prolonged computations time. The punch was defined as a rigid shell element with a boundary velocity profile for the loading onto the blank material & hence the formations of the hole.

The die was also assigned as stationery. Different punch designs (flat, shear, concave) were also to gauge the sensitivity of the results. Using such punch designs is recommended for proper distribution of the load during piercing. The punching simulations were run successfully.

Using a visco-elastic (MAT_24) allowed for further material criterions to be included (in this case MAT_ADD_EROSION). This option provided a way of including failure in models, although the option can also be applied to constitutive models with other failure/erosion criteria. The options allows setting up of failure criterion (in this case effective stress at failure), such that when the element experiences certain strain level it is deleted from the simulations. Using such criteria would force elements to be strained under loading and ultimately the formations of the hole. The limitations of the erosion criteria were that any deletion of elements resulted in energy loss in the system. These energy losses affected the accuracy of the results.

For measuring the quality of the hole pierced the roll over, burnished and fracture zone are critically. Fracture is often synonymous with tensile burr. Using such a model was causing a lot of element deletions and affecting the accuracy of the hole size. Hole size conformance is a critical factor used for the analysis also. As a result, the material definition was changed. This was also influenced by the fact that Lagrangian computational model becomes inadequate when severe element distortion is involved. This was evident by the shape of the blank shape after the piercing process. As a result a meshless method (or particle method) called SPH was used to improve the simulation.

21.3 SPH

Using SPH as material definition for the blank material gave insight on the extent of the fracturing of the material. This method allowed for the blank to be defined using particles instead of mesh. SPH material definition allows for severe material deformations and is most suitable for such applications. Several research has been conducted using such material definitions methodology (e.g. for military applications), however limited. The procedural information on implementing such a method is limited also.

When using SPH, severe fracturing was evident in the simulations using TM380. The loading was causing enough shear bands to cause the material separations in a similar pattern as in reality. Using a softer material, HR190, as a replacement reduces the stress distributions and eliminated the material separations. Even though there was evidence of burrs, or observable fracture on the that could cause the material to fail in further operations, the results where giant leap as compared to the TM380 material or other models used in this simulations. Deviation for results expected can be explained by different factors using SPH. Particles defined can be insufficient to represent the actual material behaviour. Increasing material particles has a high increase in computational time. The punching velocities assumed can also cause results to deviate. Further research using SPH needs to be conducted for further enhancement of solutions for such cases.

21.4 LIMITATIONS OF BOTH MODEL SETUPS

During the piercing process, in the practicality sense, a combination of loading from punch on material and die impression causes the blanking shape. The material shearing is often caused by the load against the die edges, and the edge ultimately causing the material to separate in the shape of the punch and edge. The results of such is the formation of burnished, metering and the shear zone in the hole (see chapter 5 Piercing Process for explanations of such phenomenon). In the piercing simulation, the boundary conditions applied to the punch (velocity) and blank (stationary). The tearing is caused by the loading of the punch to the blank material, with a failure criterion applied. In addition, minimisation of this forming load is preferable to increase die life by lowering the peak cyclic stresses.

The piercing operation forms part of a combination of operations (also) in the press tool. As a results accumulative effects, which include burr formations, material strain hardening, material forming, any stress raises, heavily influence the piercing being analysed. A pre-existing defect in the sheet metal, such as a local reduction in either thickness or strength, can have a large effect on the strain to failure. Furthermore, any post operations to the analysed areas, cropping, forming, could also be attributed to material failure in the area of focus.

The inclusion of strain rate effects in the simulation can result in variable material behaviours. For the purpose of this simulation one material flow curve at 0.16 s^{-1} strain rate was used as starting point for material behaviour. Different material flow curves can be defined in form of a table in the input deck. Different strain rates (min, max, and standard as per ASTME handbook) could be used for material flow definitions. The simulations would be such that during the simulations solving the stress versus effective plastic strain curve for the lowest strain rates is used is the strain rate fall below the minimum value. Intermediate values are found by interpolating between curves. Effective plastic strain versus yield stress is expected. Likewise, the stress versus the effective plastic strain curve for the highest value of strain rate is used if the strain rate exceeds that maximum values

Several effects can affect the reliability of the results during the simulation. During the simulations mass is added to the simulations to reduce computational time. Such mass addition can results in high internal energy. For more results reliability, an average of 10% difference between the kinetic and internal energy must be maintained in the simulations. However such a balanced is required when punching velocities are assumed or factorised to increase simulations computational times.

The simulation scope also does not take it consideration and friction between the interacting components. Frictions coefficient is a highly influential factor in controlling how material flows during such processes where material are severely stretched, formed or when material separations is involved.

The engineering used in this simulation approach also assumes that the die-face deformations during the piercing process are negligible and the industrial practice has proved the validity of this assumption. This notion of an ideally rigid die construction may nevertheless be questionable when it comes to the punching/forming of high strength steel due to higher forming loads.

Finally testing and simulation of the piercing process is recommended as it would great give an in- site to the material behaviour, mechanical properties, and press machine settings parameters. An accurate representation would greatly reduce the

amount of time spent during the tool try-out phase and the amount of prototypes required.

21.5 FUTURE WORK

Further challenges in researches of this nature remains and any developments that would provide any further manufacturing defects reduction will be of great benefit. An increase in the material data for common steels (preferably high strength steels) would hugely influence an increase capabilities of solving such problems.

This study can form foundations for further researches in using SPH for such applications where large distortions are experienced. SPH can also be used efficiently in the modelling of high speed machining of special materials. The possibility of using such methods is limitless. Further research in improving accuracy of such an applications, to reduce the possibility of errors, is also recommended. The potential benefit of solving problems using FEA and such simulations packages in a highly competitive manufacturing environment should not be in doubt. The prolonged time in tool modification and tool tryout can easily cost small companies high monetary cost which could have easily been avoided.

22 BIBLIOGRAPHY

1. Department of Trade and Industry. “Metals and Engineering study”. Jun. 2005 http://www.nedlac.org.za/research/fridge/metals/exec-summary.pdfFRIDGE study journal/article [July 2005]

2. Elanchezhian, C. Sunder C, Vijaya S.R.B. Design of Jigs, Fixtures and Press Tools. Chennai: Eswar Press, 2004.

3. Troxell, D, Clement, T. Wiskocil. The Testing and Inspection of Engineering Materials. New York: McGraw-Hill Book Company, 1964.

4. Collins, J.A. Failure of Materials in Mechanical Design: Analysis, Prediction, Prevention. New York: John Wiley & Sons, Inc, 1993

5. Benham, H.Russel, H. Thermal stress. London: Sir Isaac Pitman & Sons, 1964.

6. Widas, P. Introduction to Finite Element Analysis. Virginia Tech Material Science and Engineering, http://www.sv.vt.edu/classes/MSE2094_NoteBook/97ClassProj/num/widas/history.html [Aug. 1997].

7. ASTME Handbook

8. MacCormack, C. Monaghan, J. A finite element analysis of cold forging dies using two and three dimensional models. Journal of Materials Processing Technology 118 (2001) 286 – 292.

9. Lange, K. Hettig, A. Knoerr, M. Increasing Tool Life in Cold Forging Through Advanced Design and Tool Manufacturing Techniques, Elsevier, Amsterdam, 1992.

10. I. Jung, V. Lubich, H.-J.Wieland. Tool failure – Causes and Prevention [online], pp 1343-1360. http://www.ingvet.kau.se/mtrl/fo/pub/itc/93_1343_1362.pdf

11.. Duggan James Bryne, T.V. Fatigue as a criterion, London and Basingstoke: The Macmillan Press LTD, 1997.

13. Skov-Hansen, P et al. Fatigue in cold-forging dies: tool life analysis [online], pp 41-46. Journal of Materials Processing Technology 95 (1999) 40 - 48 http://www.sciencedirect.com, [09 July 2007].

14. Smoothed Particle Hydrodynamics. From Wikipedia, the free encyclopedia. http://en.wikipedia.org/wiki/Smoothed_particle_hydrodynamics. [2 November 2008]

15. Satorres, A. Bending Simulation of High Strength Steel by Finite Elements Master's Thesis, University of Oulu. Department of Mechanical Engineering: 2005

16. Jenberg, A. A method for modifying the tool geometry in order to compensate for spring back effects. Engineering Research Nordic AB, Linkoping, Sweden. Proceeding to the 4th LS DYNA Users Conference. 22 – 23 May 2003.Ulm, Germany.

17. Lee, S.W. Joun, M.S. Rigid-viscoplastic finite element analysis of the piercing process in the automatic simulation of multi-stage forging processes. Journal of Materials Processing Technology 104 (2000) 207 – 21. http://www.sciencedirect.com, [31 0ctober 2008].

18. Gernot, O, Dell, H. Dell, D, Gese, H. Enhanced failure prediction in sheet metal forming simulation by coupling LS DYNA with algorithm CRACH. Proceeding to the 7th Annual LS DYNA users conference. 30 - October 1, 2008, Bamberg, Germany

19. Bradley N. Maker, Xinhai Zhu. Input Parameters for Metal Forming Simulation using LS-DYNA. Livermore Software Technology Corporation, April 2000.

20. Schwer, L.E. Hacker, K. Poe, K. Perforation of Metal Plates, Laboratory Experiments and Numerical Simulations. Proceedings to the 9th Annual LS DYNA users conference. June 4 – 6 2006, Dearborn, Michigan, USA.

21. Skinner, G, Lam, D. SPH Perfomance in LS DYNA. Proceedings to the 8th Annual LS DYNA users conference. May 2-4, 2004, Dearborn, Michigan, USA.

22. Dominique, L. Lacome, J, DYNALIS, Paris, France. Simulations of Hypervelocity Impacts With Smoothed Particle Hydrodynamics.

23. Supraform TM 380 and HR datasheet. Supplied by StripSteel: South Africa

24. Hallquist, J.O, LS-DYNA Theoretical Manual, Livermore Software Technology Corporation, Report 1998

25. Brian, AC. 2002. Piercing of Aluminium beverage cans. . Proceedings to the 8th Annual LS DYNA users conference. May 2-4, 2004, Dearborn, Michigan, USA.

26. Han-Ho, C et al. Design of a piercing hole in coining process by the three-dimensional backward tracing scheme of the FEM. Pusan National University, Pusan 609 -735, South Korea

27. Dutton, T. The review of sheet metal forming simulation, progress to date, future developments. Dutton Simulation Ltd. . Proceedings to the 8th Annual LS DYNA users conference. May 2-4, 2004, Dearborn, Michigan, USA.

28. Svensson, C. The Influence Of Sheet Thickness On The Forming Limit Curve for Austenitic Stainless Steel. Maskiningenjörsprogrammet. 2004.

29. Hong Y,Jian C. Prediction Of Forming Limit Curves Using An Anisotropic Yield Function with Prestrain Induced Backstress. Department Of Mechanical Engineering, Northwestern University, Evanston, Il 60208, USA.

30. Bauer, H. Mihsein, H. State of the art in the use of (LS-DYNA) forming simulation in hydroforming and preceding processes, Third European LS-DYNA Conference Paris, France, June 18–19 (2001).

31.Roylance, D. Stress-Strain Curves, Department of Materials Science and Engineering. Massachusetts Institute of Technology. Cambridge, MA 02139 August 23, 2001.

32. Donaldson, C et al. Tool Design 3rd Edition. Tata Mcgraw-Hill Publishing Company Limited, 1976. New Dehli.

33. Paquin, J.R. Crowley, R.E. Die Design Fundamentals 2nd Edition, 1987. Industrial Press Inc, New York, New York 10016.

34. Céline, G. SPH: A solution to avoid using erosion criteria? Ensica, 31056 Toulouse Cedex.

35. Murat, B. Cing-Dao, S. K, Nabin E.B. The George Washingto University, National Crash Analysis Centre. Proceedings to the 8th Annual LS DYNA users conference. May 2-4, 2004, Dearborn, Michigan, USA.

36. Chung, TJ. Applied continuum mechanics. Cambridge, UK: Cambridge University Press, January 1996 .

37.Calladine, C.R. (1985) Plasticity for Engineers Ellis Horwood Series in Engineering Science. Ellis Horwood. Chichester.

39. Mase, G.T,Mase, G.E. Continuum mechanics for engineers. Published by CRC Press, 1999.

40. David Henwood, D. Bonet, J. Finite elements: a gentle introduction. Palgrave Macmillan November 1996.

41. Belytschko, T. Liu, WK. Brian. Nonlinear finite element analysis for continua and structures. Wiley; 1 edition. September 12, 2000.

42. Kurt Lange, Arndt Hettig and Markus Knoer. Increasing tool life in cold forging through advanced design and tool manufacturing techniques [online], pp 496-

43. Peter Vogel. Sheet Metal forming with eta/DYNAFORM and LS DYNA training notes. May 2007. Dynamore GmbH.

44. M.J. Ward, M.J. Miller, B.C. Davey, K. Simulation of a multi-stage railway wheel and tyre forming process. Journal of Materials Processing Technology 80 – 81 (1998) 206 - 212.

45. LS-DYNA Theoretical Manual. 2002. Livemore Software Tecnhology Corporation.

46. LS-DYNA support. Livemore Software Tecnhology Corporation. http://www.dynasupport.com

46. LS-DYNA Keyword Users Manual. 2002. Livemore Software Tecnhology Corporation.

47. Engineering Technology Associate, Inc. eta/DYNAFORM Modules. http://www.eta.com/index.php?option=com_content&task=view&id=1&Itemid=27

48 Smoother Particle Hydrodynamics: a new feature in LS DYNA. Jean Luc Lacome. Dynalis.

49 Smoothed Particles Hydrodynamics: Method in LS DYNA. Proceedings to the Annual LS DYNA user's conference. October 14 – 15 2004, Bamberg, Germany.

50 Ambati R. Simulation and Analysis of Orthogonal Cutting and Drilling Processes using LS-DYNA. University of Stuttgart, Germany. December 2007

23 APPENDICES

23.1 Appendix A – INPUT DECK CONTINUUM MODEL FOR TM380

```
$ ETA/DYNAFORM : DYNA3D(971) INPUT DECK
$ DATE : Oct 15, 2008 at 17:11:42
$ VERSION : eta/DYNAFORM 5.6  , built on Jan  3 2008
$ EXPORTER : AUTO-SETUP
$
$ VIEWING INFORMATION
$    -43.60229    29.50944   -47.28976    -5.92261
$   -0.1306481  -0.9880627  0.08162858
$   -0.3905243   0.1269631   0.9117956
$   -0.9112741  0.08724742  -0.4024518
$
$ UNIT SYSTEM : MM, TON, SEC, N
$
$ SIMULATION  : SHEET FORMING
$
$---+----1----+----2----+----3----+----4----+----5----+----6----+----
7----+----8
$
$*KEYWORD_ID
$piercing_mbavhi
*KEYWORD
$
$---+----1----+----2----+----3----+----4----+----5----+----6----+----
7----+----8
$
$                    (1) TITLE CARD
$
$---+----1----+----2----+----3----+----4----+----5----+----6----+----
7----+----8
*TITLE
SIM_MBAVHI
$---+----1----+----2----+----3----+----4----+----5----+----6----+----
7----+----8
$
$                    (2) CONTROL CARDS
$
$---+----1----+----2----+----3----+----4----+----5----+----6----+----
7----+----8
*CONTROL_TERMINATION
$   ENDTIM    ENDCYC     DTMIN    ENDNEG    ENDMAS
 0.0230225         0                           0.0
*CONTROL_TIMESTEP
$   DTINIT    TSSFAC      ISDO    TSLIMT     DT2MS      LCTM
ERODE     MS1ST
       0.0       0.9         0       0.0 -1.00E-07
*CONTROL_RIGID
$      LMF      JNTF    ORTHMD     PARTM    SPARSE    METALF
                                                           1
*CONTROL_HOURGLASS
$      IHQ        QH
         4       0.1
*CONTROL_BULK_VISCOSITY
$       Q1        Q2      TYPE
       1.5      0.06         1
*CONTROL_SHELL
```

```
$   WRPANG     ESORT     IRNXX    ISTUPD    THEORY       BWC
MITER      PROJ
      20.0         1        -1         1         2         2
1         0
$  ROTASCL    INTGRD    LAMSHT    CSTYP6    TSHELL    NFAIL1
NFAIL4

$  PSSTUPD    IRQUAD

*CONTROL_CONTACT
$   SLSFAC    RWPNAL    ISLCHK    SHLTHK    PENOPT    THKCHG
ORIEN
       0.1       0.0         2         1         4         0
1
$   USRSTR    USRFAC     NSBCS    INTERM     XPENE     SSTHK
ECDT   TIEDPRJ
         0         0        10         0       4.0         0
*CONTROL_ENERGY
$     HGEN      RWEN    SLNTEN     RYLEN
         2         1         2         1
*CONTROL_OUTPUT
$    NPOPT    NEECHO    NREFUP    IACCOP     OPIFS    IPNINT
IKEDIT
         1         0         0         0       0.0         0
100
*CONTROL_PARALLEL
$     NCPU    NUMRHS     CONST
         1         0         2
*CONTROL_ACCURACY
$      OSU       INN
         0         1
$*CONTROL_ADAPTIVE
$  ADPFREQ    ADPTOL    ADPOPT    MAXLVL    TBIRTH    TDEATH
LCADP    IOFLAG
$0.0011511       5.0         2         3       0.0 1.000E+20
1
$  ADPSIZE    ADPASS    IREFLG    ADPENE     ADPTH    MEMORY
ORIENT     MAXEL
$    1.0         1         0       1.0      -0.5                    0
0
$  IADPE90              NCFREQ    IADPCL    ADPCTL    CBIRTH
CDEATH
$     -1                   0         1       0.0       0.0 1.000E+20
$*CONTROL_ADAPSTEP
$   FACTIN    DFACTR
$    1.0      0.01
$*INTERFACE_SPRINGBACK_LSDYNA
$     PSID
$      1
*CONTROL_SOLID
1
$---+----1----+----2----+----3----+----4----+----5----+----6----+----
7----+----8
$*DATABASE_OPTION
$       DT    BINARY
$OPTION : SECFORC RWFORC NODOUT ELOUT  GLSTAT
$         DEFORC  MATSUM NCFORC RCFORC DEFGEO
$         SPCFORC SWFORC ABSTAT NODFOR BNDOUT
$         RBDOUT  GCEOUT SLEOUT MPGS   SBTOUT
$         JNTFORC AVSFLT MOVIE
$*DATABASE_RCFORCE
```

```
*DATABASE_RCFORC
 4.604E-05
*DATABASE_MATSUM
 4.604E-05
*DATABASE_GLSTAT
 4.604E-05
*DATABASE_SLEOUT
 4.604E-05
*DATABASE_RBDOUT
 4.604E-05
*DATABASE_BNDOUT
 4.604E-05
$*DATABASE_ABSTAT
$ 4.604E-05
$---+----1----+----2----+----3----+----4----+----5----+----6----+----
7----+----8
*DATABASE_BINARY_D3PLOT
$  DT/CYCL      LCDT      BEAM
                   1
*DATABASE_EXTENT_BINARY
$    NEIPH     NEIPS    MAXINT    STRFLG    SIGFLG    EPSFLG
RLTFLG    ENGFLG
                               5         1
$   CMPFLG    IEVERP    BEAMIP     DCOMP      SHGE     STSSZ
                   1                    2
$---+----1----+----2----+----3----+----4----+----5----+----6----+----
7----+----8
$
$                    (3) DEFINE BLANK
$
$---+----1----+----2----+----3----+----4----+----5----+----6----+----
7----+----8
*SET_PART_LIST
$SET_PART_NAME: BLANK
$      SID       DA1       DA2       DA3       DA4
         1
$     PID1      PID2      PID3      PID4      PID5      PID6
PID7      PID8
         1
*PART
$HEADING
 PART PID =        1 PART NAME :001V000
$      PID     SECID       MID     EOSID      HGID      GRAV
ADPOPT      TMID
         1         1         1
*MAT_PIECEWISE_LINEAR_PLASTICITY
$MATERIAL NAME:DQSK
$      MID        RO         E        PR      SIGY      ETAN
FAIL      TDEL
         1 7.850E-09 2.070E+05      0.28
$        C         P      LCSS      LCSR
       0.0       0.0         2
$     EPS1      EPS2      EPS3      EPS4      EPS5      EPS6
EPS7      EPS8
       0.0       0.0       0.0       0.0       0.0       0.0
0.0       0.0
$      ES1       ES2       ES3       ES4       ES5       ES6
ES7       ES8
       0.0       0.0       0.0       0.0       0.0       0.0
0.0       0.0
*SECTION_SOLID
```

```
$       SID    ELFORM       AET
          1         1
*MAT_ADD_EROSION
$#     mid      excl
          1
$#   pfail     sigp1     sigvm     epsp1     epssh     sigth
impulse    failtm
     0.000     0.000    670.35
$---+----1----+----2----+----3----+----4----+----5----+----6----+----
7----+----8
$
$                    (4) DEFINE TOOLS
$
$---+----1----+----2----+----3----+----4----+----5----+----6----+----
7----+----8
$---+----1----+----2----+----3----+----4----+----5----+----6----+----
7----+----8
$                     TOOL < 10_die >
$---+----1----+----2----+----3----+----4----+----5----+----6----+----
7----+----8
*SET_PART_LIST
$SET_PART_NAME: 10_die
$       SID       DA1       DA2       DA3       DA4
          2
$     PID1      PID2      PID3      PID4      PID5      PID6
PID7      PID8
          4
*PART
$HEADING
 PART PID =         4 PART NAME :IE
$       PID     SECID       MID     EOSID      HGID      GRAV
ADPOPT      TMID
          4         2         2
*MAT_RIGID
$       MID        RO         E        PR         N    COUPLE
M     ALIAS
          2 7.830E-09 2.070E+05      0.28
$       CMO      CON1      CON2
          1         7         7
$LCO or A1        A2        A3        V1        V2        V3

*SECTION_SHELL
$       SID    ELFORM      SHRF       NIP     PROPT   QR/IRID
ICOMP     SETYP
          2         2       1.0       3.0       0.0
$        T1        T2        T3        T4      NLOC
        1.0       1.0       1.0       1.0
*CONTACT_AUTOMATIC_SINGLE_SURFACE
$#     cid
title
$#    ssid      msid     sstyp     mstyp    sboxid    mboxid
spr       mpr
         50         0         2         0         0         0
1         1
$#      fs        fd        dc        vc       vdc    penchk
bt        dt
  0.125000  0.125000     0.000     0.000     0.000         0
0.0001.0000E+20
$#     sfs       sfm       sst       mst      sfst      sfmt
fsf       vsf
```

```
  2.000000  2.000000     0.000     0.000  1.000000  1.000000
0.000  1.000000
$#    soft    sofscl    lcidab    maxpar     sbopt     depth
bsort    frcfrq
         2     0.200         0     0.000         3         5
$#  penmax    thkopt    shlthk     snlog      isym     i2d3d
sldthk    sldstf
     0.000         0         0         0         0         0
0.000     0.000
$     IGAP    IGNORE    DPRFAC    DTSTIF
FLANGL
*SET_PART_LIST
$#     sid       da1       da2       da3       da4
        50
$#    pid1      pid2      pid3      pid4      pid5      pid6
pid7      pid8
         1         3         4
$*DEFINE_BOX
$$#   boxid       xmn       xmx       ymn       ymx       zmn
zmx
$         1-1.000E+201.0000E+20-1.000E+201.0000E+20-
1.000E+201.0000E+20
$$     IGAP    IGNORE    DPRFAC    DTSTIF
FLANGL
*CONTACT_FORCE_TRANSDUCER_PENALTY
3,,3
0
0
*CONTACT_FORCE_TRANSDUCER_PENALTY
4,,3
0
0
$---+----1----+----2----+----3----+----4----+----5----+----6----+----
7----+----8
$                    TOOL < 10_punch >
$---+----1----+----2----+----3----+----4----+----5----+----6----+----
7----+----8
*SET_PART_LIST
$SET_PART_NAME: 10_punch
$      SID       DA1       DA2       DA3       DA4
         3
$     PID1      PID2      PID3      PID4      PID5      PID6
PID7      PID8
         3
*PART
$HEADING
 PART PID =         3 PART NAME :002V000
$      PID     SECID       MID     EOSID      HGID      GRAV
ADPOPT      TMID
         3         3         3
*MAT_RIGID
$      MID        RO         E        PR         N    COUPLE
M     ALIAS
         3 7.830E-09 2.070E+05      0.28
$      CMO      CON1      CON2
         1         4         7
$LCO or A1        A2        A3        V1        V2        V3

*SECTION_SHELL
$      SID    ELFORM      SHRF       NIP     PROPT   QR/IRID
ICOMP     SETYP
```

```
         3         2       1.0       3.0       0.0
$       T1        T2        T3        T4      NLOC
       1.0       1.0       1.0       1.0
$---+----1----+----2----+----3----+----4----+----5----+----6----+----
7----+----8
$
$                    (5) DEFINE PROCESS STEPS
$
$---+----1----+----2----+----3----+----4----+----5----+----6----+----
7----+----8
$---+----1----+----2----+----3----+----4----+----5----+----6----+----
7----+----8
$                     STEP < drawing >
$---+----1----+----2----+----3----+----4----+----5----+----6----+----
7----+----8
$10_die : stationary
$10_punch : velocity
*BOUNDARY_PRESCRIBED_MOTION_RIGID
$   typeID       DOF       VAD      LCID        SF       VID
DEATH     BIRTH
         3         3         0         3        2          0
0.0460450       0.0
$---+----1----+----2----+----3----+----4----+----5----+----6----+----
7----+----8
$
$                    (6) DEFINE CURVES
$
$---+----1----+----2----+----3----+----4----+----5----+----6----+----
7----+----8
*DEFINE_CURVE
$D3PLOT
$     LCID      SIDR      SCLA      SCLO      OFFA      OFFO
DATTYP
         1         0
$                  A1                  O1
    0.0000000000E+00    7.2288985248E-04
    7.2288985248E-04    7.2288985248E-04
    1.4457797050E-03    7.2288985248E-04
    2.1686695574E-03    7.2288985248E-04
    2.8915594099E-03    7.2288985248E-04
    3.6144492624E-03    7.2288985248E-04
    4.3373391149E-03    7.2288985248E-04
    5.0602289673E-03    7.2288985248E-04
    5.7831188198E-03    7.2288985248E-04
    6.5060086723E-03    3.0029948810E-03
    9.5090035533E-03    3.0029948810E-03
    1.2511998434E-02    3.0029948810E-03
    1.5514993315E-02    3.0029948810E-03
    1.8517988196E-02    3.0029948810E-03
    2.1520983077E-02    3.0030788903E-03
    2.4524061968E-02    3.0029948810E-03
    2.7527056849E-02    3.0029948810E-03
    3.0530051730E-02    3.0029948810E-03
    3.3533046611E-02    3.0029948810E-03
    3.6536041492E-02    1.5014974405E-03
    3.8037538932E-02    1.5014974405E-03
    3.9539036373E-02    1.5014974405E-03
    4.1040533813E-02    1.5014974405E-03
    4.2542031254E-02    1.5014974405E-03
    4.4043528694E-02    2.0015163508E-03
    4.6045045045E-02    2.0015163508E-03
```

```
*DEFINE_CURVE
$     LCID      SIDR      SCLA      SCLO      OFFA      OFFO
DATTYP
         2         0
$                 A1                  O1
    0.0000000000E+00    6.6780000000E+00
    2.3300000000E-02    6.8356000000E+00
    4.9900000000E-02    1.7192000000E+01
    7.5700000000E-02    3.6388000000E+01
    1.0000000000E-01    5.8800000000E+01
    1.2550000000E-01    8.8700000000E+01
    1.4960000000E-01    1.2698000000E+02
    1.7300000000E-01    1.7743500000E+02
    1.9590000000E-01    2.6860080000E+02
    2.1800000000E-01    4.4186000000E+02
    2.6100000000E-01    5.1908000000E+02
    2.8200000000E-01    5.5268000000E+02
    3.0300000000E-01    5.8079600000E+02
    3.2000000000E-01    6.0419800000E+02
    3.4000000000E-01    6.2509000000E+02
    3.6000000000E-01    6.4270000000E+02
    3.8110000000E-01    6.5772000000E+02
    4.0000000000E-01    6.7035400000E+02
*DEFINE_CURVE
$MOTION OF 10_punch
$     LCID      SIDR      SCLA      SCLO      OFFA      OFFO
DATTYP
         3         0
$                 A1                  O1
    0.0000000000E+00    0.0000000000E+00
    1.0000000000E-03    3.3300000000E+02
    4.5045045045E-02    3.3300000000E+02
    4.6045045045E-02    0.0000000000E+00
$---+----1----+----2----+----3----+----4----+----5----+----6----+----
7----+----8
$
$                    (7) MODEL DATA
$
$---+----1----+----2----+----3----+----4----+----5----+----6----+----
7----+----8
*INCLUDE
piercing_mbavhi.blk
$
*INCLUDE
piercing_mbavhi.mod
$
$---+----1----+----2----+----3----+----4----+----5----+----6----+----
7----+----8
${{DYNAFORM-AUTOSETUP-CMPRS1->>>DO NOT MODIFY>>>
$!"f,0!<E9$!!!&^!!>S1"o&&s6LR,@o"R%oB</aS2hM2Oq'Wq=C7*m]*;mK"#q[1`s6m
_j!!\G+7rgg
$DDD/+Aq'Wr'CZC2n7rl@</i".,s6m](jo>KN*sME=s$H0="7j2aAnS0Y?oN]?)u1krOD
:0?=WI?&.L@
$[Ili6E<mJmHNb=?Tf.W-oA.etGVcYMQrb=?S;9J/(7li6E<"8i-
"!=8]Z!ARXS0EE9srVup!r;ZhJrr
$<N7!5+8rSr9Yob6141;bR&h#@(&m8<qpp55bHi^dJJplqt86L$R,N'_VM3I6TSq\k*c)
qdom65gB5N!
$CT3MAe>eDHPEVQiTaZ5+,0#X\/leYqZ$\25gB5N&gflR*eioWcu21FE'4Q[UF\[TrQG=
*EBsCW+Yc6%
$4UTf9\8jhKY".Gs'Jr'GiHc3@[rXh.-
sVhMoeo)5!#f6e5hDcM4UTe$5d!W9H5,L`5e%khlVY/S5l:T
```

```
$a0QfXLr0]9(5iI#'Y"*2K5WoJ+UMr@^5e%khlVWI\5d!W9H5*MK5Y0j['X!dF5SU@kiH
c2+5l:TpTQN
$M\_Y#<^O$u;JY".GsOEEhc!%LK(EBOZ\UNgoHEBOZ\UMrah_t>E_O&C*ciHc3@8)[$)E
BOZ\UD.i9Rf
$/W]=\M(Y\/p@irGk/S!6kN@1BJ4T!WE'!"o\K.%P=uWn#,G8!!rTY!A[^T0EE9urVup#
r;Zm)8O`M!!
$!N9$!!<*!%"J?Y#6;DqXHKZOMZM!$!!3#u!.b(L'*nTNN3%rJOH#D'#A.mpD/!m#$Mj`
0$<'Mj?VNjQ
$<_,gX!!!)u!!!*"!!EC7Bk7kP!!%QG!!%QH!!2T(`rH)CpAb2DqZ$Z45N;_F1dD0B!!W
UGF`(]&+R9"
$.n3=qn!!W?%!1NhR!<L"5!!0l"irBHD5_8j4n^:-
@:d5!X!!ig?Eaa0+DJ'%J!!!*"!!!&u!!!-#!!!
$)n!!:Mh5l1Na!rr?%"8Dj!/jKF;)?'U9!r)`r#XJ7e!T63>!!+?1qZ$]e56:6R#^1h0o
^sB7^'+E8!!
$<-
"!!;us!1NhR!kCMsrVup!rVup$oDeq(5QUia!!2or!!3'!!!W?%!!<&u!%@UB!Ydm$rVu
p#p](Bb5
$6:BV!Ur>N!!2#mo)K*d5C4*I8)\cI5Q1W\!!!&f!!bcJ[<N^q'h&'%!!iK'%JKhps7H?
_s763[s7$'D
$!!2RRq#CYH'WssbHA"M5
$}}DYNAFORM-AUTOSETUP
$---+----1----+----2----+----3----+----4----+----5----+----6----+----
7----+----8
$---+----1----+----2----+----3----+----4----+----5----+----6----+----
7----+----8
*END
```

23.2 Appendix B – INPUT DECK SPH MODEL FOR TM380

```
$ ETA/DYNAFORM : DYNA3D(971) INPUT DECK
$ DATE : Oct 15, 2008 at 17:11:42
$ VERSION : eta/DYNAFORM 5.6  , built on Jan  3 2008
$ EXPORTER : AUTO-SETUP
$
$ VIEWING INFORMATION
$    -43.60229    29.50944   -47.28976    -5.92261
$   -0.1306481  -0.9880627  0.08162858
$   -0.3905243   0.1269631   0.9117956
$   -0.9112741  0.08724742  -0.4024518
$
$ UNIT SYSTEM : MM, TON, SEC, N
$
$ SIMULATION  : SHEET FORMING
$
$---+----1----+----2----+----3----+----4----+----5----+----6----+----
7----+----8
$
$KEYWORD_ID
*KEYWORD
$
$---+----1----+----2----+----3----+----4----+----5----+----6----+----
7----+----8
$
$                    (1) TITLE CARD
$
$---+----1----+----2----+----3----+----4----+----5----+----6----+----
7----+----8
*TITLE
SIM_MBAVHI
$---+----1----+----2----+----3----+----4----+----5----+----6----+----
7----+----8
$
$                    (2) CONTROL CARDS
$
$---+----1----+----2----+----3----+----4----+----5----+----6----+----
7----+----8
*CONTROL_TERMINATION
$   ENDTIM    ENDCYC     DTMIN    ENDNEG    ENDMAS
$0.0230225         0                           0.0
$*CONTROL_TIMESTEP
$$   DTINIT    TSSFAC      ISDO    TSLIMT     DT2MS      LCTM
ERODE     MS1ST
      0.0       0.9         0       0.0 -4.00E-07
*CONTROL_CONTACT
$#  slsfac    rwpnal    islchk    shlthk    penopt    thkchg
orien    enmass
  0.100000     0.000         2         1         0         0
1
$#  usrstr    usrfrc     nsbcs    interm     xpene     ssthk
ecdt   tiedprj
         0         0         0         0  4.000000
$#   sfric     dfric       edc       vfc        th     th_sf
pen_sf
  0.200000  0.100000
$#  ignore    frceng   skiprwg    outseg   spotstp   spotdel
spothin
         2
```

```
$#    isym    nserod    rwgaps    rwgdth     rwksf      icov
swradf    ithoff
         0         0         0     0.000     0.000         0
0.000         0
$#  shledg
$        1
*CONTROL_ENERGY
$#    hgen      rwen    slnten     rylen
         2         2         1         1
*CONTROL_HOURGLASS
$#     ihq        qh
         4
*CONTROL_OUTPUT
$#   npopt    neecho    nrefup    iaccop     opifs    ipnint
ikedit    iflush
         0         0         0         1     0.000         0
100      5000
$#   iprtf    ierode     tet10    msgmax    ipcurv
         0         0         0         0         0
*CONTROL_PARALLEL
$#    ncpu    numrhs     const      para
         2         0         2
*CONTROL_SOLUTION
$#    soln       nlq     isnan
         0         0         1
*CONTROL_SPH
$#    ncbs     boxid        dt       dim    memory      form
start      maxv
         1         01.0000E+20         3      5000         0
0.0001.0000E+15
$#    cont     deriv
         0         0
$CONTROL_ADAPTIVE
$  ADPFREQ    ADPTOL    ADPOPT    MAXLVL    TBIRTH    TDEATH
LCADP    IOFLAG
$0.0011511       5.0         2         3       0.0 1.000E+20
1
$  ADPSIZE    ADPASS    IREFLG    ADPENE     ADPTH    MEMORY
ORIENT     MAXEL
$   1.0         1         0       1.0      -0.5                    0
0
$  IADPE90              NCFREQ    IADPCL    ADPCTL    CBIRTH
CDEATH
$    -1                    0         1       0.0       0.0 1.000E+20
$*CONTROL_ADAPSTEP
$   FACTIN    DFACTR
$    1.0      0.01
$*INTERFACE_SPRINGBACK_LSDYNA
$     PSID
$      1
$---+----1----+----2----+----3----+----4----+----5----+----6----+----
7----+----8
$*DATABASE_OPTION
$       DT    BINARY
$OPTION : SECFORC RWFORC NODOUT ELOUT  GLSTAT
$         DEFORC  MATSUM NCFORC RCFORC DEFGEO
$         SPCFORC SWFORC ABSTAT NODFOR BNDOUT
$         RBDOUT  GCEOUT SLEOUT MPGS   SBTOUT
$         JNTFORC AVSFLT MOVIE
$*DATABASE_RCFORCE
*DATABASE_RCFORC
```

```
 4.604E-05
*DATABASE_MATSUM
 4.604E-05
*DATABASE_GLSTAT
 4.604E-05
*DATABASE_SLEOUT
 4.604E-05
*DATABASE_RBDOUT
 4.604E-05
*DATABASE_BNDOUT
 4.604E-05
*DATABASE_ABSTAT
 4.604E-05
*DATABASE_ELOUT
 4.604E-05
*DATABASE_NCFORC
 4.604E-05
*DATABASE_NODFOR
 4.604E-05
*DATABASE_NODOUT
 4.604E-05
*DATABASE_SECFORC
 4.604E-05
*DATABASE_SPCFORC
 4.604E-05
$*DATABASE_ABSTAT
$ 4.604E-05
$---+----1----+----2----+----3----+----4----+----5----+----6----+----
7----+----8
*DATABASE_BINARY_D3PLOT
$  DT/CYCL      LCDT      BEAM
   5.0e-05
$#   ioopt
         0
*DATABASE_EXTENT_BINARY
$#   neiph     neips    maxint    strflg    sigflg    epsflg
rltflg    engflg
         0         0         3         0         1         1
1         1
$#  cmpflg    ieverp    beamip     dcomp      shge     stssz
n3thdt   ialemat
         0         0         0         1         2         2
2         1
$# nintsld   pkp_sen      sclp    unused     msscl     therm
iniout    iniout
         0         0  1.000000         0         0         0
$---+----1----+----2----+----3----+----4----+----5----+----6----+----
7----+----8
$
$                    (3) DEFINE BLANK
$
$---+----1----+----2----+----3----+----4----+----5----+----6----+----
7----+----8
*SET_PART_LIST
$SET_PART_NAME: BLANK
$      SID       DA1       DA2       DA3       DA4
         6
$     PID1      PID2      PID3      PID4      PID5      PID6
PID7      PID8
$         1
         6
```

```
*PART
$HEADING
 PART PID =         1 PART NAME :001V000
$      PID     SECID       MID     EOSID      HGID      GRAV
ADPOPT      TMID
$         1         1         1
         6        11         1
*MAT_PIECEWISE_LINEAR_PLASTICITY
$MATERIAL NAME:DQSK
$      MID        RO         E        PR      SIGY      ETAN
FAIL      TDEL
         1 7.850E-09 2.070E+05      0.28
$        C         P      LCSS      LCSR
       0.0       0.0         4
$     EPS1      EPS2      EPS3      EPS4      EPS5      EPS6
EPS7      EPS8
       0.0       0.0       0.0       0.0       0.0       0.0
0.0       0.0
$      ES1       ES2       ES3       ES4       ES5       ES6
ES7       ES8
       0.0       0.0       0.0       0.0       0.0       0.0
0.0       0.0
*SECTION_SPH
$    secid      cslh      hmin      hmax    sphini     death
start
        11  1.200000  0.200000  2.000000     0.000  1.00E+20
$---+----1----+----2----+----3----+----4----+----5----+----6----+----
7----+----8
$
$                    (4) DEFINE TOOLS
$
$---+----1----+----2----+----3----+----4----+----5----+----6----+----
7----+----8
$---+----1----+----2----+----3----+----4----+----5----+----6----+----
7----+----8
$                     TOOL < 10_die >
$---+----1----+----2----+----3----+----4----+----5----+----6----+----
7----+----8
*SET_PART_LIST
$SET_PART_NAME: 10_die
$      SID       DA1       DA2       DA3       DA4
         2
$     PID1      PID2      PID3      PID4      PID5      PID6
PID7      PID8
         4
*PART
$HEADING
 PART PID =         4 PART NAME :IE
$      PID     SECID       MID     EOSID      HGID      GRAV
ADPOPT      TMID
         4         2         2
*MAT_RIGID
$      MID        RO         E        PR         N    COUPLE
M     ALIAS
         2 7.830E-09 2.070E+05      0.28
$      CMO      CON1      CON2
         1         7         7
$LCO or A1        A2        A3        V1        V2        V3

*SECTION_SHELL
```

```
$      SID    ELFORM      SHRF       NIP     PROPT   QR/IRID
ICOMP     SETYP
$         2         2       1.0       3.0       0.0
          2         2       1.0       2.0       1.0
$       T1        T2        T3        T4      NLOC
        1.0       1.0       1.0       1.0
*CONTACT_AUTOMATIC_NODES_TO_SURFACE_TITLE
$*     cidtitle
          1
$*    ssid      msid     sstyp     mstyp    sboxid    mboxid
spr       mpr
          6         2         4         2
1         1
$#      fs        fd        dc        vc       vdc    penchk
bt        dt
  0.500000  0.350000     0.000     0.000 20.000000         0
0.0001.0000E+20
$#     sfs       sfm       sst       mst      sfst      sfmt
fsf       vsf
  1.000000  1.000000     0.000     0.000  1.000000  1.000000
1.000000  1.000000
$*CONTACT_AUTOMATIC_SINGLE_SURFACE
$$#     cid
title
$$#    ssid      msid     sstyp     mstyp    sboxid    mboxid
spr       mpr
$         50         0         2         0         0         0
1         1
$$#      fs        fd        dc        vc       vdc    penchk
bt        dt
$  0.125000  0.125000     0.000     0.000     0.000         0
0.0001.0000E+20
$$#     sfs       sfm       sst       mst      sfst      sfmt
fsf       vsf
$  2.000000  2.000000     0.000     0.000  1.000000  1.000000
0.000  1.000000
$$#    soft    sofscl    lcidab    maxpar     sbopt     depth
bsort    frcfrq
$$      2     0.000         0     0.000  2.000000         5
$         2     0.200         0     0.000         3         5
$$#  penmax    thkopt    shlthk     snlog      isym     i2d3d
sldthk    sldstf
$     0.000         0         0         0         0         0
0.000     0.000
$$     IGAP    IGNORE    DPRFAC    DTSTIF
FLANGL
$*SET_PART_LIST
$$#     sid       da1       da2       da3       da4
$         50
$$#    pid1      pid2      pid3      pid4      pid5      pid6
pid7      pid8
$       103         3         4
$*DEFINE_BOX
$$#   boxid       xmn       xmx       ymn       ymx       zmn
zmx
$         1-1.000E+201.0000E+20-1.000E+201.0000E+20-
1.000E+201.0000E+20
$$     IGAP    IGNORE    DPRFAC    DTSTIF
FLANGL
$*CONTACT_FORCE_TRANSDUCER_PENALTY
$3,,3
```

```
$0
$0
$*CONTACT_FORCE_TRANSDUCER_PENALTY
$4,,3
$0
$0
$---+----1----+----2----+----3----+----4----+----5----+----6----+----
7----+----8
$                    TOOL < 10_punch >
$---+----1----+----2----+----3----+----4----+----5----+----6----+----
7----+----8
*SET_PART_LIST
$SET_PART_NAME: 10_punch
$      SID       DA1       DA2       DA3       DA4
         3
$     PID1      PID2      PID3      PID4      PID5      PID6
PID7      PID8
         3
*PART
$HEADING
 PART PID =         3 PART NAME :002V000
$      PID     SECID       MID     EOSID      HGID      GRAV
ADPOPT      TMID
         3         3         3
*MAT_RIGID
$      MID        RO         E        PR         N    COUPLE
M     ALIAS
         3 7.830E-09 2.070E+05      0.28
$      CMO      CON1      CON2
         1         4         7
$LCO or A1        A2        A3        V1        V2        V3
*SECTION_SHELL
$      SID    ELFORM      SHRF       NIP     PROPT   QR/IRID
ICOMP     SETYP
$         3         2       1.0       3.0       0.0
         3         2       1.0       2.0       1.0
$       T1        T2        T3        T4      NLOC
       1.0       1.0       1.0       1.0
*CONTACT_AUTOMATIC_NODES_TO_SURFACE_TITLE
$*     cidtitle
         2
$*    ssid      msid     sstyp     mstyp    sboxid    mboxid
spr       mpr
         6         3         4         2
1         1
$#      fs        fd        dc        vc       vdc    penchk
bt        dt
  0.500000  0.350000     0.000     0.000 20.000000         0
0.0001.0000E+20
$#     sfs       sfm       sst       mst      sfst      sfmt
fsf       vsf
  1.000000  1.000000     0.000     0.000  1.000000  1.000000
1.000000  1.000000
$---+----1----+----2----+----3----+----4----+----5----+----6----+----
7----+----8
$
$                    (5) DEFINE PROCESS STEPS
$
$---+----1----+----2----+----3----+----4----+----5----+----6----+----
7----+----8
```

```
$---+----1----+----2----+----3----+----4----+----5----+----6----+----
7----+----8
$                    STEP < drawing >
$---+----1----+----2----+----3----+----4----+----5----+----6----+----
7----+----8
$10_die : stationary
$10_punch : velocity
*BOUNDARY_PRESCRIBED_MOTION_RIGID
$   typeID       DOF       VAD      LCID        SF       VID
DEATH     BIRTH
         3         3         0         3         3         0
0.0460450       0.0
$---+----1----+----2----+----3----+----4----+----5----+----6----+----
7----+----8
$
$                    (6) DEFINE CURVES
$
$---+----1----+----2----+----3----+----4----+----5----+----6----+----
7----+----8
*DEFINE_CURVE
$D3PLOT
$     LCID      SIDR      SCLA      SCLO      OFFA      OFFO
DATTYP
         1         0
$                 A1                  O1
    0.0000000000E+00    5.1161111111E-04
    5.1161111111E-04    5.1161111111E-04
    1.0232222222E-03    5.1161111111E-04
    1.5348333333E-03    5.1161111111E-04
    2.0464444444E-03    5.1161111111E-04
    2.5580555556E-03    5.1161111111E-04
    3.0696666667E-03    5.1161111111E-04
    3.5812777778E-03    5.1161111111E-04
    4.0928888889E-03    5.1161111111E-04
    4.6045000000E-03    5.1161111111E-04
    5.1161111111E-03    5.1161111111E-04
    5.6277222222E-03    5.1161111111E-04
    6.1393333333E-03    5.1161111111E-04
    6.6509444444E-03    5.1161111111E-04
    7.1625555556E-03    5.1161111111E-04
    7.6741666667E-03    5.1161111111E-04
    8.1857777778E-03    5.1161111111E-04
    8.6973888889E-03    5.1161111111E-04
    9.2090000000E-03    5.1161111111E-04
    9.7206111111E-03    5.1161111111E-04
    1.0232222222E-02    5.1161111111E-04
    1.0743833333E-02    5.1161111111E-04
    1.1255444444E-02    5.1161111111E-04
    1.1767055556E-02    5.1161111111E-04
    1.2278666667E-02    5.1161111111E-04
    1.2790277778E-02    5.1161111111E-04
    1.3301888889E-02    5.1161111111E-04
    1.3813500000E-02    5.1161111111E-04
    1.4325111111E-02    5.1161111111E-04
    1.4836722222E-02    5.1161111111E-04
    1.5348333333E-02    5.1161111111E-04
    1.5859944444E-02    5.1161111111E-04
    1.6371555556E-02    5.1161111111E-04
    1.6883166667E-02    5.1161111111E-04
    1.7394777778E-02    5.1161111111E-04
    1.7906388889E-02    5.1161111111E-04
```

```
    1.8418000000E-02    5.1161111111E-04
    1.8929611111E-02    5.1161111111E-04
    1.9441222222E-02    5.1161111111E-04
    1.9952833333E-02    5.1161111111E-04
    2.0464444444E-02    5.1161111111E-04
    2.0976055556E-02    5.1161111111E-04
    2.1487666667E-02    5.1161111111E-04
    2.1999277778E-02    5.1161111111E-04
    2.2510888889E-02    5.1161111111E-04
    2.3022500000E-02    5.1161111111E-04
*DEFINE_CURVE
$MOTION OF 10_punch
$     LCID      SIDR       SCLA      SCLO      OFFA      OFFO
DATTYP
         3         0
$                 A1                  O1
    0.0000000000E+00    0.0000000000E+00
    1.5045045045E-02    3.3300000000E+02
    4.5045045045E-02    3.3300000000E+02
    4.6045045045E-02    0.0000000000E+00
*DEFINE_CURVE
$     LCID      SIDR       SCLA      SCLO      OFFA      OFFO
DATTYP
         4         0
$                 A1                  O1
    0.0000000000E+00    6.6780000000E+00
    2.3300000000E-02    6.8356000000E+00
    4.9900000000E-02    1.7192000000E+01
    7.5700000000E-02    3.6388000000E+01
    1.0000000000E-01    5.8800000000E+01
    1.2550000000E-01    8.8700000000E+01
    1.4960000000E-01    1.2698000000E+02
    1.7300000000E-01    1.7743500000E+02
    1.9590000000E-01    2.6860080000E+02
    2.1800000000E-01    4.4186000000E+02
    2.6100000000E-01    5.1908000000E+02
    2.8200000000E-01    5.5268000000E+02
    3.0300000000E-01    5.8079600000E+02
    3.2000000000E-01    6.0419800000E+02
    3.4000000000E-01    6.2509000000E+02
    3.6000000000E-01    6.4270000000E+02
    3.8110000000E-01    6.5772000000E+02
    4.0000000000E-01    6.7035400000E+02
$---+----1----+----2----+----3----+----4----+----5----+----6----+----
7----+----8
$
$                   (7) MODEL DATA
$
$---+----1----+----2----+----3----+----4----+----5----+----6----+----
7----+----8
*INCLUDE
piercing_dmore_sph.blk
*INCLUDE
piercing_dmore_9.mod
$
$---+----1----+----2----+----3----+----4----+----5----+----6----+----
7----+----8
${{DYNAFORM-AUTOSETUP-CMPRS1->>>DO NOT MODIFY>>>
$!"f,0!<E9$!!!&^!!>S1"o&&s6LR,@o"R%oB</aS2hM2Oq'Wq=C7*m]*;mK"#q[1`s6m
_j!!\G+7rgg
```

```
$DDD/+Aq'Wr'CZC2n7rl@</i".,s6m](jo>KN*sME=s$H0="7j2aAnS0Y?oN]?)u1krOD
:0?=WI?&.L@
$[Ili6E<mJmHNb=?Tf.W-oA.etGVcYMQrb=?S;9J/(7li6E<"8i-
"!=8]Z!ARXS0EE9srVup!r;ZhJrr
$<N7!5+8rSr9Yob6141;bR&h#@(&m8<qpp55bHi^dJJplqt86L$R,N'_VM3I6TSq\k*c)
qdom65gB5N!
$CT3MAe>eDHPEVQiTaZ5+,0#X\/leYqZ$\25gB5N&gflR*eioWcu21FE'4Q[UF\[TrQG=
*EBsCW+Yc6%
$4UTf9\8jhKY".Gs'Jr'GiHc3@[rXh.-
sVhMoeo)5!#f6e5hDcM4UTe$5d!W9H5,L`5e%khlVY/S5l:T
$a0QfXLr0]9(5iI#'Y"*2K5WoJ+UMr@^5e%khlVWI\5d!W9H5*MK5Y0j['X!dF5SU@kiH
c2+5l:TpTQN
$M\_Y#<^O$u;JY".GsOEEhc!%LK(EBOZ\UNgoHEBOZ\UMrah_t>E_O&C*ciHc3@8)[$)E
BOZ\UD.i9Rf
$/W]=\M(Y\/p@irGk/S!6kN@1BJ4T!WE'!"o\K.%P=uWn#,G8!!rTY!A[^T0EE9urVup#
r;Zm)8O`M!!
$!N9$!!<*!%"J?Y#6;DqXHKZOMZM!$!!3#u!.b(L'*nTNN3%rJOH#D'#A.mpD/!m#$Mj`
0$<'Mj?VNjQ
$<_,gX!!!)u!!!*"!!EC7Bk7kP!!%QG!!%QH!!2T(`rH)CpAb2DqZ$Z45N;_F1dD0B!!W
UGF`()&+R9"
$.n3=qn!!W?%!1NhR!<L"5!!0l"irBHD5_8j4n^:-
@:d5!X!!ig?Eaa0+DJ'%J!!!*"!!!&u!!!-#!!!
$)n!!:Mh5l1Na!rr?%"8Dj!/jKF;)?'U9!r)`r#XJ7e!T63>!!+?1qZ$]e56:6R#^1h0o
^sB7^'+E8!!
$<-
"!!;us!1NhR!kCMsrVup!rVup$oDeq(5QUia!!2or!!3'!!!W?%!!<&u!%@UB!Ydm$rVu
p#p](Bb5
$6:BV!Ur>N!!2#mo)K*d5C4*I8)\cI5Q1W\!!!&f!!bcJ[<N^q'h&'%!!iK'%JKhps7H?
_s763[s7$'D
$!!2RRq#CYH'WssbHA"M5
$}}DYNAFORM-AUTOSETUP
$---+----1----+----2----+----3----+----4----+----5----+----6----+----
7----+----8
$---+----1----+----2----+----3----+----4----+----5----+----6----+----
7----+----8
*END
```